April 2015
contact: qualif@mercator-ocean.fr

QuO Va Dis?
Quarterly Ocean Validation Display #19

Validation bulletin for October-November-December (OND) 2014

Edition:
Charly Régnier, Marie Drévillon, Bruno Levier, Charles Desportes, Coralie Perruche,
(MERCATOR OCEAN/Production Dep./Products Quality)

Contributions :
Eric Greiner (CLS)
Jean-Michel Lellouche, Olivier Le Galloudec (MERCATOR OCEAN/ Production Dep./R&D)

Credits for validation methodology and tools:
Eric Greiner, Mounir Benkiran, Nathalie Verbrugge, Hélène Etienne (CLS)
Fabrice Hernandez, Laurence Crosnier (MERCATOR OCEAN)
Nicolas Ferry, Gilles Garric, Jean-Michel Lellouche (MERCATOR OCEAN)
Stéphane Law Chune (Météo-France), Julien Paul (MERCATOR OCEAN), Lionel Zawadzki (CLS)
Jean-Marc Molines (LGGE), Sébastien Theeten (Ifremer), Mélanie Juza (IMEDEA), the DRAKKAR and NEMO groups, the BCG group (Météo-France, CERFACS)
Bruno Blanke, Nicolas Grima, Rob Scott (LPO)

Information on input data:
Christine Boone, Gaël Nicolas (CLS/ARMOR team)

Abstract

This bulletin gives an estimate of the accuracy of MERCATOR OCEAN's analyses and forecast for the season of ***October-November-December 2014****. It also provides a summary of useful information on the context of the production for this period. Diagnostics will be displayed for the global 1/12° (PSY4), global ¼° (PSY3), the Atlantic and Mediterranean zoom at 1/12° (PSY2), and the Iberia-Biscay-Ireland (IBI) monitoring and forecasting systems currently producing daily 3D temperature, salinity and current products. Surface Chlorophyll concentrations from the BIOMER biogeochemical monitoring and forecasting system are also displayed and compared with simultaneous observations.*

Table of contents

I Executive summary 4
II Status and evolutions of the systems 5
II.1. Short description and current status of the systems 5
II.2. Incidents in the course of OND 2014 10
III Summary of the availability and quality control of the input data 10
III.1. Observations available for data assimilation 10
III.1.1. In situ observations of T/S profiles 10
III.1.2. Sea Surface Temperature 10
III.1.3. Sea level anomalies along track 10
III.2. Observations available for validation 11
IV Information on the large scale climatic conditions 11
V Accuracy of the products 13
V.1. Data assimilation performance 13
V.1.1. Sea surface height 13
V.1.2. Sea surface temperature 18
V.1.3. Temperature and salinity profiles 22
V.2. Accuracy of the daily average products with respect to observations 38
V.2.1. T/S profiles observations 38
V.2.2. SST Comparisons 49
V.2.3. Drifting buoys velocity measurements 50
V.2.4. Sea ice concentration 56
V.2.5. Closer to the coast with the IBI36V2 system: multiple comparisons 59
V.2.5.1. Comparisons with SST from CMS 59
V.2.5.2. Comparisons with in situ data from EN3/ENSEMBLE for OND 2014 60
V.2.5.3. MLD Comparisons with in situ data 62
V.2.5.4. Comparisons with moorings and tide gauges 63
V.2.6. Biogeochemistry validation: ocean colour maps 66
VI Forecast error statistics 68
VI.1. General considerations 68
VI.2. Forecast accuracy: comparisons with T and S observations when and where available 68
VI.2.1. North Atlantic region 68
VI.2.2. Mediterranean Sea 70
VI.2.3. Tropical Oceans and global 71
VI.3. Forecast accuracy: skill scores for T and S 74
VI.4. Forecast verification: comparison with analysis everywhere 76
VII Monitoring of ocean and sea ice physics 77
VII.1. Global mean SST and SSS 77
VII.2. Surface EKE 78
VII.3. Mediterranean outflow 79
VII.4. Sea Ice extent and area 79
I Annex A 81
I.1. Table of figures 81

II Annex B..... 85
II.1. Maps of regions for data assimilation statistics..... 85
II.1.1. Tropical and North Atlantic..... 85
I.1.1. Mediterranean Sea..... 86
I.1.2. Global ocean..... 87
III Annex C..... 88
III.1. Quality control algorithm for the Mercator Ocean drifter data correction (Eric Greiner) 88
III.2. Algorithm of the Lagrangian verification of the Mercator Ocean surface currents forecast..... 89

I Executive summary

T & S

The Mercator Ocean monitoring and forecasting systems are evaluated for the **period October-November-December 2014**. The 1/12° global system providing products for MyOcean V3 global MFC, and the other Mercator "off shore" systems (global ¼° and Atlantic+Mediterranean 1/12°) display similar performance in terms of water masses accuracy. The system's analysis of the **ocean water masses is very accurate on global average** and almost everywhere between the bottom and 200m. Between 0 and 500m departures from *in situ* observations **rarely exceed 1 °C and 0.2 psu** (mostly in high variability regions like the Gulf Stream or the Eastern Tropical Pacific). At the global scale PSY4 is fresh (up to 0.02) at the surface and warm in the whole water column (below 0.05°C) whereas PSY3 is salty (up to 0.01) in the 0-300m layer and globally cold (below to 0.05). PSY3 seems to be close to PSY4 but most accurate in the Pacific and Atlantic basins. PSY4 is the best in the Indian basin. The evolution of this difference between the global systems will be monitored in the next issues.
The temperature and salinity forecast have **significant skill** in many regions of the ocean in the 0-500m layer, but the signal is noisy.

Surface fields: SST, SSS, SSH, currents

A **warm SST bias** of 0.1 °C on global average is diagnosed this quarter, mainly due to the tropics and the ACC. The SST bias is cold in the Arctic.

Especially in the high resolution systems PSY2 and PSY4, a **strong fresh bias is diagnosed in the tropics,** in link with the overestimated convective precipitations in the ECMWF atmospheric fields.

The monitoring systems are generally very close to altimetric observations (global average of 6 cm residual RMS error). Biases persist locally that correspond to known uncertainties in the mean dynamic topography (for instance in the Indonesian region).

For the **high resolution system PSY4**, the **surface currents are overestimated** in the mid-latitudes and for the **Equatorial Pacific currents** (South Equatorial Current and North Equatorial Counter Current) with respect to *in situ* measurements of drifting buoys (drifter velocities are corrected of windage and slippage with a method developed by Mercator Ocean). He also overestimates the Kuroshio region, the Gulf of Alaska and the Southern oceans. PSY3 underestimates the South Pacific Equatorial Current, the Western Subarctic gyre and the South Indian Ocean. Both overestimate the Southern oceans and the Gulf Stream region.

The underestimation ranges from 20% in strong currents up to 60% in weak currents. On the contrary the orientation of the current vectors is well represented**.** Lagrangian metrics show that after 1 day, 80% of the virtual drifters trajectories performed with Mercator Ocean forecast velocities stay within a 25 km distance of the actual drifters observed trajectories.

Regional North East Atlantic

The high resolution North East Atlantic at 1/36° (IBI36V1) with no data assimilation is accurate on average. **Tidal and residual sea surface elevations are well represented**. Zones of intense tidal mixing are less accurate. The mixed layer is too shallow in the Bay of Biscay (the thermocline is too diffusive). The upwelling along the Iberian coasts is underestimated.

Sea Ice

Sea ice observations are not yet assimilated, nevertheless sea ice concentrations are realistic. In OND 2014, there is an underestimation of modelled sea ice concentration with observed sea ice concentration near the marginal zones and an overestimation in the Canadian Archipelago. This could be partly explains by to much melting during the summer and a bad resolved sea ice circulation. In the Antarctic the summer sea ice concentration is underestimated on average by both PSY3 and PSY4, On the contrary it is overestimated along the sea ice edge in the Bellingshausen Sea and in the south of Kerguelen Island.

Biogeochemistry

The **new version** of BIOMER4 seems to be **closer to the observations,** the serious discrepancies in the tropical band are corrected. Due to a **bad timing of the blooms**, some **discrepancies** are still present in the **Peru-Chili coast** and in the **Ziapola region**.

II Status and evolutions of the systems

II.1. Short description and current status of the systems

A bit of history

PSY3V3 (global ¼°) and PSY2V4 (Altantic and Mediterranean 1/12°) systems have been operated at MERCATOR OCEAN since 2010 December, 15th. These systems provide the version 1 (PSY3V3*R1*/PSY2V4*R1, see QuOVaDis?* #2) and version 2 (PSY3V3*R1*/PSY2V4*R2, see QuOVaDis?* #5) products of the MyOcean global monitoring and forecasting centre. As reminded in table 1 (and illustrated for PSY2V2 in Figure 1) the atmospheric forcing is updated daily with the latest ECMWF analysis and forecast, and a new oceanic forecast is run every day for both PSY3V3R1 and PSY2V4R2.

The PSY3V3R1 system is started in October 2006 from a 3D climatology of temperature and salinity (World Ocean Atlas Levitus 2005) while the PSY2V4R2 is started in October 2009. After a short 3-month spin up of the model and data assimilation, the performance of PSY3V3R1 has been evaluated on the 2007-2009 period (MyOcean internal calibration report, which results are synthesised in *QuOVaDis?* #2).

The PSY4 system (global 1/12°) is delivering operational products since the beginning of 2010, and was developed in 2009. Its first version PSY4V1 did not benefit from the scientific improvements of PSY3V3R1 and PSY2V4R2, developed in 2010 and 2011. This system delivers 7-day forecast (and not 14-day like PSY3V3R1 and PSY2V4R2).

An upgrade of the data assimilation systems was performed in March 2012 in order to assimilate MyOcean V2 altimetric observations and in situ observations (instead of respectively AVISO and CORIOLIS observations, corresponding to MyOcean V0 observations).

In consequence, more in situ observations are assimilated by all systems in the European seas since March 2012.

Current global systems

The whole Mercator Ocean global analysis and forecasting system (including PSY4, PSY2 and PSY3) has been updated in April 2013 (MyOcean products version 3). **The current versions names are PSY3V3R3, PSY2V4R4 and PSY4V2R2. Results from these current systems only will be described in this issue. For more simplicity they will be called PSY3, PSY2 and PSY4 in this document.** A description of most updates, as well as the evaluation process, can be found in Lellouche et al (2013)[1]. With respect to this article, several additional modifications were made in order to stabilize the performance of the system (see table 1). A specific paragraph is dedicated to the evaluation of these new systems: in Quo Va Dis?#12.

North east Atlantic

The IBI36 system is described in QuOVaDis? #5 and #6 (see also table 1 and Figure 1). The nominal MyOcean production unit for IBI36 is Puertos Del Estado (Spain) while Mercator Océan produces the back up products. The Mercator Océan IBI36V1 system was officially operational in June 2011. The version IBI36V2 of the system was operated from December 2011 to April 2014 and was very similar to IBI36V1 except it used realistic river runoffs from SHMI and Prévimer instead of climatological runoffs. The version IBI36V4 of the system is operated since April 2014: the only difference with IBI36V2 is the switch of the NEMO code version, from 2.3 to 3.4. There are however minor code upgrades. The leapfrog time stepping scheme of 3d variables has been modified according to the work of Leclair and Madec (2009)[2]; this should have a small impact on the results. The computation of coriolis terms in the barotropic equations has been corrected in order to be fully compliant with the 3d calculation. The locally enhanced bottom friction in the Gulf of Cadiz implemented in IBI-V3 has been suppressed, since this leads to a relatively minor improvement of Mediterranean overflow.

---

[1] J.-M. Lellouche, O. Le Galloudec, M. Drévillon, C. Régnier, E. Greiner, G. Garric, N. Ferry, C. Desportes, C.-E. Testut, C. Bricaud, R. Bourdallé-Badie, B. Tranchant, M. Benkiran, Y. Drillet, A. Daudin, and C. De Nicola, Evaluation of global monitoring and forecasting systems at Mercator Océan, Ocean Sci., 9, 57-81, 2013, www.ocean-sci.net/9/57/2013/, doi:10.5194/os-9-57-2013

[2] M. Leclerc, G. Madec, A conservative Leap-Frog time stepping method, Ocean Modelling 30(2-3), 88-94, 2009, http://dx.doi.org/10.1016/j.ocemod.2009.06.006

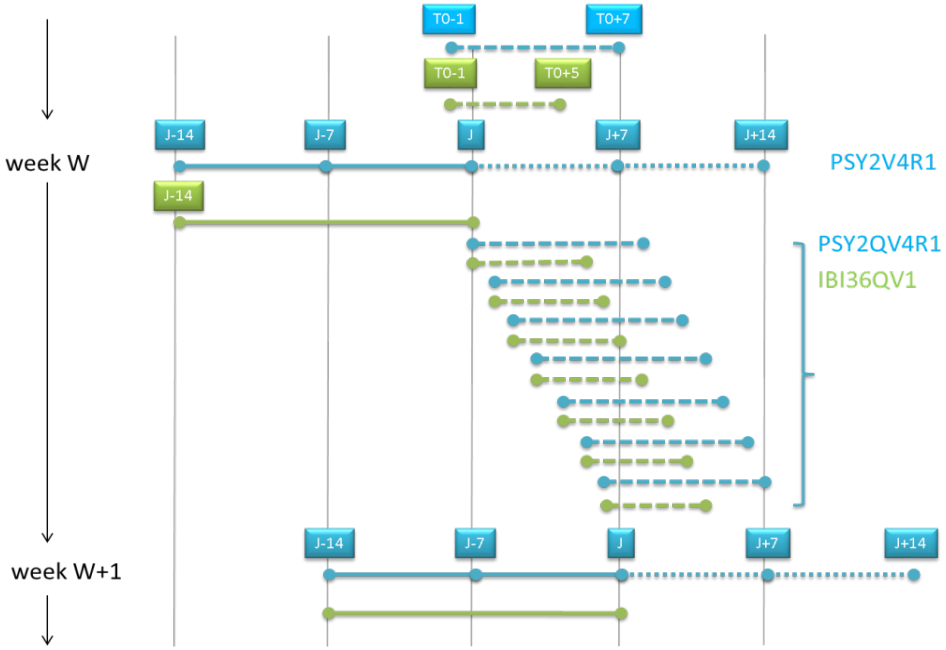

Figure 1: schematic of the operational forecast scenario for IBI36Q (green) and PSY2Q (blue). Solid lines are the PSY2 weekly hindcast and nowcast experiments, and the IBI36 spin up. Dotted lines are the weekly 14-day forecast, dashed lines are daily updates of the ocean forecast forced with the latest ECMWF atmospheric analysis and forecast. The operational scenario of PSY3, PSY4 and PSY3Q, PSY4Q is similar to PSY2's scenario. In the case of PSY4, only weekly hindcast, nowcast and 7-day forecast are performed.

Biogeochemistry

The BIOMER4 system is described in QuOVaDis? #18 (see also table 1). It is a global hindcast biogeochemical model forced by physical ocean fields. The biogeochemical model used is PISCES. The coupling between ocean physics and biogeochemistry is performed offline. The physical fields from PSY3 have a 1/4° horizontal resolution and 7-day time resolution.

System name	domain	resolution	Physical Model	Assimilation	Assimilated observations	Inter dependencies	Status of production
PSY4V1R3 (operational in OND 2013) PSY4V2R2 (operational in AMJ 2013)	Global	1/12° on the horizontal, 50 levels on the vertical	ORCA12 LIM2 NEMO 1.09 Bulk CLIO 24-h atmospheric forcing LIM2 EVP NEMO 3.1 Bulk CORE 3-h atmospheric forcing mix, colour, iceberg, EMP init WOA09: oct 2012	SAM2V1 (SEEK) + IAU 3D-Var bias correction coast error, shelf error new MDT, radii Increase of Envisat error new QC, SST bulk corr	RTG-SST, MyOcean SLA along track, MyOcean T/S vertical profiles AVHRR-AMSR SST, new MDT Sea Mammals T/S profiles in CUTRR Black Sea SLA files		Weekly 7-day forecast Weekly 7-day forecast Daily update of atmospheric forcing for daily 7-day forecast
PSY3V3R1 (operational in OND 2013) PSY3V3R2 (described in Lellouche et al, 2013) PSY3V3R3 (operational in AMJ 2013)	Global	1/4° on the horizontal, 50 levels on the vertical	ORCA025 LIM2 EVP NEMO 3.1 Bulk CORE 3-h atmospheric forcing mix, colour, iceberg, EMP flux corr no flux corr current in wind init WOA09:oct 2006	SAM2V1 (SEEK) + IAU 3D-Var bias correction coast error, shelf error MDT error adjusted first update of radii Increase of Envisat error new QC radii, SST bulk corr	RTG-SST, MyOcean SLA along track, MyOcean T/S vertical profiles AVHRR-AMSR SST, new MDT Sea Mammals T/S profiles in CUTRR Black Sea SLA files		Weekly 14-day forecast Daily update of atmospheric forcing for daily 7-day forecast
PSY2V4R2 (operational in OND 2013) PSY2V4R3 (described in Lellouche et al., 2013) PSY2V4R4 (operational in AMJ 2013)	Tropical North Atlantic Mediterranean	1/12° on the horizontal, 50 levels on the vertical	NATL12 LIM2 EVP NEMO 3.1 Bulk CORE 3-h atmospheric forcing mix, colour flux corr no flux corr current in wind init WOA09:oct 2006	SAM2V1 (SEEK) + IAU 3D-3D-Var bias correction coast error, shelf error first update of radii Increase of Envisat error QC on T/S vertical profiles radii, SST bulk corr Larger weight of Bogus OBC on TSUV	AVHRR-AMSR SST, MyOcean SLA along track , MyOcean T/S vertical profiles new MDT Sea Mammals T/S profiles in CUTRR	OBC from PSY3V3R1 OBC and SMEMP from PSY3V3R2 OBC and SMEMP from PSY3V3R3	Weekly 14-day forecast Daily update of atmospheric forcing for daily 7-day forecast
BIOMER4 upgrade in September 2014	Global	1/4° on the horizontal, 50 levels on the vertical	PISCES, NEMO 3.2, offline	none	none	Two weeks hindcast, nowcast with PSY3V3R3 1/4° phy	Weekly 14-day analysis Weekly 7-day forecast
IBI36V4 upgrade in AMJ 2014	North East Atlantic and West Mediterranean Sea (Iberian, Biscay and Ireland) region	1/36° on the horizontal, 50 levels on the vertical	NEATL36 NEMO 3.4 3-hourly atmospheric forcing from ECMWF, bulk CORE, tides, time-splitting, GLS vertical mixing, corrected bathymetry, river runoffs from SMHI & Prévimer	none	none	Two weeks spin up initialized with PSY2V4R4 and OBC from PSY2V4R4	Weekly spin up two weeks back in time. Daily update of atmospheric forcings for daily 5-day forecast IBI36QV4

Table 1: Main characteristics and latest updates of the Mercator Ocean global analysis and forecasting systems. The systems studied in Lellouche et al (2013) include the main characteristics (in black) plus the updates in blue. The 2013 systems (in red) include the main characteristics (in black) plus the updates in blue and red. In the legend below one can find a description of the updates referred to as "mix", "colour", etc…

Mix = New parameterization of vertical mixing
Colour = Taking into account ocean colour monthly climatology for depth of light extinction
Current in wind = taking 50 % of surface current for the computation of wind stress with bulk CORE
EMP = Adding seasonal cycle for surface mass budget
SMEMP = spatial mean EMP correction
Iceberg = Adding runoff for iceberg melting
Flux corr = Large scale correction to the downward radiative and precipitation fluxes
Coast error = Observation error s higher near the coast (SST and SLA)
Shelf error = Observation error s higher on continental shelves (SLA)

New MDT = MDT CNES/CLS09 adjusted with model solutions (bias corrected)
Radii = New correlation radii (minimum =130km)
New QC = additional QC on T/S vertical profiles computed from the innovations
SST bulk corr = Procedure to avoid the damping of SST increments via the bulk forcing function
OBC = Open Boundary Conditions
1° phy= physical forcings are “degraded” from ¼° horizontal resolution to 1° horizontal resolution, and weekly averaged.
CUTRR= Catch Up to Real Time Run, or calibration hindcast run (before 2013)
Init WOA09= initialisation with World Ocean Atlas climatology

II.2. Incidents in the course of OND 2014

No special event to report for this quarter.

III Summary of the availability and quality control of the input data

III.1. Observations available for data assimilation

III.1.1. In situ observations of T/S profiles

System	PSY3V3R3	PSY4V2R2	PSY2V4R4
Min/max number of T profiles per DA cycle	2600/3200	2600/3500	500/800
Min/max number of S profiles per DA cycle	2000/2500	2000/2500	400/600

Table 2: minimum and maximum number of observations (orders of magnitude of vertical profiles) of subsurface temperature and salinity assimilated weekly in OND 2014 by the Mercator Ocean monitoring and forecasting systems.

The maximum number of in situ observations is displayed in Table 2. It is unchanged with respect to the previous quarter.

III.1.2. Sea Surface Temperature

System	PSY3V3R3	PSY4V2R2	PSY2V4R42
Min/max number (in 10^3) of SST observations	135/144	137/146	26/27

Table 3: minimum and maximum number (orders of magnitude in thousands) of SST observations (from Reynolds AVHRR ¼°) assimilated weekly in OND 2014 by the Mercator Ocean monitoring and forecasting systems.

In the Atlantic (PSY2) the number of assimilated SST observations decreases with the increase of Arctic sea ice cover from January to March.

III.1.3. Sea level anomalies along track

As shown in Table 4 the data assimilated this OND 2014 season come from AltiKa, Jason 2, Cryosat 2 and HY-2A.

system	PSY3V3R3	PSY4V2R2	PSY2V4R4
Min/max number (in 103) of Jason 2 SLA observations	161/174	161/175	29/31
Min/max number (in 103) of HY-2A SLA observations	45/154	45/155	8/29
Min/max number (in 103) of AltiKa SLA observations	112/161	113/162	24/31
Min/max number (in 103) of Cryosat 2 SLA observations	141/163	142/165	27/32

Table 4: minimum and maximum number (orders of magnitude in thousands) of SLA observations from AltiKa, Jason 2, Cryosat 2 and HY-2A assimilated weekly in OND 2014 by the Mercator Ocean monitoring and forecasting systems.

III.2. Observations available for validation

Both observational data and statistical combinations of observations are used for the real time validation of the products:

- T/S profiles from MyOcean
- OSTIA SST from MyOcean
- Arctic sea ice concentration and drift from CERSAT
- SURCOUF surface currents from CLS
- ARMOR-3D 3D temperature and salinity fields from CLS
- Drifters velocities from Météo-France reprocessed by CLS
- Tide gauges from CLS
- Chlorophyll-a concentrations daily L3 and monthly L4 maps from MyOcean

All products were available in real time during the OND 2014 season, except tropical moorings from 29/11 to 09/12 and from 23/12 to 07/01/2015. All profiles have been retrieved then and the delays had no significant impact on the Mercator Ocean production and validation procedure.
Grodsky et al (GRL, May 2011) show that drifters' velocities overestimate current velocities in regions and periods of strong winds due to undetected undrogued drifters. This information is taken into account for comparisons with Mercator Ocean currents.

IV Information on the large scale climatic conditions

Mercator Ocean participates in the monthly seasonal forecast expertise at Météo France. This chapter summarizes the state of the ocean and atmosphere during the OND 2014 season, as discussed in the "Bulletin Climatique Global" of Météo France.

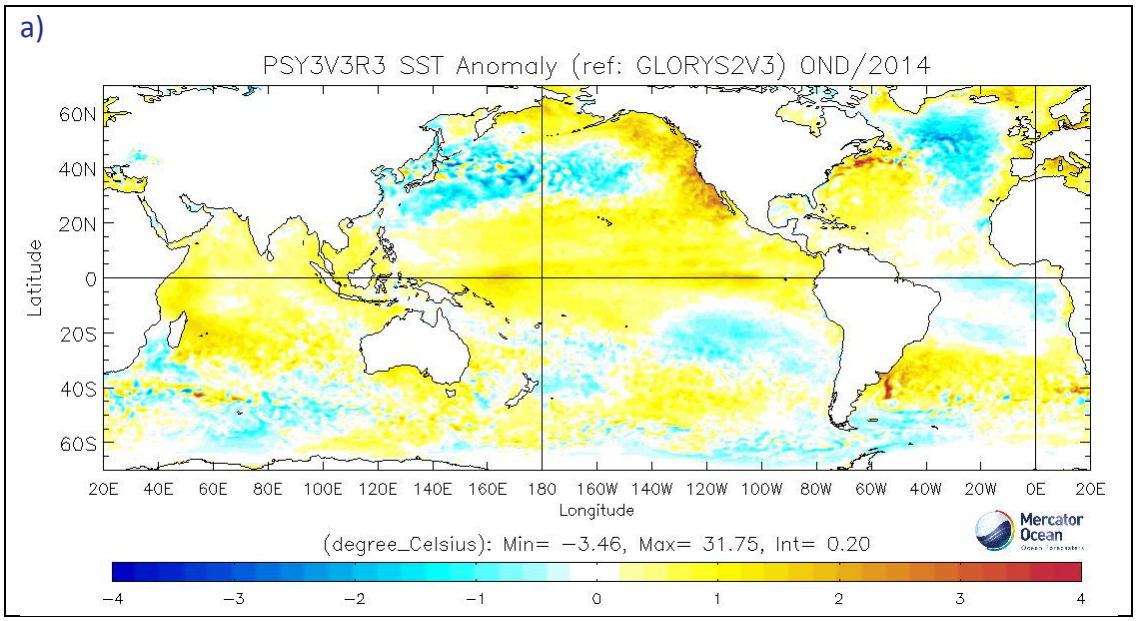

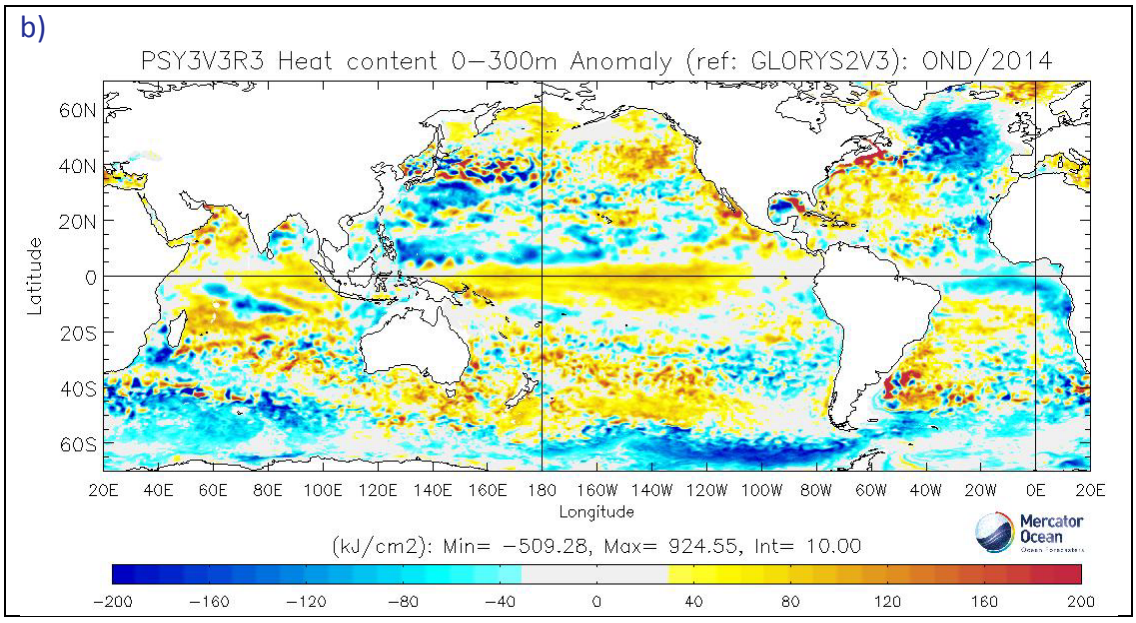

Figure 2: Seasonal OND 2014 temperature anomalies with respect to GLORYS2V3 climatology (1993-2011). (a): SST anomaly (°C) at the global scale from the 1/4° ocean monitoring and forecasting system PSY3V3R3. (b): heat content anomaly ($\rho_0 C_p \Delta T$, with constant ρ_0=1020 kg/m3) from the surface to 300m.

In the tropical Pacific, the ENSO conditions were neutral. The equatorial pacific is slightly warmer than the GLORYS2V3 climatology, as well as most of the Tropical Indian Ocean and the Indonesian throughflow. As can be seen in Figure 3, a downwelling Kelvin wave has propagated in subsurface, and temperature anomalies up to 3°C can be diagnosed on average over OND 2014 near 150m in the central Tropical pacific.

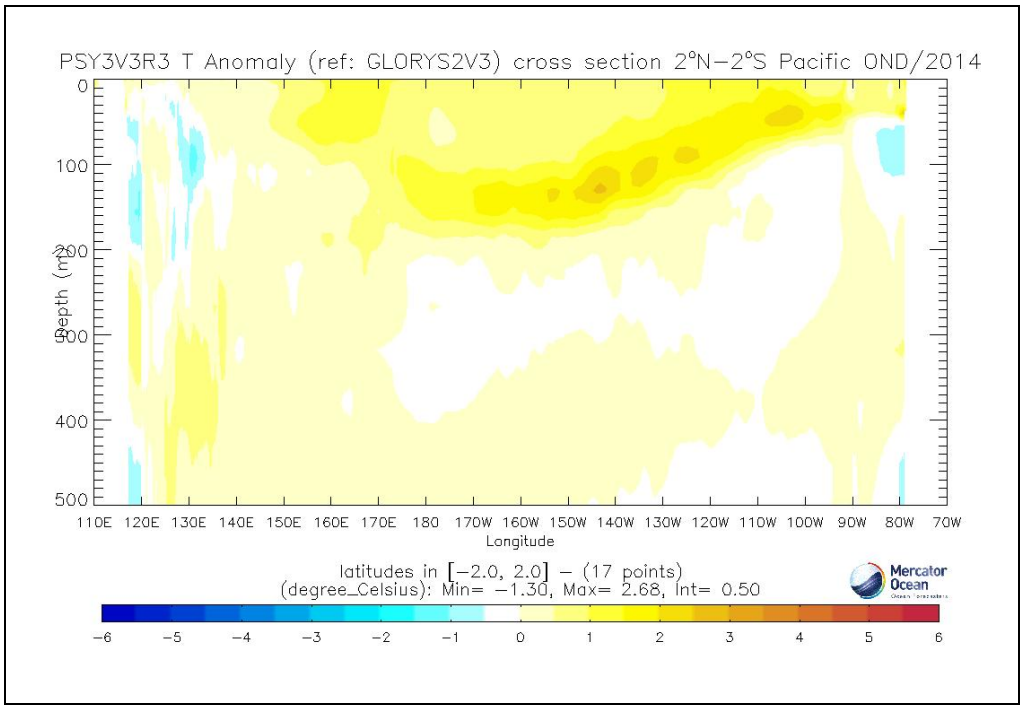

Figure 3: Seasonal OND 2014 temperature anomaly (°C) with respect to GLORYS2V3 climatology (1993-2011), vertical section 2°S-2°N mean, Pacific Ocean, PSY3V3R3.

The cold SST anomaly in the North Pacific surrounded by warm anomalies along the west coast of the US is linked with the persistent positive phase of the Pacific Decadal Oscillation[3] in 2014. In the Norway Sea the persisting Scandinavian blocking as given rise to warm SST anomalies. In December the positive phase of the North Atlantic Oscillation dominates the atmospheric circulation, strengthening the warm anomaly in the subtropical gyre, and the cold anomaly in the centre of the basin. Note a cold SST anomaly in the outflow of the Mozambique Channel that can be due to the late start of the South African rainy season in December.

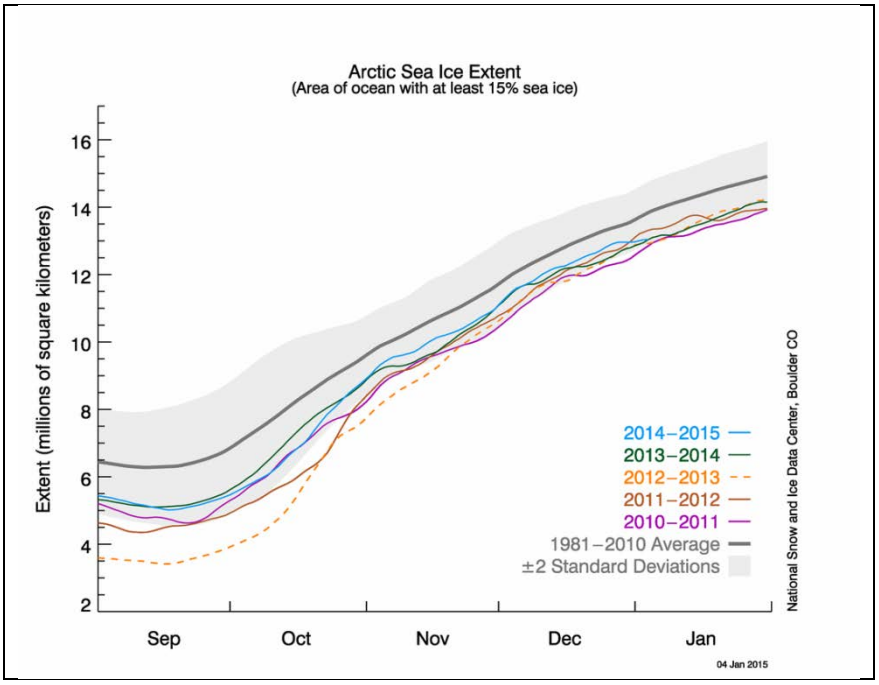

Figure 4 : Arctic sea ice extent from the NSIDC, available at http://nsidc.org/arcticseaicenews

As can be seen in Figure 4, the Arctic sea ice extent in OND 2014 is within the envelope of the last 30 years records of sea ice extent.

V Accuracy of the products

V.1. Data assimilation performance

V.1.1. Sea surface height

V.1.1.1. Basin scale statistics (GODAE metrics)

[3]http://www.climate.gov/news-features/understanding-climate/2013-state-climate-sea-surface-temperature

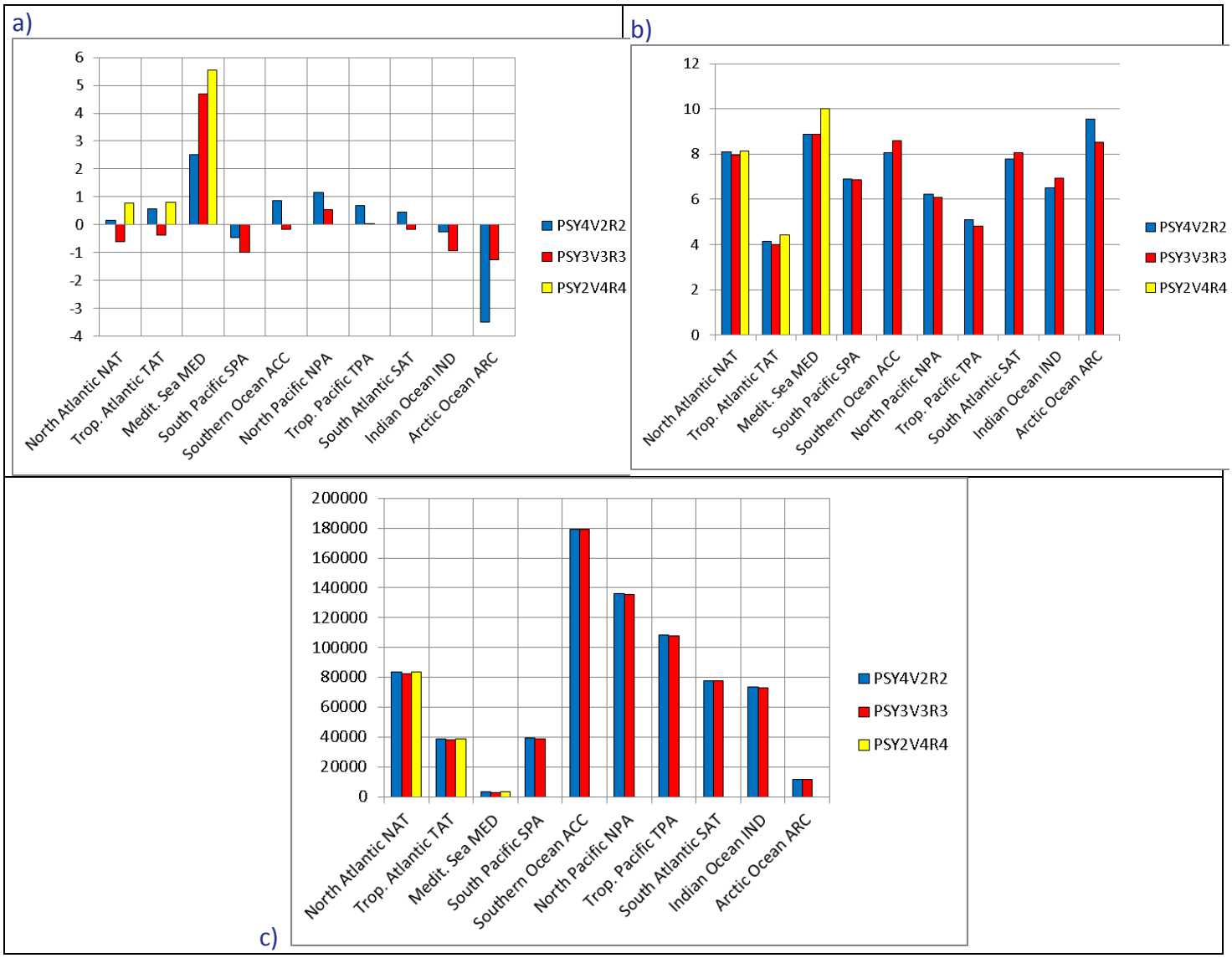

Figure 5 : Comparison between SLA data assimilation scores (a: average misfit in cm, b: RMS misfit in cm, c: number of observations) for all available Mercator Ocean systems in OND 2014. The scores are averaged for all available satellite along track data (Saral/altiKa, Jason 2, Cryosat 2). For each region the bars refer to PSY2V4R4 (yellow), PSY3V3R3 (red), PSY4V2R2 (blue).

SLA assimilation scores for PSY4, PSY3, and PSY2 in OND 2014 are displayed in Figure 5. The different systems reach similar levels of performance on average. The basin scale SLA bias does not exceed 2 cm except in the Arctic in PSY4 where it reaches 3 cm (Figure 5 a), and in the Mediterranean Sea where PSY4 is slightly greater than 2cm and PSY3 with PSY2 reach 5cm . The Arctic SSH undergoes large uncertainties (MSSH, measurement errors, sea ice limit). In the Mediterranean Sea this quarter, the high resolution 1/12° global system (PSY4) is less biased than the others. PSY4 is less biased than the other systems in the Atlantic. The three systems have consistent RMS errors. The RMS error (Figure 5 b) is of the order of 9 cm in the Mediterranean Sea and in the Arctic, 8cm in the Atlantic and in the Southern Oceans. It is of the order of 5-7 cm, the Indian and Pacific oceans, and it is close to 4-5 cm in the Tropical Atlantic and Tropical Pacific oceans. The error amplitude is proportional to the region's internal variability.

V.1.1.2. North Atlantic Ocean and Mediterranean Sea in all systems

The SLA assimilation scores for PSY4, PSY3, and PSY2 in OND 2014 are displayed for sub-regions of the Tropical and North Atlantic Ocean in Figure 6. The different systems reach identical levels of performance on average: except for three regions (Iceland, North Madeira and Yoyo Pomme) the biases are less than 2 cm during this season. The largest biases (4cm) appear in PSY4 and PSY2, in small regions assimilating few data. Note that consistently with Figure 5 results. Part of the biases can be attributed to local errors in the current mean dynamical topography (MDT).

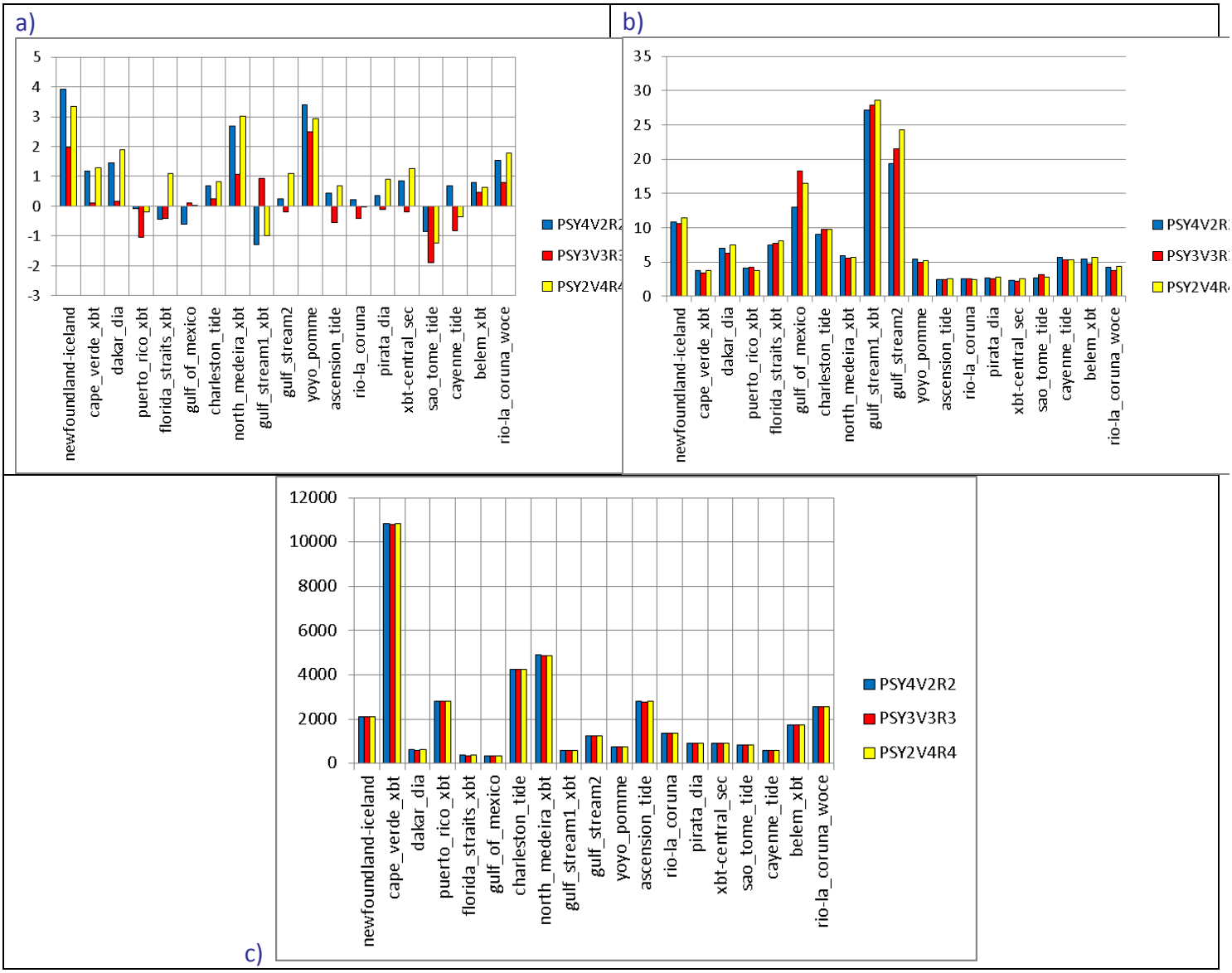

Figure 6: Comparison between SLA data assimilation scores (a: average misfit in cm, b: RMS misfit in cm, c: number of observations) for all available Mercator Ocean systems in OND 2014 in sub-regions of the Tropical Atlantic (TAT) and North Atlantic (NAT). The scores are averaged for all available satellite along track data (Jason 1 G, Jason 2, Cryosat 2). For each region the bars refer respectively to PSY2V4R4 (yellow), PSY3V3R3 (red), and PSY4V2R2 (blue).

The RMS errors are almost identical in all systems, and stay below 10 cm in most regions, except regions of high mesoscale variability (Gulf Stream, Gulf of Mexico). This OND 2014 season, the RMS error in the Gulf Stream 1 region is larger in PSY2 and lower in PSY4. PSY4 biases are small but positive in many regions, meaning that PSY4 is slightly lower than the observations over these regions. PSY2 exhibits positive biases on average where PSY3 seems to be more balanced than the previous quarter (consistently with Figure 5).

In the eastern Mediterranean Sea (Figure 7), significant positive biases (the model is lower than the observations) appear this autumn. PSY2 displays biases of 4 to 11 cm, while the global systems PSY3 and PSY4 present smaller biases of 1 to 8 cm. A bias of 11 cm is present in PSY2 in the Aegean Sea (it was nearly 10 cm last quarter). The Mediterranean sub-regions are circled by coasts, and consequently few observations are assimilated. Figure 7 c gives the number of observations taken into account by the system, but the observation error that is applied reduces strongly the influence of observations within a 50 km distance of the coast.

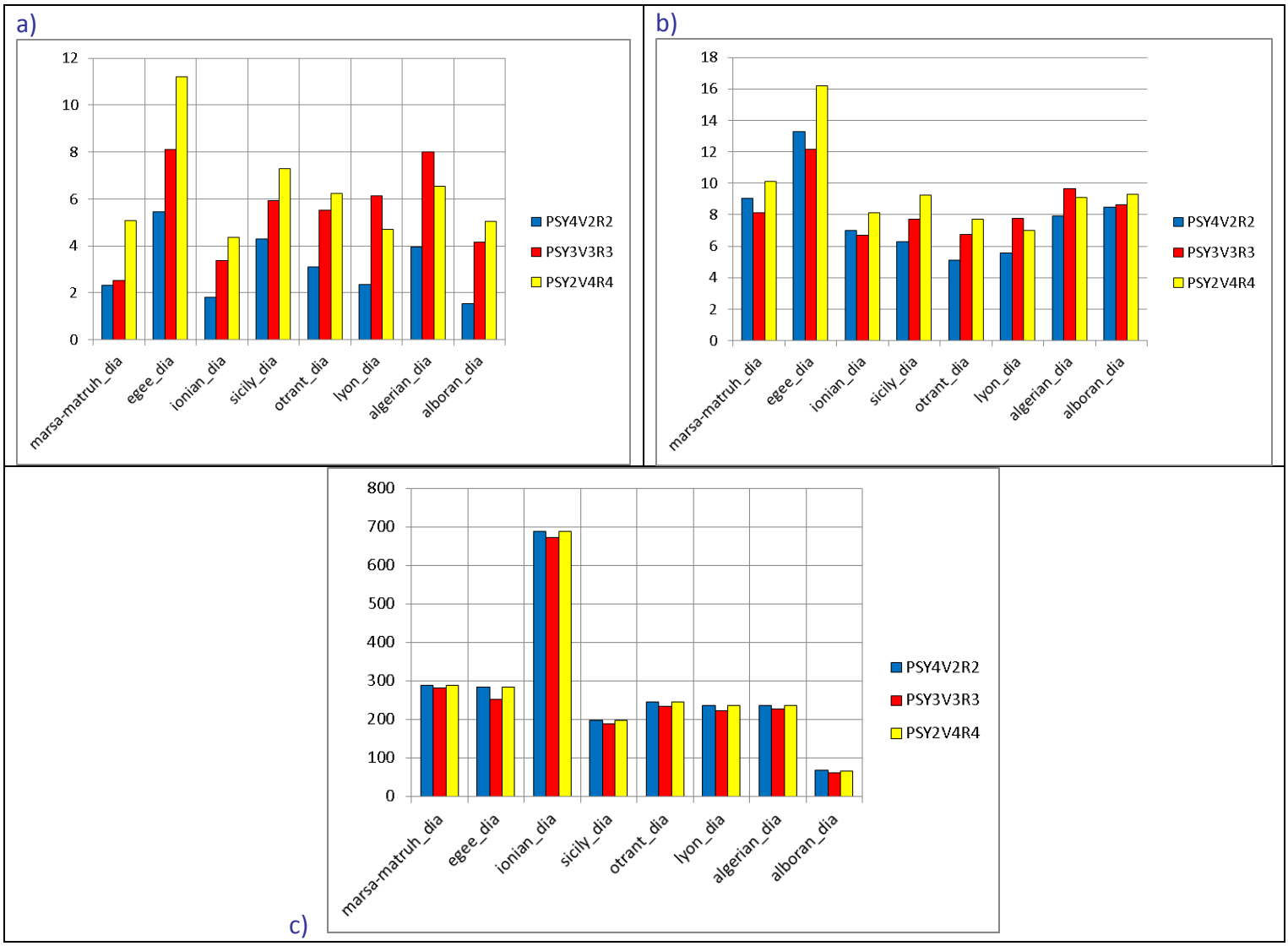

Figure 7: Comparison between SLA data assimilation scores (a: average misfit in cm, b: RMS misfit in cm, c: number of observations) for all available Mercator Ocean systems in OND 2014 in the Mediterranean Sea MED sub-regions: PSY2V4R4 (yellow), PSY3V3R3 (red) and PSY4V2R2 (blue). The scores are averaged for all available satellite along track data (Jason 1 G, Jason 2, Cryosat 2). See annex B for geographical location of regions.

One can also note that the variability in the Aegean Sea is difficult to model because of the presence of many islands. PSY4 may perform better in this region due to the presence of the Black sea in the global configuration PSY4, which is not present in PSY2.

Except in the Aegean Sea, and in the Alboran Sea where very few observations are available, the RMS of the innovation (misfit) is generally less than 7 cm for all systems in OND 2014.

V.1.1.3. Performance at global scale in PSY3 (1/4°) and PSY4 (1/12°)

Figure 8: Comparison between SLA data assimilation scores (a: average misfit in cm, b: RMS misfit in cm, c: number of observations) for all available global Mercator Ocean systems in OND 2014 in sub-regions of the SAT, IND, NPA, SPA, TPA, and ACC basins: PSY3V3R3 (red) and PSY4V2R2 (blue). The scores are averaged for all available along track satellite data (Jason 1 G, Jason 2, Cryosat 2). The geographical location of regions is displayed in annex B.

As can be seen in Figure 8 the performance of intermediate resolution global PSY3 and the performance of high resolution global PSY4 in terms of SLA assimilation are of the same order of magnitude. A small positive bias (less than 3 cm) is present in many regions in PSY4. A strong bias of around 10 cm persists in the “Nino 5” box centred on the Banda Sea in Indonesia, which corresponds to a MDT problem. Except the Nino 5 region, the RMS error reaches its highest values in the Agulhas current where the variability is high.

Other regions with high variability, especially in the ACC region but also in eastern Australia, consistently display RMS errors of more than 8 cm.

V.1.2. Sea surface temperature

V.1.2.1. Basin scale statistics (GODAE metrics)

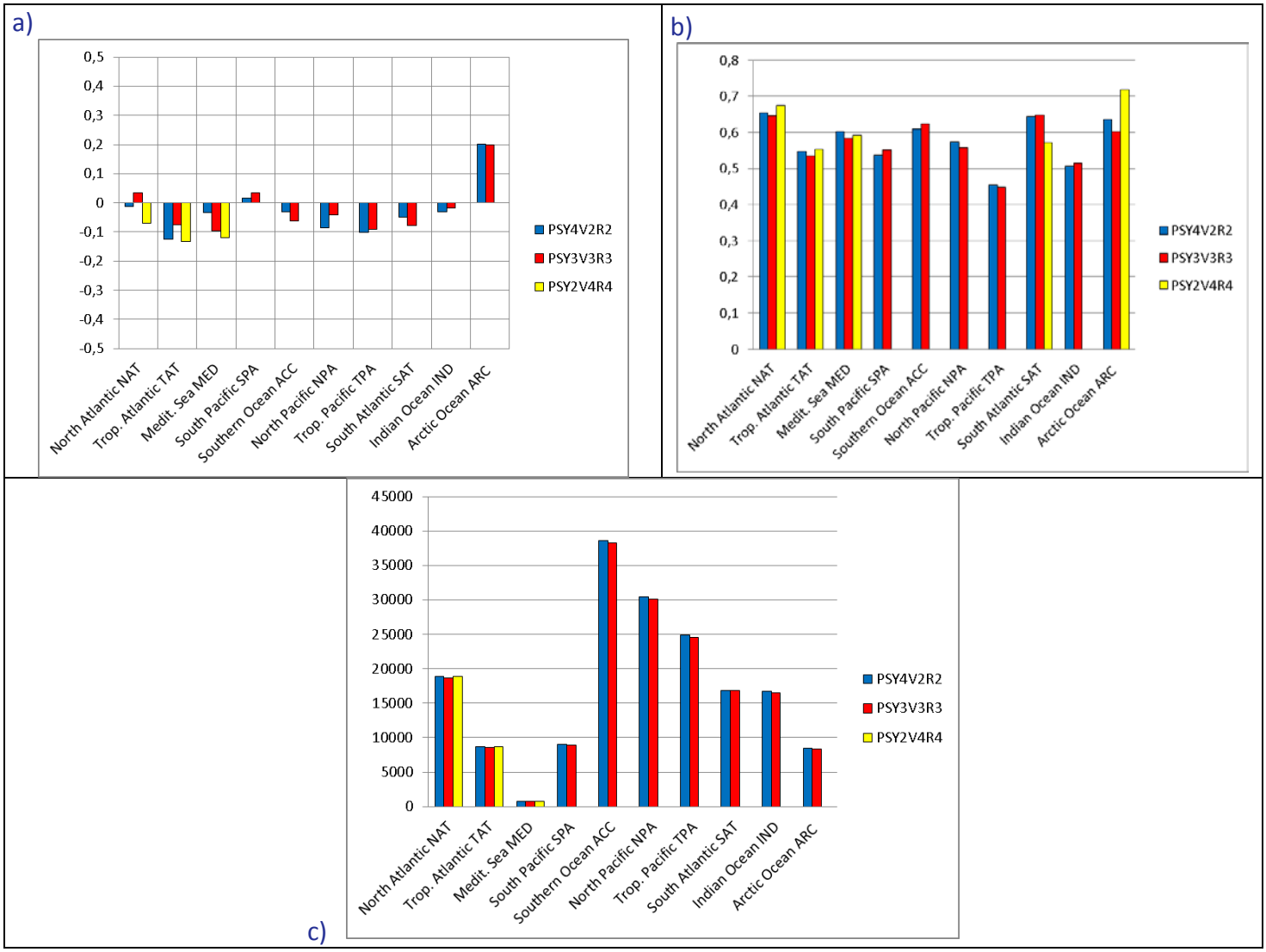

Figure 9: Comparison between Reynolds ¼°AVHRR-data assimilation scores (a: average misfit in °C, b: RMS misfit in °C, c: number of observations) for all available Mercator Ocean systems in OND 2014: PSY4V2R2 (blue), PSY3V3R3 (red), and PSY2V4R4 (yellow).

This OND season, a warm bias of 0.1 to 0.2 °C persists in all systems on average over the Tropical Atlantic and Pacific (Figure 9). On the contrary, the Arctic Ocean is colder (0.2 °C) than the observations. It is known that not enough Atlantic (warm) waters enter the Arctic in both PSY3 and PSY4 and during the Summer season there is too much sea ice melting in the centre of the Arctic (see QUOVADIS 18).
The Mediterranean is warmer than the observations on average over the basin (0.1°C). The RMS error is lower than 0.7 °C except in the Arctic Ocean due to the strong biases in marginal zones.

V.1.2.2. North and Tropical Atlantic Ocean and Mediterranean Sea

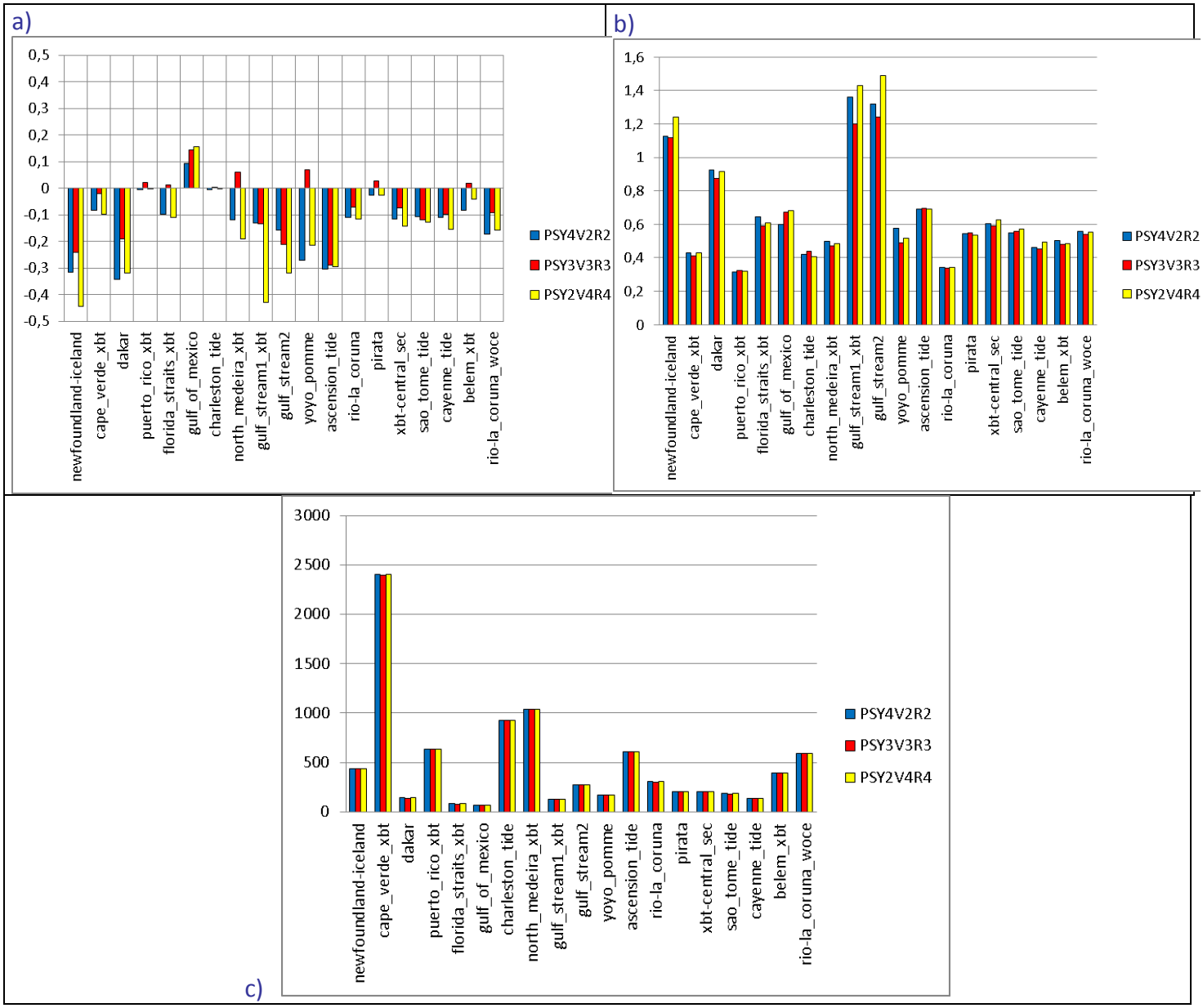

Figure 10: Comparison between Reynolds ¼°AVHRR SST data assimilation scores (a: average misfit in °C, b: RMS misfit in °C, c: number of observations) for all available Mercator Ocean systems in OND 2014 in sub-regions of the Tropical Atlantic (TAT) and of the North Atlantic (NAT): PSY4V2R2 (blue), PSY3V3R3 (red) and PSY2V4R4 (yellow). The geographical location of regions is displayed in annex B.

In the Atlantic the three systems display consistent regional behaviours in terms of SST bias as illustrated in Figure 10. In most regions the bias stays below 0.3 °C. A warm bias of around 0.3 to 0.5°C is diagnosed in the Tropical Atlantic in the Dakar region due to an underestimation of the upwelling by all systems. PSY2 display strong warm biases in Newfoundland and Gulf Stream region. Note that as for SLA, prescribed SST errors are higher within 50km off the coast. The RMS error reaches more than 1.5°C in the Gulf Stream regions, and in the Newfoundland Iceland region where it reaches 1.2°C this season.

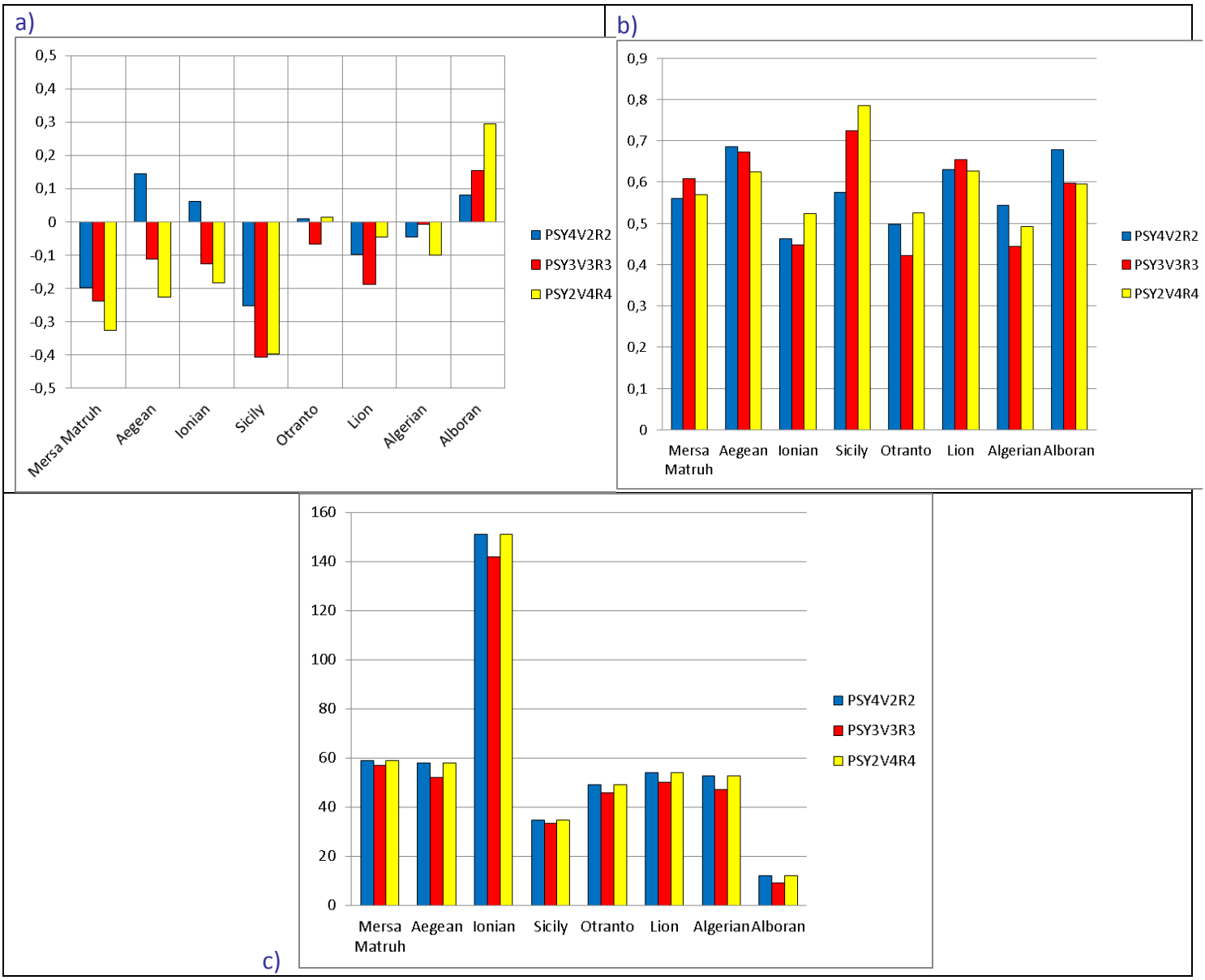

Figure 11: Comparison between Reynolds ¼° AVHRR SST data assimilation scores (a: average misfit in °C, b: RMS misfit in °C, c: number of observations) for all available Mercator Ocean systems in OND 2014 in the Mediterranean Sea: PSY4V2R2 (blue), PSY3V3R3 (red) and PSY2V4R4 (yellow). The geographical location of regions is displayed in annex B.

This season, the Mediterranean regions are more strongly biased in Mersa Matruh and Sicily regions (up to 0.4°C Figure 11**)**. In the Aegan and Ionean Sea PSY3 and PSY4 display opposite bias (the Black Sea is present in PSY4 and not in PSY3 which can explain this result). The RMS error is generally of the order of 0.5-0.8°. As in SLA, the performance of the systems is lower in the Aegean Sea. Errors are also higher in the Alboran Sea, Aegean and Siciliy regions but one can note that not many observations are available in this small region. (see **Figure 11**). The low rms error in the Ionian region is associated with a high number of observations.

V.1.2.3. Performance at global scale in PSY3 (1/4°) and PSY4 (1/12°)

Figure 12: Comparison between Reynolds ¼° AVHRR SST data assimilation scores (a: average misfit in °C, b: RMS misfit in °C, c: number of observations) for all available global Mercator Ocean systems in OND 2014 in the SAT, NPA, TPA, SPA, IND and ACC basins: PSY3V3R3 (red) and PSY4V2R2 (blue). See annex B for geographical location of regions.

The global products exhibit a warm surface bias in most regions this OND 2014 season (Figure 12), of magnitude 0.1°C to 0.4°C. This warm bias is present in (small) coastal regions: in the cold waters of the California current, in the Peru upwelling or in the Angola upwelling but also in the Pacific Ocean especially in the Tropical Pacific Ocean (Niño boxes 5,6, 1-2). The strongest warm bias is diagnosed in the Nino 1-2 box probably with very few data near the coast. A cold bias (0.1°C) is diagnosed in the North Pacific region and in the Eastern Australia.

PSY3 and PSY4 exhibit the same levels of performance but the warm bias is generally stronger in PSY4 than in PSY3 by 0.05°C, and so is the RMS error, meaning that the variability is at least as well represented in PSY4 than in PSY3. The RMS error stands between 0.8 °C and 1°C in the tropical Pacific and in the Agulhas current and the Angola region. It stands between 0.4°C and 0.7°C in the other regions.

V.1.3. Temperature and salinity profiles

V.1.3.1. Methodology

All systems innovation (**observation – model first guess**) profiles from the **hindcast or "best analysis" week (J-14 to J-7)** are systematically inter-compared in all regions given in annex B. In the following, intercomparison results are shown on the main regions of interest for Mercator Ocean users in OND 2014. Some more regions are shown when interesting differences take place, or when the regional statistics illustrate the large scale behaviour of the systems.

V.1.3.1.1. Basin scale statistics (GODAE metrics)

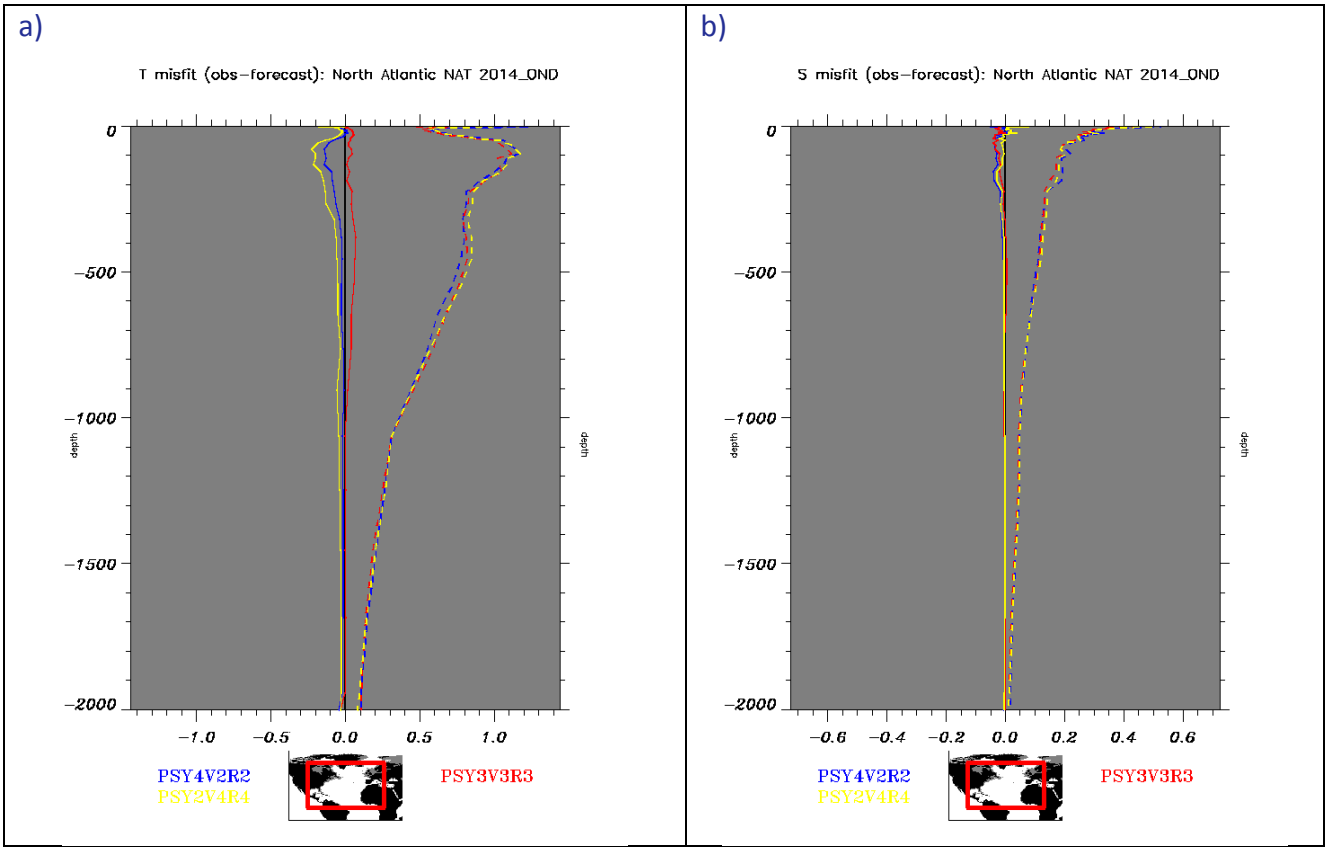

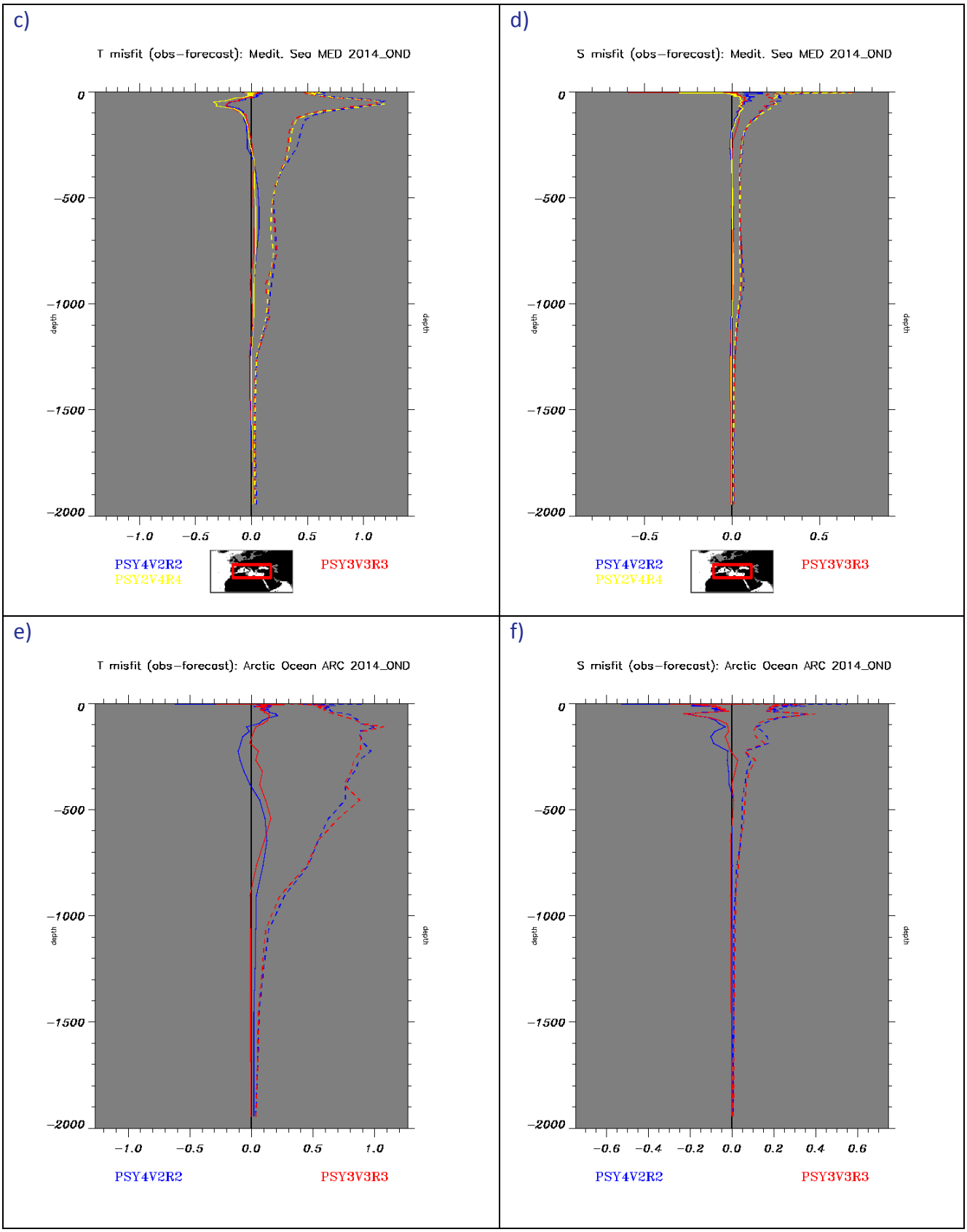

Figure 13: Profiles of OND 2014 innovations of temperature (°C, left column) and salinity (psu, right column), mean (solid line) and RMS (dashed line) for PSY3V3R3 (red), PSY2V4R4 (yellow) and PSY4V1R3 (blue) in the North Atlantic NAT (a and b), Mediterranean Sea MED (c and d) and Arctic Ocean ARC (e an fl, the region starts of north of 67°N). Basin masks are applied to keep only the main basin of interest (no Mediterranean in the Altantic NAT, no Black Sea in the Mediterranean MED, etc…).

On average over the **North Atlantic**, PSY4 and PSY2 display a **warm bias** from 50 m to 400 m that is not present in PSY3 (Figure 13). In the meantime, a slight salty bias of around 0.02 psu is diagnosed in PSY2 and PSY4 near 100m.

On average over the **Mediterranean Sea**, the three systems display a warm bias around 100m, and a slight cold bias between 500 and 800m, they appear too fresh between 50 and 200m. PSY2 displays the best performance in salinity and PSY4 in temperature.

In the Arctic, a cold bias is diagnosed in both PSY3 and PSY4 near the surface up to 100m (0.2°C), and then we have a warm bias between 150 and 400m (0.1°C) and again a cold bias between 500 and 900m (0.2°C). A salty bias of around 0.2 psu can be found at the surface and decreases with depth until 200m. Theses error profiles show a bad stratification of the systems in this region.

On average over **the Tropical Atlantic basin** PSY4 and PSY2 exhibit warm (0.3°C) and salty (around 0.05 psu) biases in the 50-300m layer (Figure 14). No significant temperature or salinity biases appear underneath the surface layer. PSY4 (closely followed by PSY3) exhibits the best performance in this region. For PSY3, a small cold bias appears near the surface (0.1°C).

PSY3 is less biased than PSY4 in the **South Atlantic Basin**, where PSY4 is too warm in the 50-900 m layer. PSY3 is too salty near the surface and PSY4 is too salty in the subsurface near 200m.

In the **Indian Ocean,** PSY3 exhibits a cold bias (0.2°C near 100m and then 0.1 °C between 150 and 500m). PSY4 also exhibits just a small cold bias in the surface layer (0-100m). On average the subsurface layer (up to 200m) is slightly too salty for PSY4 and slightly too salty for PSY3 near the surface (0.02 psu). PSY4 exhibits the best performance in this region.

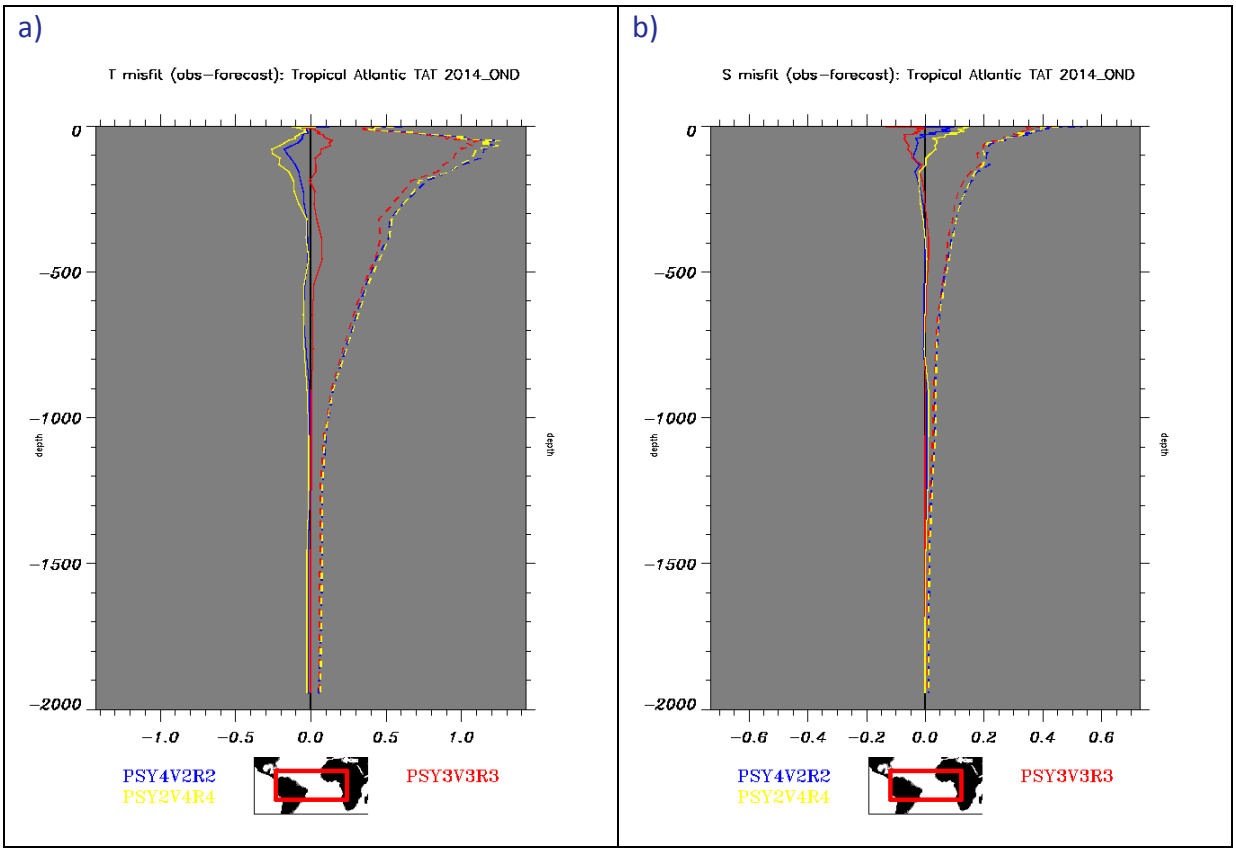

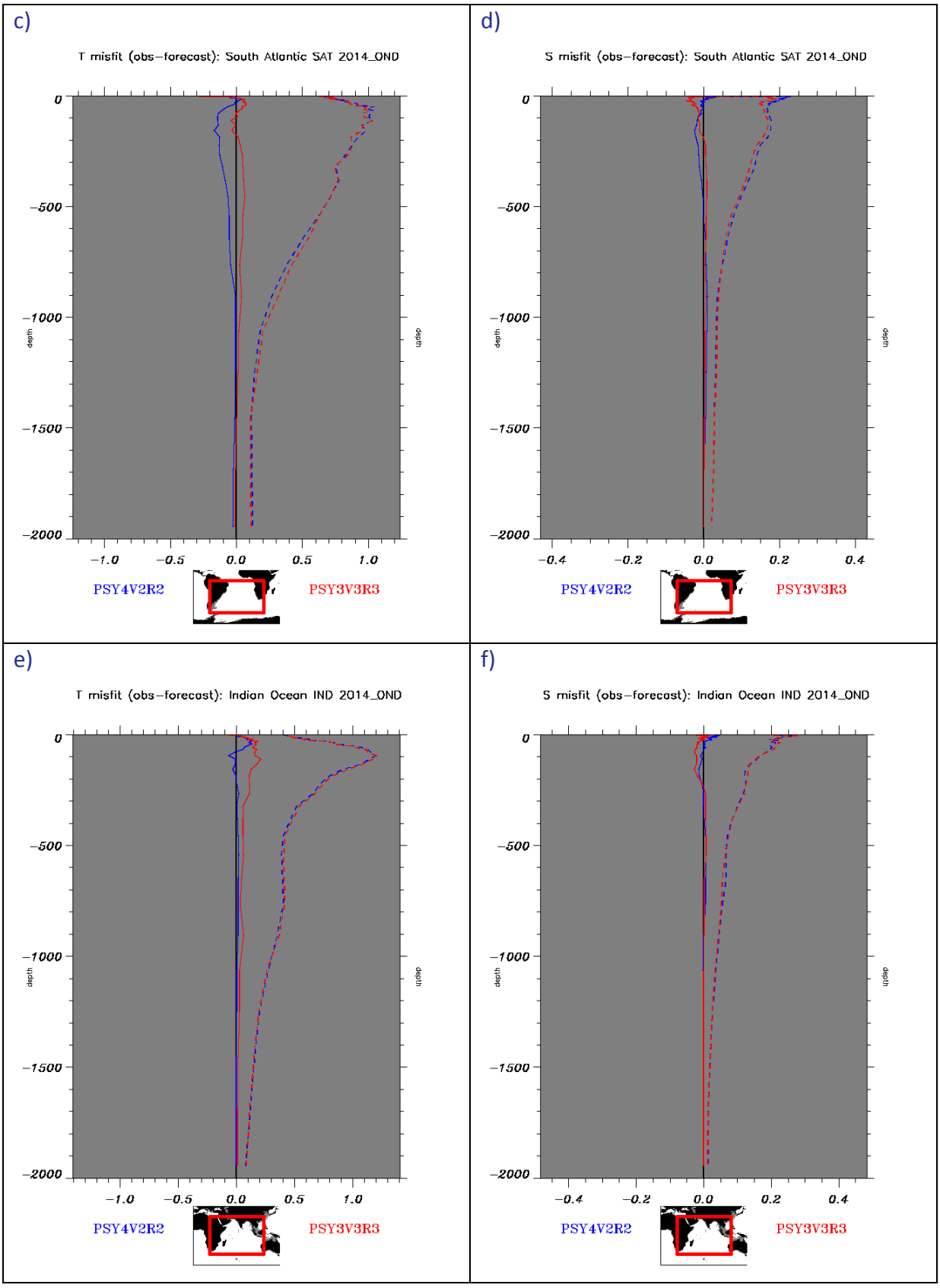

Figure 14: As Figure 13 in the Tropical Atlantic TAT (a and b), South Atlantic SAT (c and d) and Indian IND (e and f) basins.

On average over the **Pacific Ocean and the Tropical Pacific** (Figure 15), PSY4 is warmer (0.1 to 0.2 °C) than the observations (and than PSY3) from the surface to 800 m. On the contrary PSY3 is close to the observations and exhibits a small cold bias of around 0.1°C near 200m.

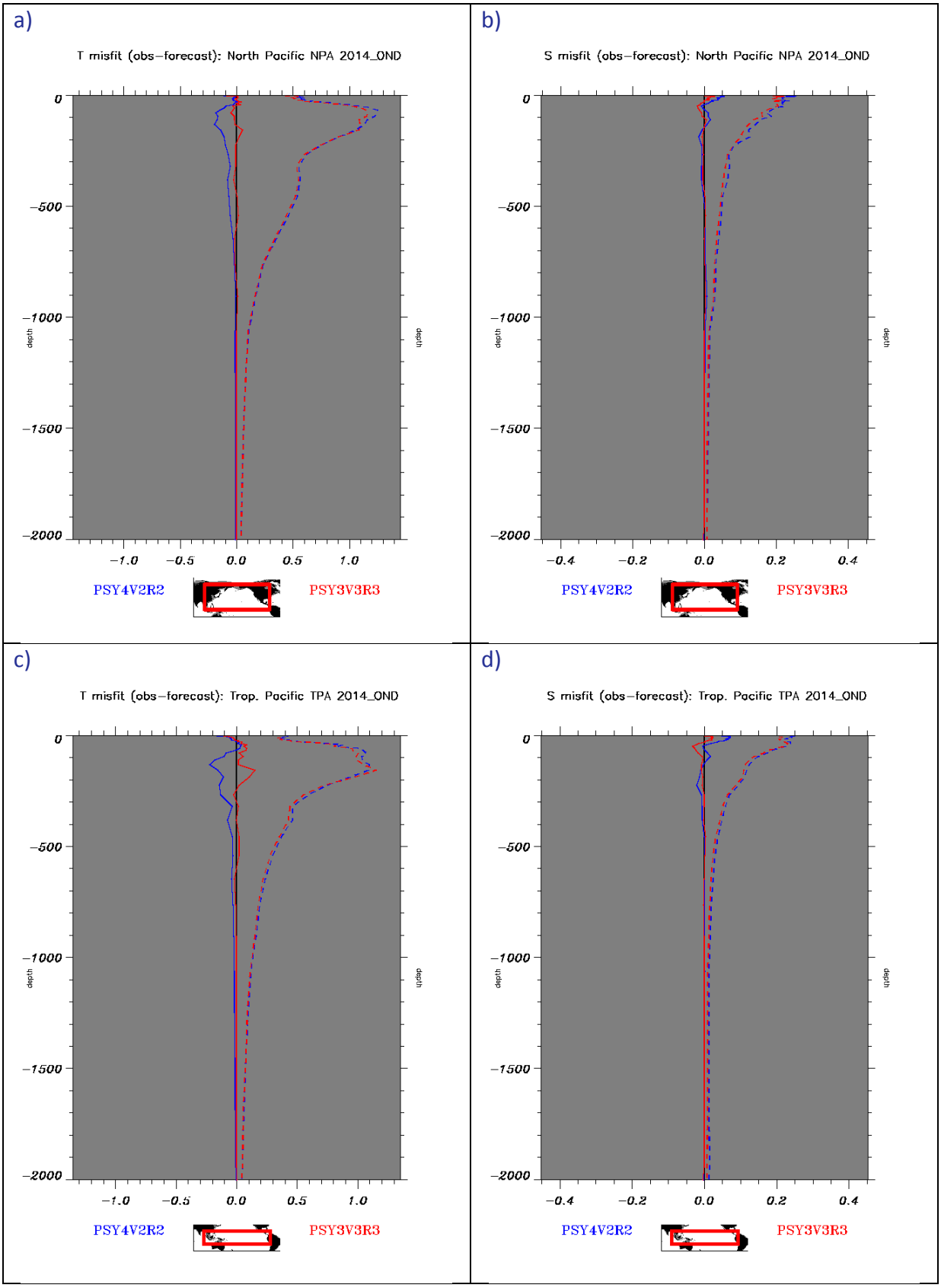

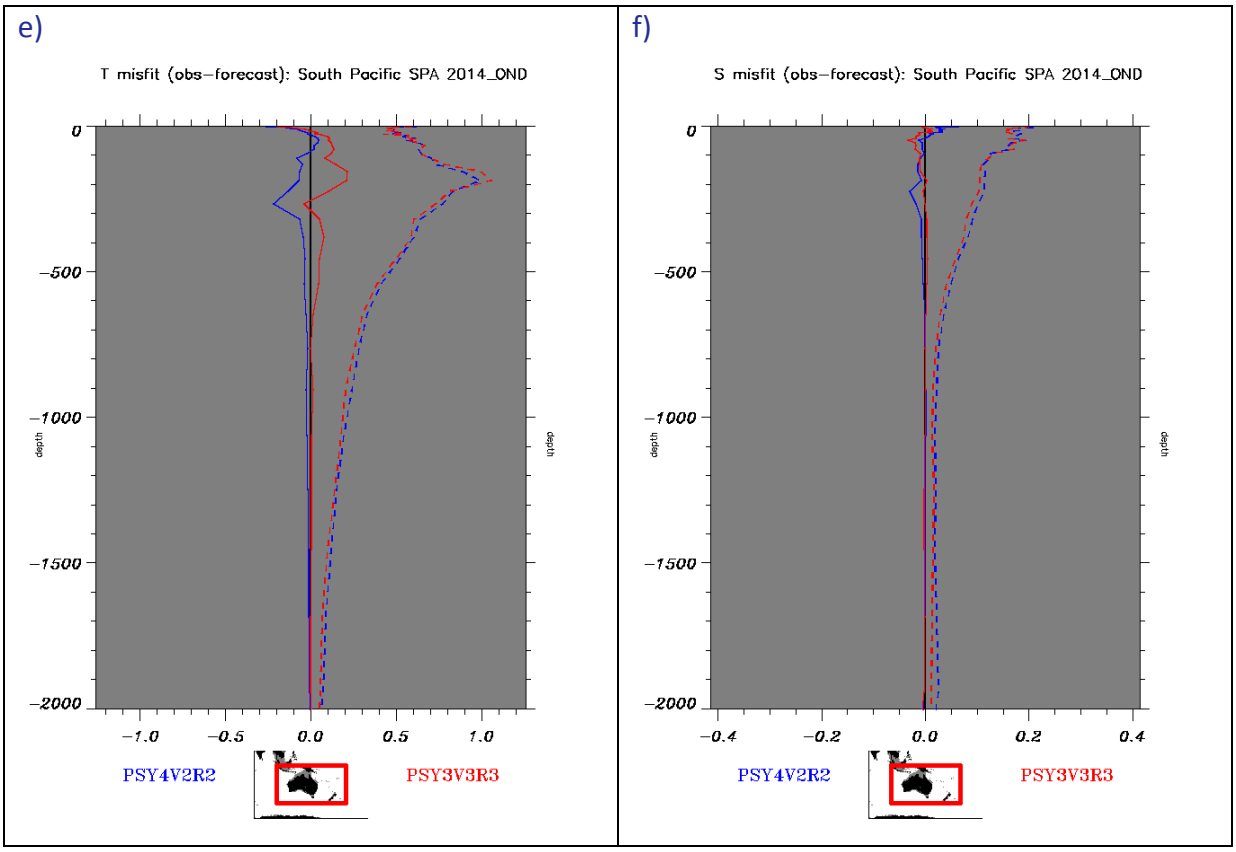

Figure 15: As Figure 13 in the North Pacific NPA (a and b), Tropical Pacific TPA (c and d) and South Pacific SPA (e and f).

For the **South Pacific Region**, in the 100-500m layer PSY4 exhibits a warm bias and PSY3 a cold bias as the same order (0.1 to 0.2°C).
For the three regions in Figure 15 these systems have the same salinity bias vertical structure with small amplitude (less than 0.05 psu, with a maximum fresh bias at the surface). The temperature and salinity RMS errors of PSY3 and PSY4 are identical while the bias is stronger in PSY4 which means that the variability is probably better represented in PSY4 than in PSY3.

In the Southern Ocean in Figure 16, a warm temperature bias is observed again in PSY4 (up to 0.2 °C) in the 100-1000m layer. PSY3 exhibits the best performance in this region with just a small warm bias (0.1 °C) between 100 and 200m. For the two systems the salinity is very close to the observations.

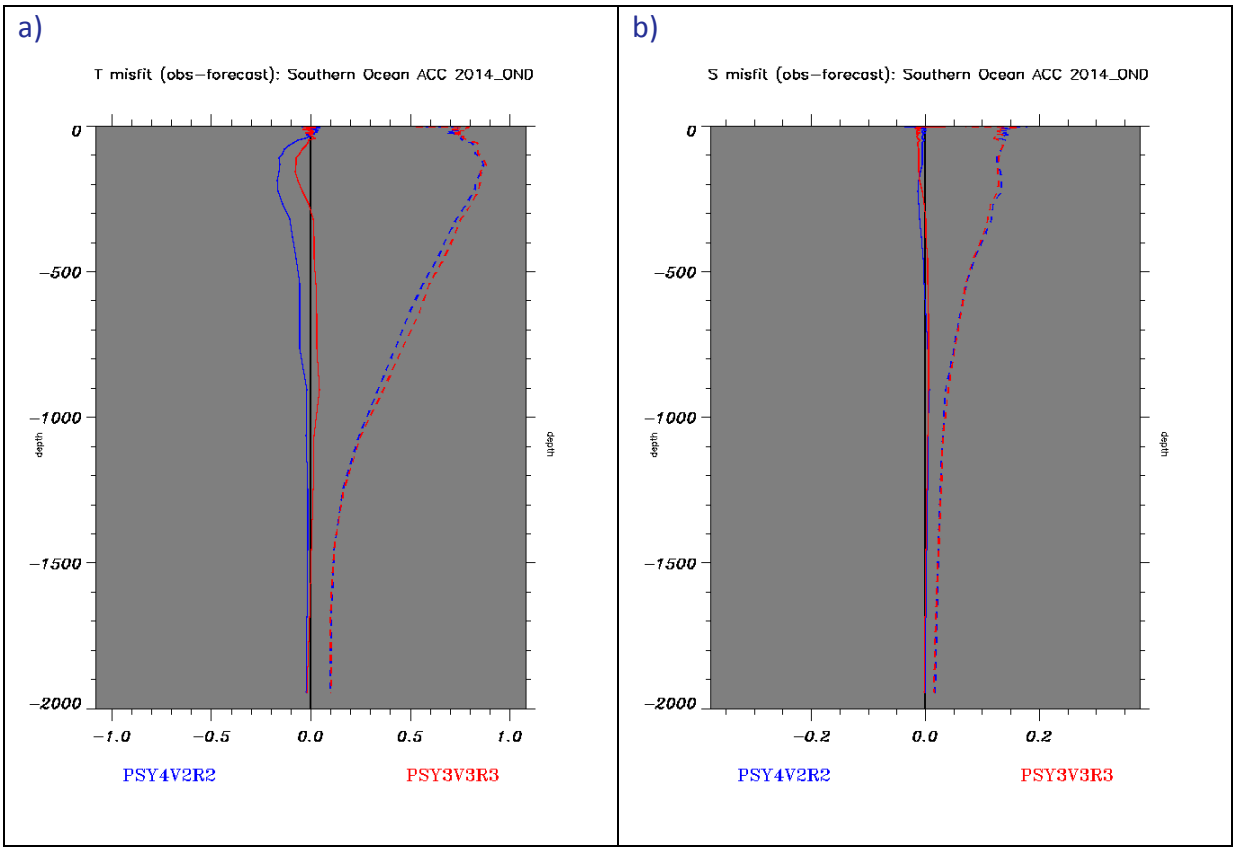

Figure 16: As Figure 13 in the ACC Southern Ocean basin (from 35°S).

V.1.3.1.2. Atlantic sub-regions

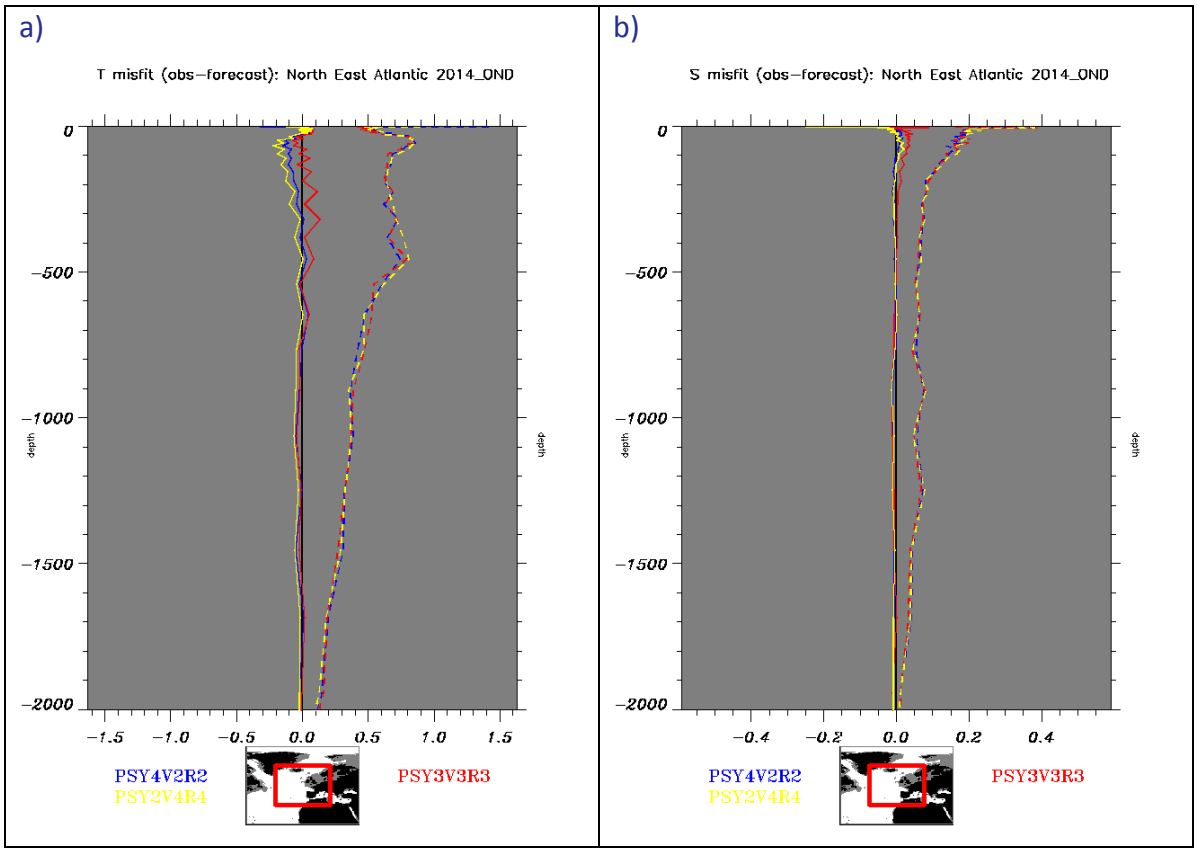

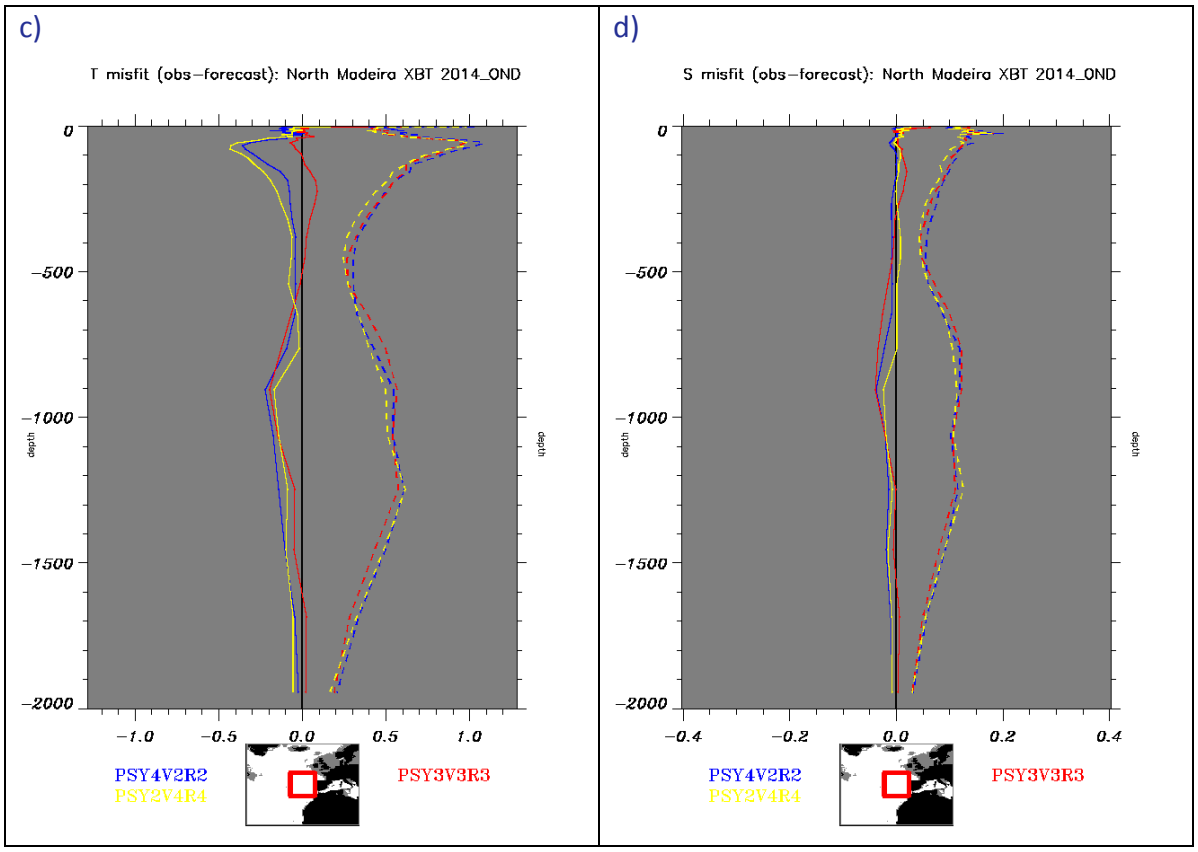

Figure 17: As Figure 13 in the North East Atlantic (IBI) and the North Madeira XBT regions.

As shown in Figure 17, in the **North East Atlantic Ocean** the RMS error appears very noisy and the high resolution systems are a little bit too warm (0.2 to 0.1°C) in the 100-500m layer.
For the high resolution systems PSY2 and PSY4 the signature of the **Mediterranean waters** is clear in the T and S RMS error (Figure 17 c and d). This quarter is characterized by the warm bias in both high resolution systems PSY2 and PSY4 in the 50-500 m layer. PSY3 on the contrary, exhibits a smaller cold bias in the same layer. All systems exhibit a warm bias near 1000m. PSY4 and PSY3 (in the North Madeira region) are more biased than PSY2 this OND season. In the Mediterranean water outflow the RMS error of PSY4 is higher than that of the other systems, which may be due to the ring off of Portugal (see description in previous QUOVADIS 17).

In sub-regions of the **Tropical Atlantic** (Figure 18), and in the **Gulf Stream** (Figure 19) the vertical structure of the biases is more complex. It reflects the underestimation of the upwelling in the Dakar region, and the errors in the vertical structure of the currents. In the Dakar region PSY3 exhibits the best performance I temperature for this OND quarter.

In the **Gulf of Mexico** the systems are too cold in the 0-500m layer and too fresh near 200m.
In the **Gulf Stream**, all systems are too warm (up to 1°C near 200m) and salty in the 0-800m layer. Underneath PSY4 is too cold and fresh until 1500m, while PSY4 is too cold from 800 to 1500m. PSY2 is the worst system in this region with a RMS error growing up to 1°C.

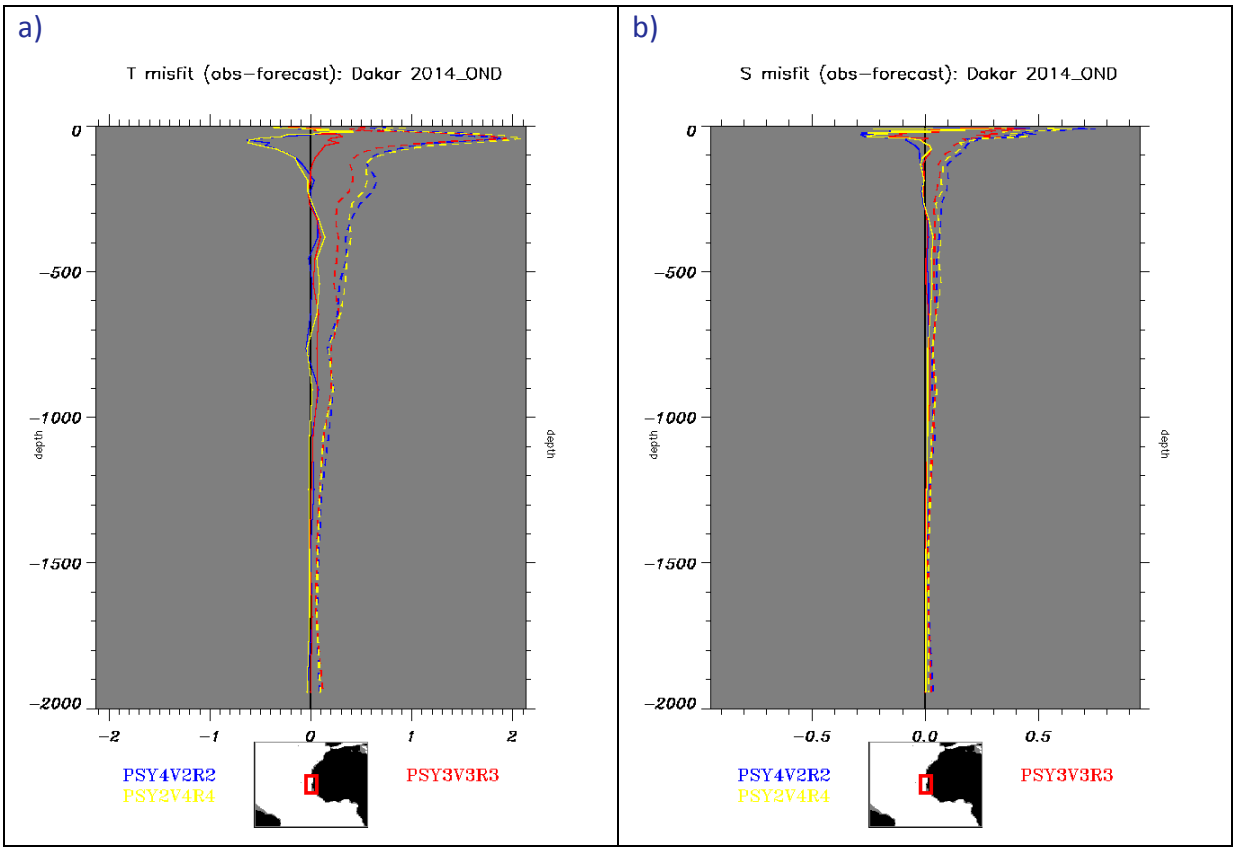

Figure 18: As Figure 13 in the Dakar region.

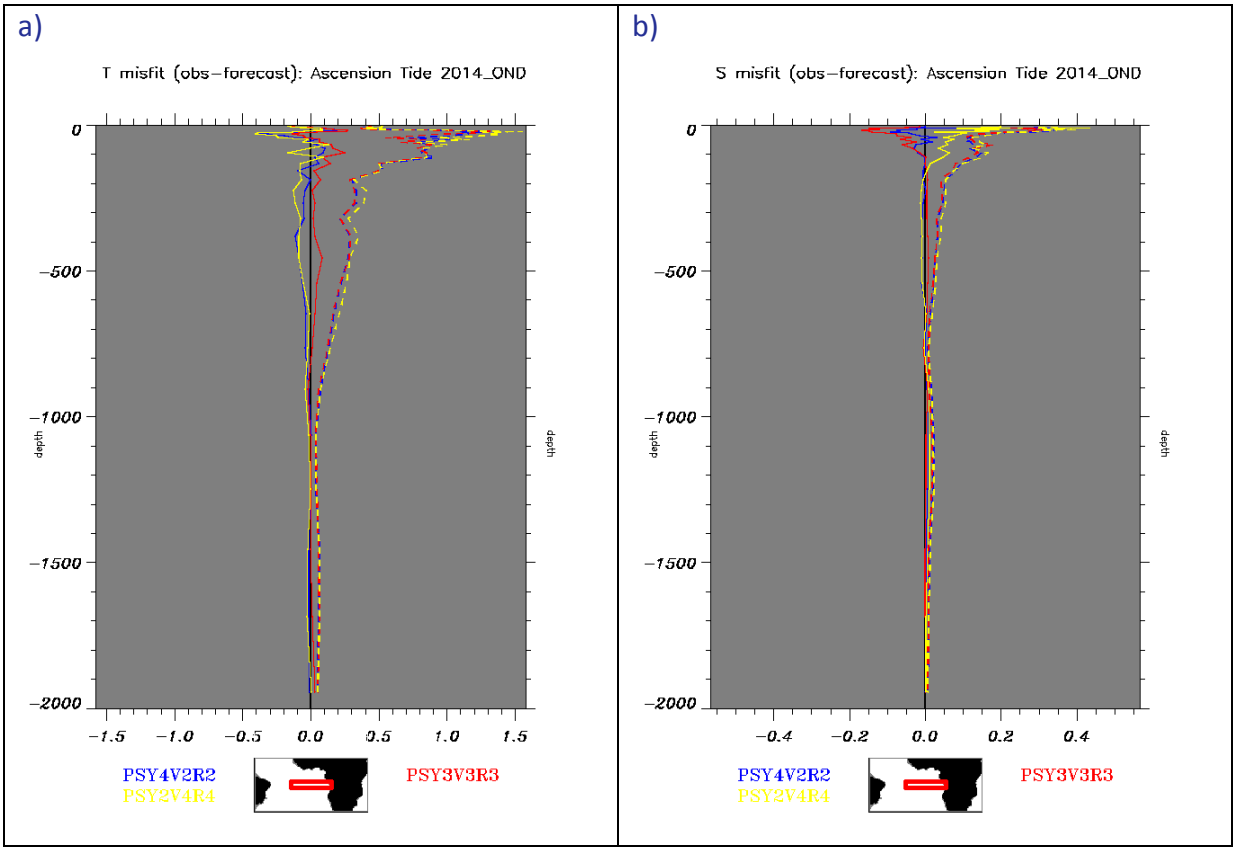

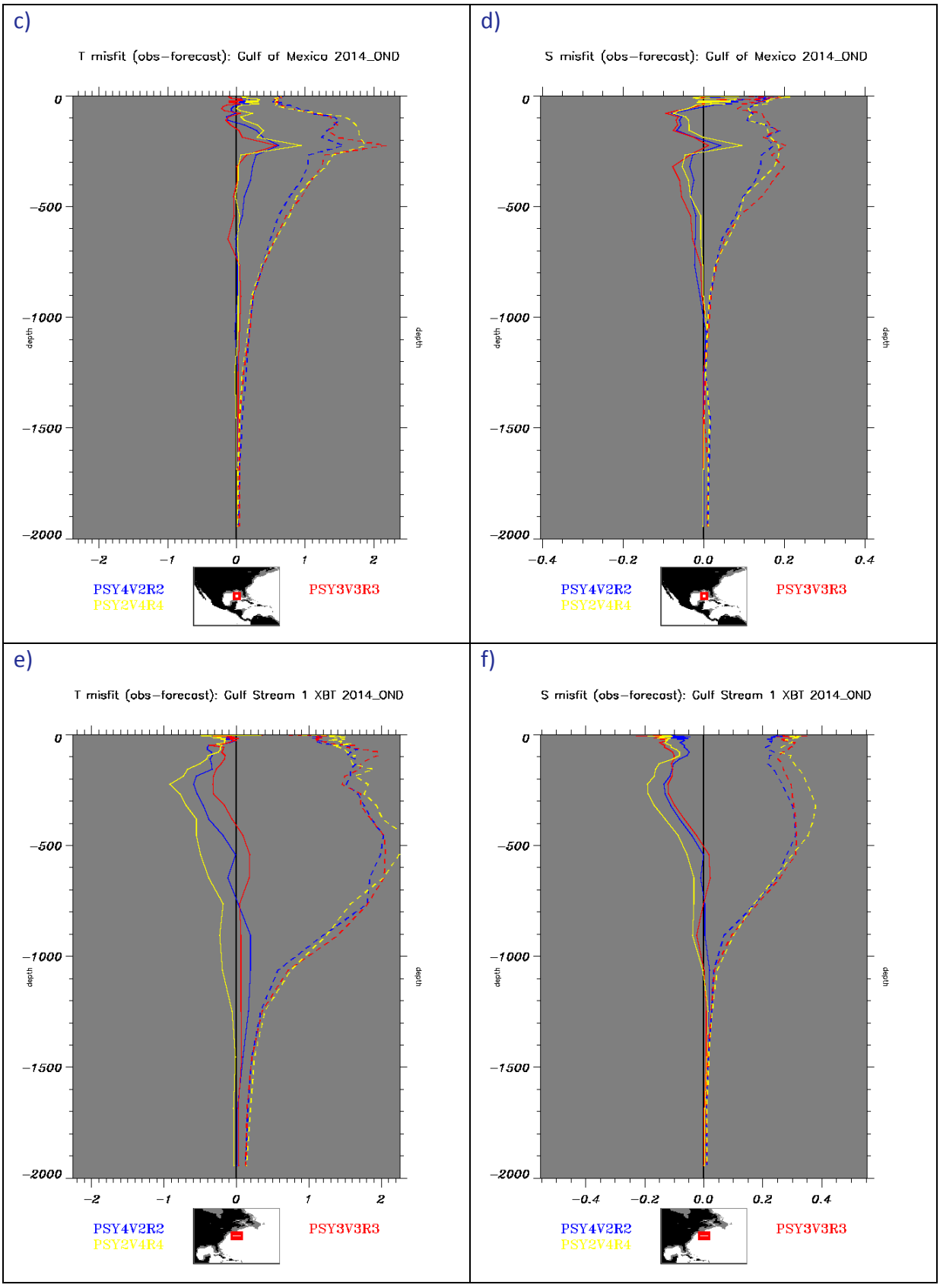

Figure 19: As Figure 13 in the Ascension tide (a and b), the Gulf of Mexico (c and d) and the Gulf Stream 1 regions (e and f)

However, one must keep in mind that the smallest sub-regions contain only a few data per assimilation cycle and that in this case the statistics may not be representative of the whole period.

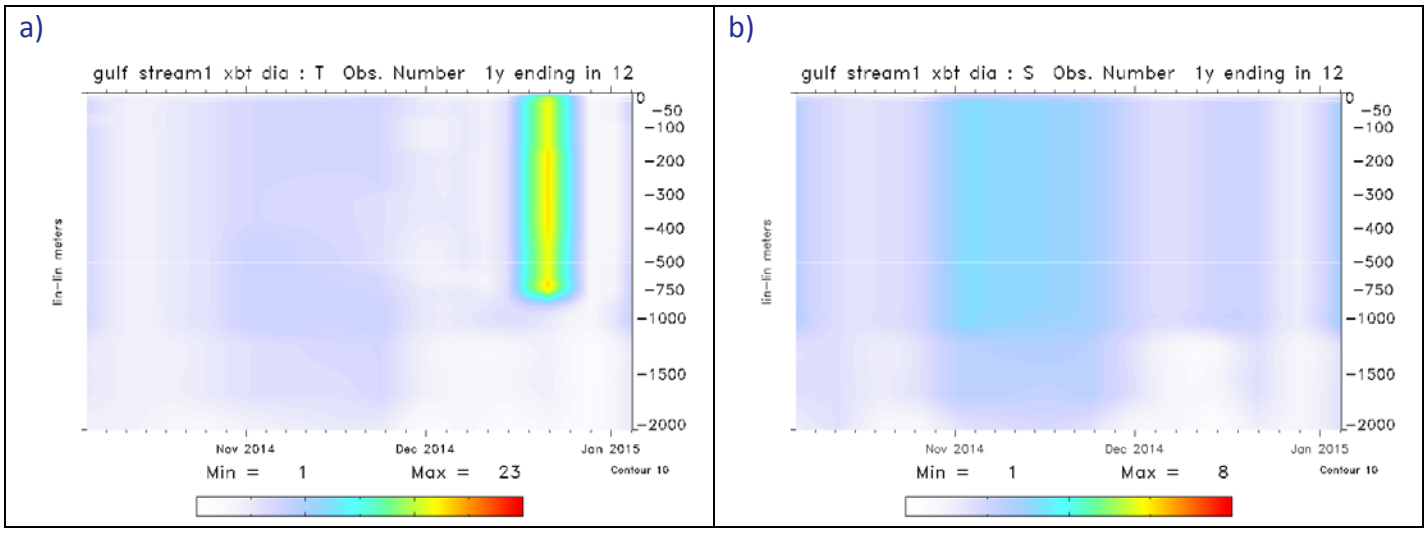

Figure 20 : number of observations of T (a) and S (b) assimilated in PSY4V2R2 in the Gulf Stream 1 region during the OND 2014 quarter.

V.1.3.1.3. Mediterranean Sea sub-regions

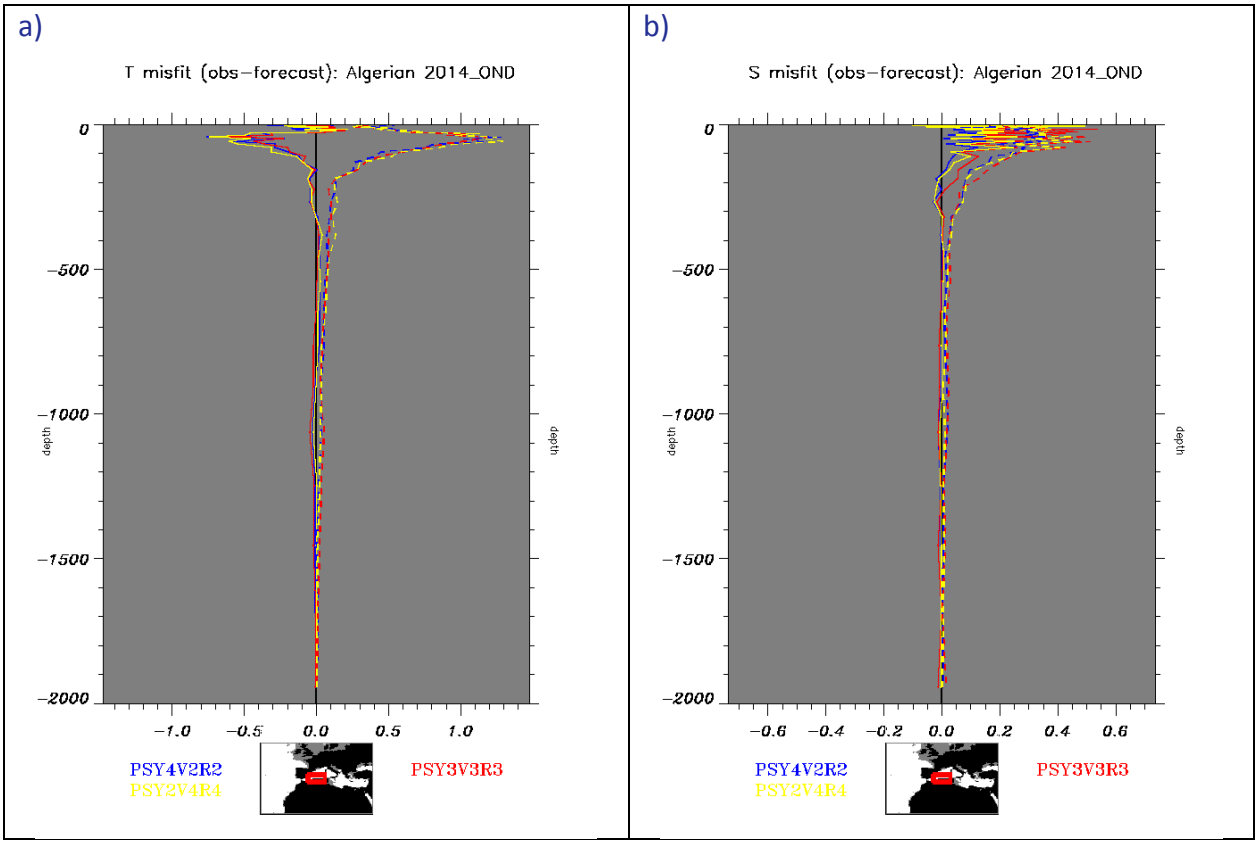

c)

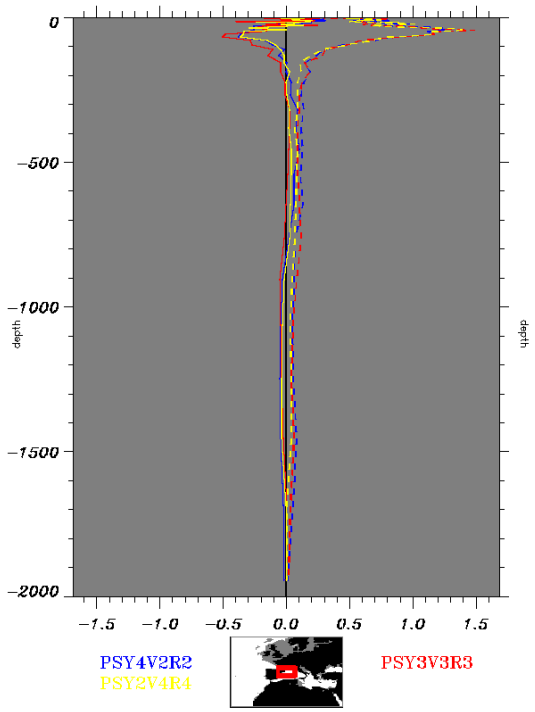
T misfit (obs−forecast): Gulf of Lion 2014_OND
0
−500
−1000
−1500
−2000
depth
−1.5 −1.0 −0.5 0.0 0.5 1.0 1.5
PSY4V2R2
PSY2V4R4
PSY3V3R3

d)

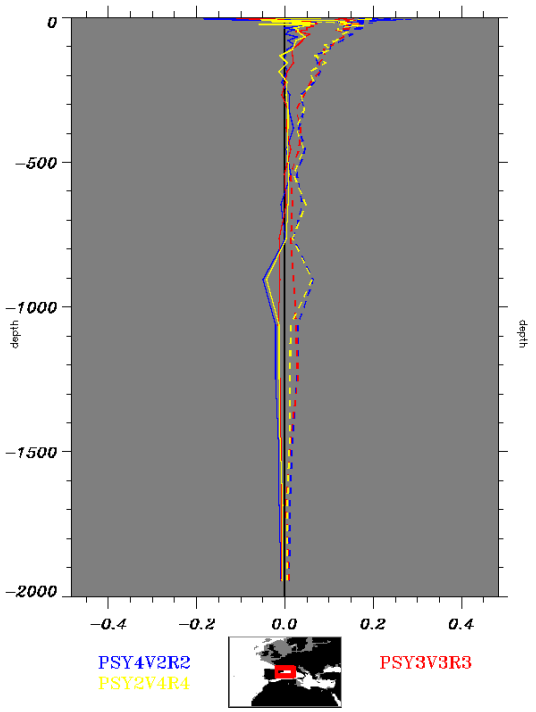
S misfit (obs−forecast): Gulf of Lion 2014_OND
0
−500
−1000
−1500
−2000
depth
−0.4 −0.2 0.0 0.2 0.4
PSY4V2R2
PSY2V4R4
PSY3V3R3

e)

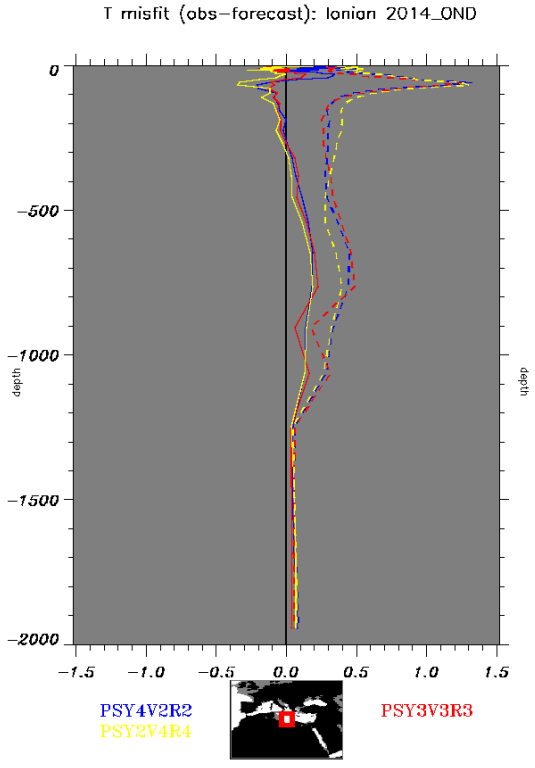
T misfit (obs−forecast): Ionian 2014_OND
0
−500
−1000
−1500
−2000
depth
−1.5 −1.0 −0.5 0.0 0.5 1.0 1.5
PSY4V2R2
PSY2V4R4
PSY3V3R3

f)

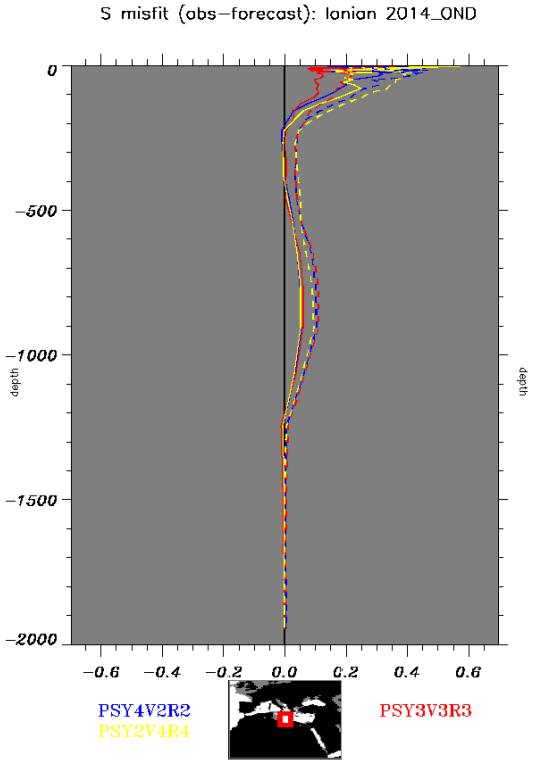
S misfit (obs−forecast): Ionian 2014_OND
0
−500
−1000
−1500
−2000
depth
−0.6 −0.4 −0.2 0.0 0.2 0.4 0.6
PSY4V2R2
PSY2V4R4
PSY3V3R3

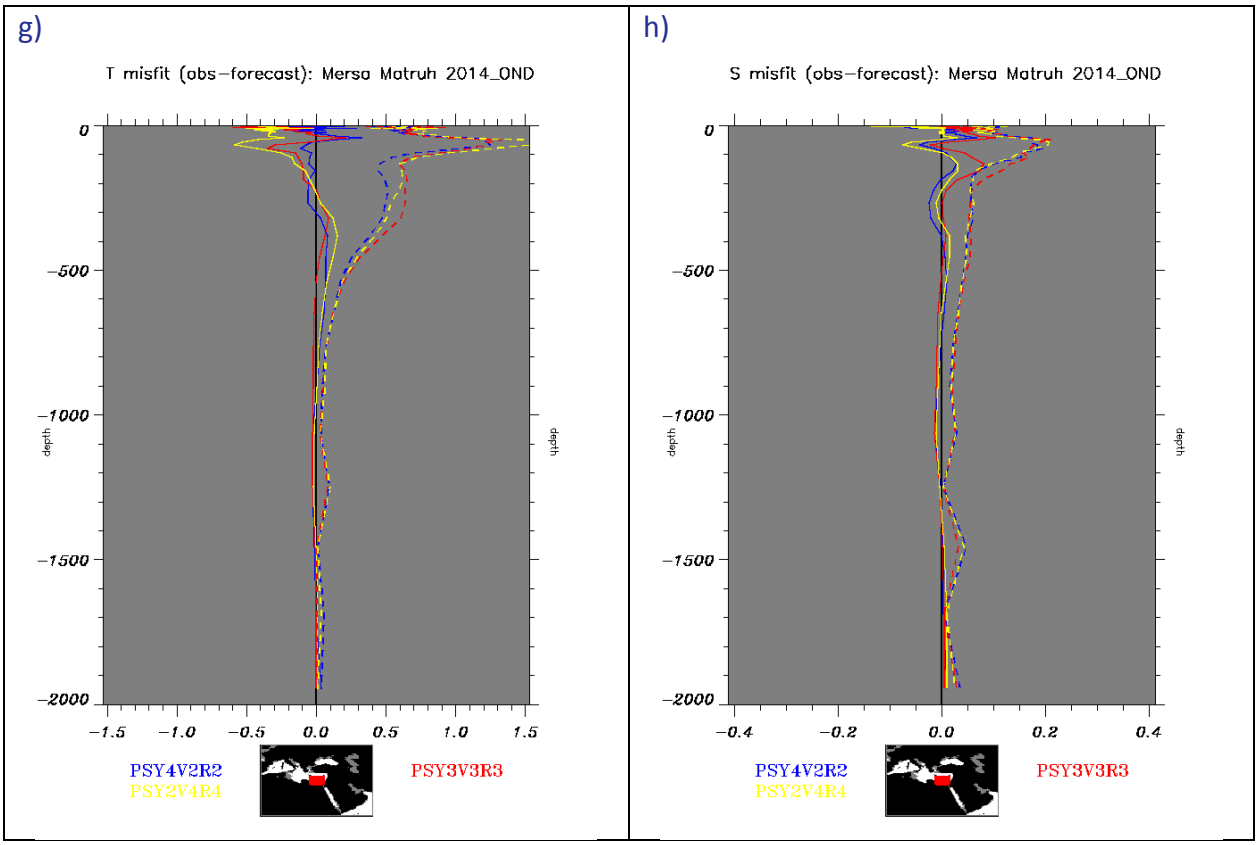

Figure 21: As Figure 13 in the Algerian (a and b), the gulf of Lion (c and d), the Ionian (e and f) and the Mersa Matruh (g and h) regions.

Figure 21 shows the T and S error profiles in sub-regions of the Mediterranean Sea. In the Algerian region the systems are too warm (0.8°C) and fresh (0.1 PSU). The same characteristics, with smaller amplitude, are presents in the Gulf of Lion. In the central Ionian region, a surface fresh bias is present between 0 and 200m (up to 0.2 PSU) and between 500m and 1200m (0.05 PSU) with a cold bias (0.2°C). In Mersa Matruh region PSY4 seems to be the best system, there is a fresh bias of 0.08 PSU for PSY3 near 200m.

V.1.3.1.4. Indian Ocean sub-regions

a)

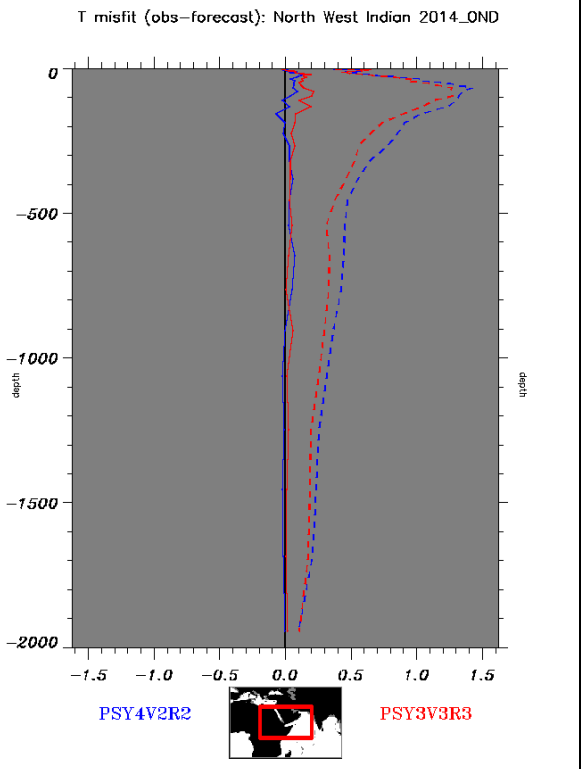
T misfit (obs−forecast): North West Indian 2014_OND
0
−500
−1000
−1500
−2000
depth
−1.5 −1.0 −0.5 0.0 0.5 1.0 1.5
PSY4V2R2
PSY3V3R3

b)

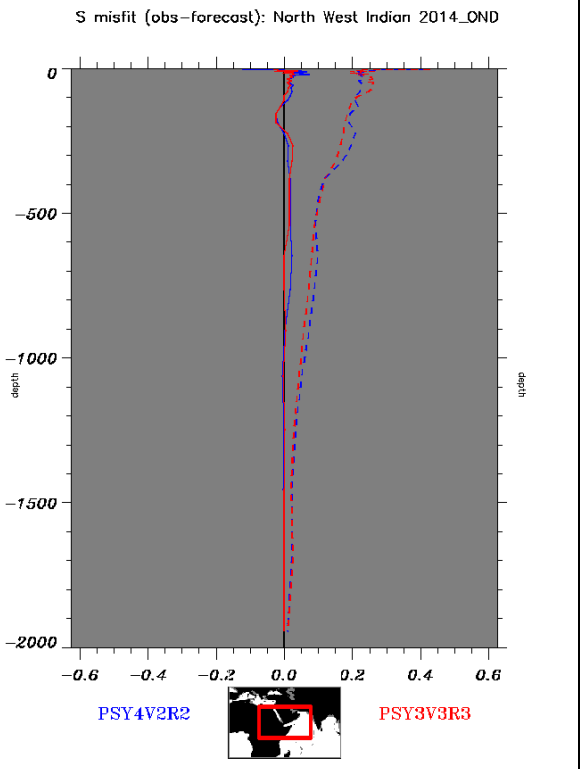
S misfit (obs−forecast): North West Indian 2014_OND
0
−500
−1000
−1500
−2000
depth
−0.6 −0.4 −0.2 0.0 0.2 0.4 0.6
PSY4V2R2
PSY3V3R3

c)

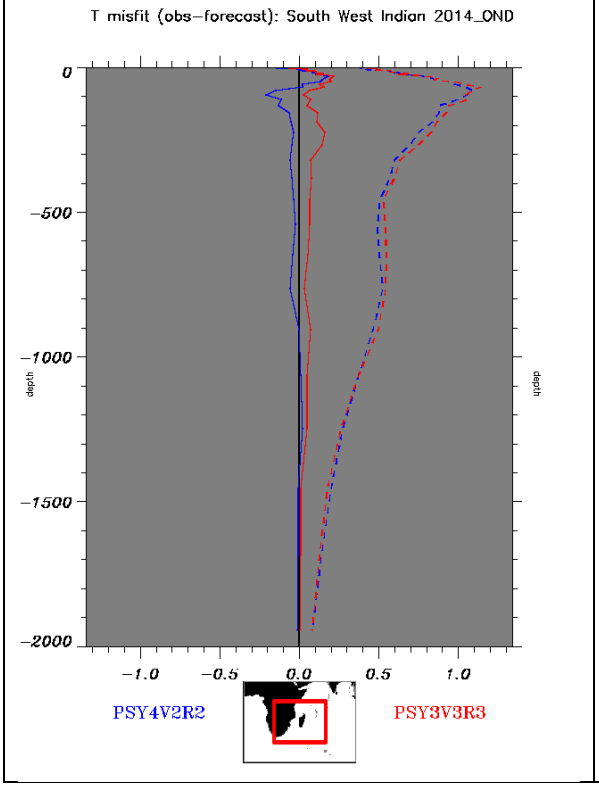
T misfit (obs−forecast): South West Indian 2014_OND
0
−500
−1000
−1500
−2000
depth
−1.0 −0.5 0.0 0.5 1.0
PSY4V2R2
PSY3V3R3

d)

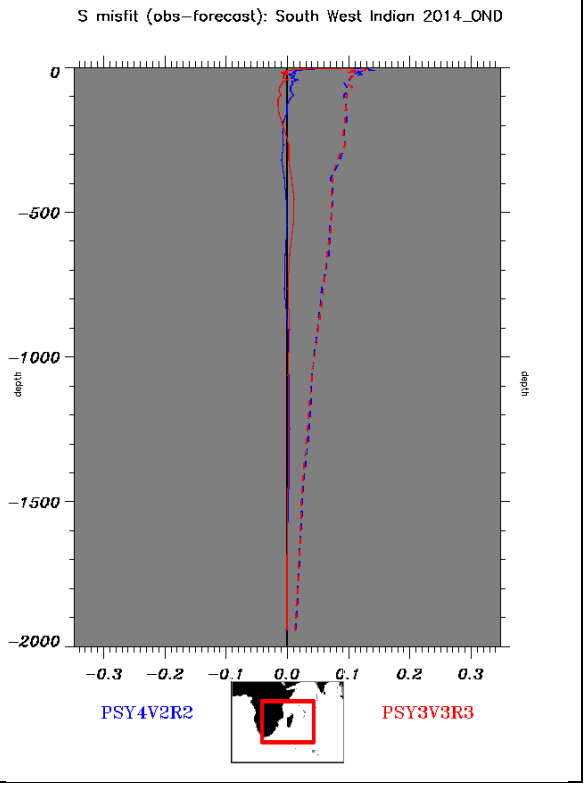
S misfit (obs−forecast): South West Indian 2014_OND
0
−500
−1000
−1500
−2000
depth
−0.3 −0.2 −0.1 0.0 0.1 0.2 0.3
PSY4V2R2
PSY3V3R3

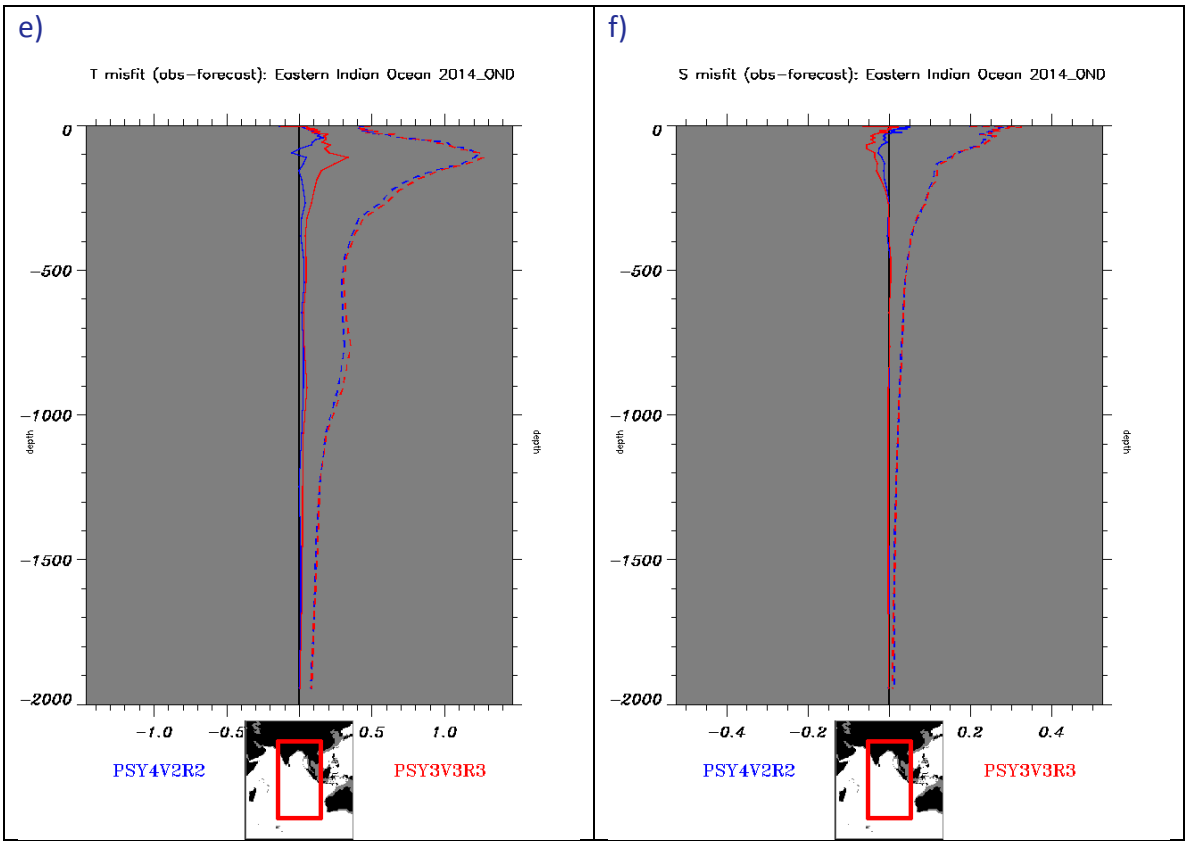

Figure 22: As Figure 13 in the North West Indian (a and b), the South West Indian (c and d) and the East Indian (e and f) regions

The analysis of the sub-regions of the Indian basin (Figure 22) shows that PSY3 displays a cold bias (0.2°C) in the thermocline in all sub-regions. PSY4 displays a warm bias mainly in the South western part of the basin. Otherwise the two systems display consistent errors in salinity, they are very close to the observations for that variable, but PSY4 seems to be the best system in this region.

SUMMARY: Starting in April 2013, the PSY2, PSY3 and PSY4 systems converge in terms of model version and parameterizations. The data assimilation method and tunings are the same, and so do the data sets assimilated by the three systems. In consequence**, the three Mercator Ocean systems display consistent data assimilation statistics** for the quarter OND 2014. **The systems are close to the observations**, and misfits lie within the prescribed error (most of the time misfit in T is less than 0.1 °C, misfit in S less then 0.05, misfit in SLA less than 7 cm). **The average and RMS errors are larger in regions of high spatial and/or temporal variability** (thermocline, regions of high mesoscale activity, upwelling, fronts, etc…). **PSY4 displays a warm bias in the 0-500m layer** in the Pacific zone that is not present in PSY3. This difference is mainly due to the initialization of PSY4 which took place in October 2012 (in October 2009 for PSY2 and PSY3) from the WOA09 climatology. The analysis of the GLORYS2V3 reanalysis has shown that the first cycles of SLA data assimilation induce a large warming of the ocean in the 0-800m layer that the in situ observations have to correct. The SEEK and the 3D-var bias correction need at least a one year period to correct this bias, which is then propagated to the deep layers (under 1000m) within 5 to 10 years, if no correction is applied.. PSY4 also displays low biases in SLA concurrent with warm biases in SST. **Coastal regions are weakly constrained in all systems**, and consistent biases appear in SLA and SST (warm and high, or cold and low). There are still many uncertainties in the MDT, mainly near the coasts and in the Polar Regions. The systems do not use the SLA misfit information in coastal regions, but problems can appear in open ocean regions where there are still errors in the MDT. Seasonal biases have been reduced with respect to previous versions of the systems, thanks to the use of a procedure to avoid the damping of SST increments via the bulk forcing function. A warm bias is diagnosed in SST this quarter. **Globally, there is a warm bias in a mixing layer especially between 50 and 150m. This bias is a consequence of a too diffuse thermocline.** The bias correction is not as efficient on reducing seasonal biases as it is on reducing long term systematic biases. No precipitation correction is applied in the systems, and uncertainties (overestimation) of the convective precipitations induce **large fresh biases in the tropical oceans (Pacific and Atlantic).**

V.2. Accuracy of the daily average products with respect to observations

V.2.1. T/S profiles observations

V.2.1.1. Global statistics for OND 2014

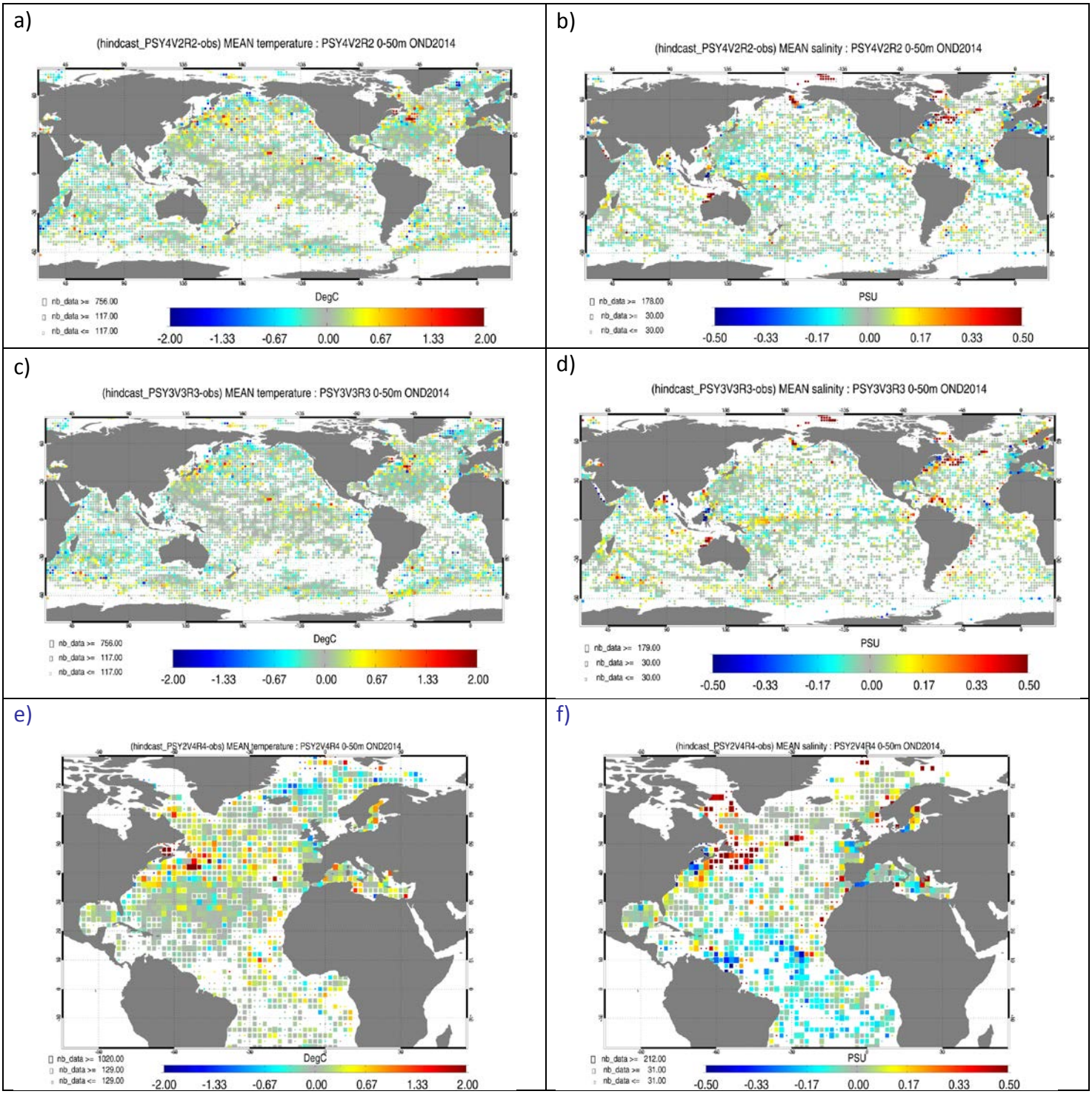

Figure 23: Average difference MODEL-OBSERVATION of temperature (a, c, and e, in °C) and salinity (b, d, and f, in psu) in OND 2014 between the daily average hindcast PSY4V2R2 (a and b), PSY3V3R3 (c and d) and PSY2V4R4 (e and f) hindcast products and all available T/S observations from the Coriolis database. The Mercator hindcast products are taken at the time and location of the observations. Averages are performed in the 0-50m layer. The size of the pixel is proportional to the number of observations used to compute the RMS in 2°x2° boxes.

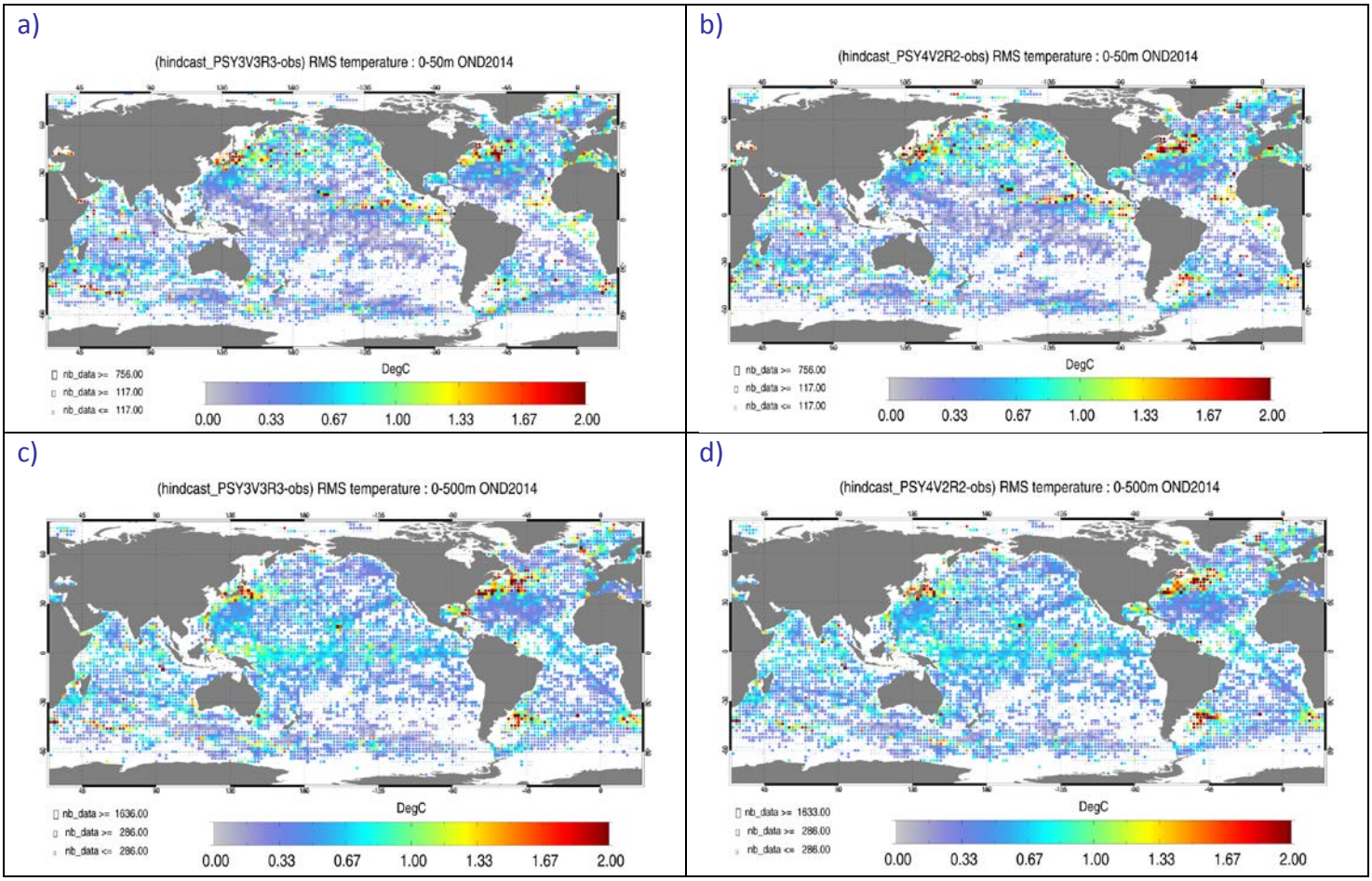

Figure 24: RMS temperature (°C) difference (model-observation) in OND 2014 between all available T/S observations from the Coriolis database and the daily average hindcast PSY3V3R3 products on the left and hindcast PSY4V2R2 on the right column colocalised with the observations. Averages are performed in the 0-50m layer (a and b) and in the 0-500m layer (c and d). The size of the pixel is proportional to the number of observations used to compute the RMS in 2°x2° boxes.

Consistently with the data assimilation statistics the systems PSY4 and PSY2 are slightly warmer (~0.1°C) than the observations at the global scale in the surface layer (0-50m) as can be seen in Figure 23, especially in Tropical Pacific and in the Gulf Stream and Kuroshio region. PSY3 is slightly colder in the same layer. Especially for high resolution systems PSY2 and PSY4, fresh biases also appear in the tropics, linked with overestimated convective precipitations in the ECMWF analyses, and also to the climatological runoffs that are prescribed. This quarter the bias is significantly stronger in PSY4 than in PSY2 or PSY3.

As can be seen in Figure 24, in both PSY3 and PSY4 temperature errors in the 0-500m layer have similar amplitude and spatial patterns, and stand between 0.5 and 1°C in most regions of the globe. RMS errors in the tropical thermocline can reach 1°C. Regions of high mesoscale activity (Kuroshio, Gulf Stream, Agulhas current) and regions of upwelling in the tropical Atlantic and Tropical Pacific display higher errors (up to 3°C).

The salinity RMS errors (Figure 25) are usually less than 0.2 but can reach higher values in regions of high runoff (Amazon, Sea Ice limit) or precipitations (ITCZ, SPCZ, Gulf of Bengal), and in regions of high mesoscale variability. RMS errors of around 0.2 in the Tropics in the 0-50m layer correspond to the fresh bias linked with overestimated precipitation. High RMS error in the Beaufort Sea correspond to a salty and cold bias in the Summer Pacific Water (also called summer Pacific halocline water) for both PSY3 and PSY4 see Focus on Beaufort Sea for a longer description.

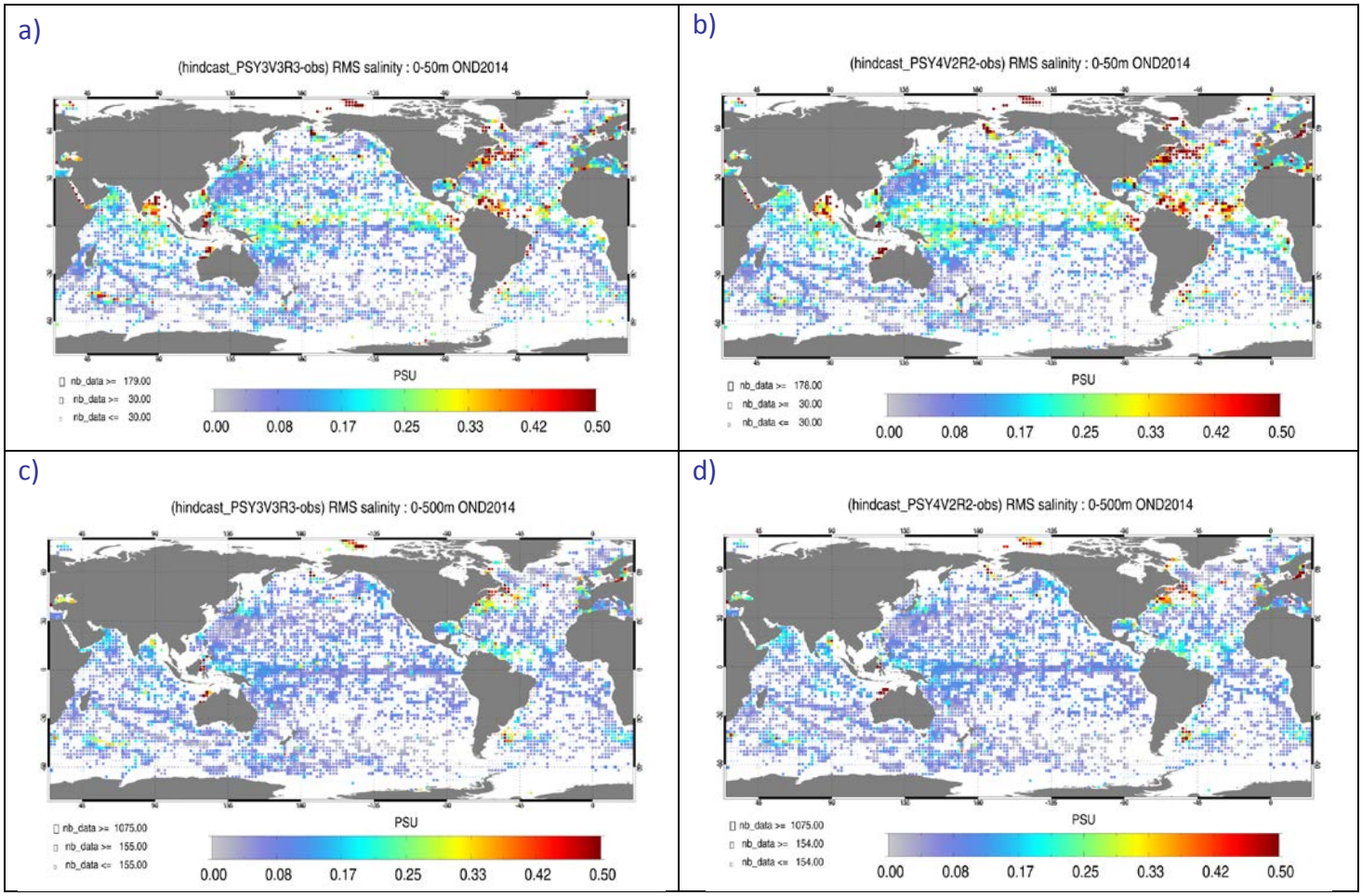

Figure 25: RMS salinity (psu) difference (model-observation) in OND 2014 between all available T/S observations from the Coriolis database and the daily average hindcast PSY3V3R3 products (a and c) and hindcast PSY4V2R2 (b and d), colocalised with the observations. Averages are performed in the 0-50m layer (a and b) and in the 0-500m layer (c and d). The size of the pixel is proportional to the number of observations used to compute the RMS in 2°x2° boxes.

As can be seen in Figure 26, the intermediate resolution model (PSY3) and the high resolution model (PSY4) display comparable temperature and salinity RMS differences.

For the surface layers: PSY4 displays a global average fresh bias (0.02 psu) at the surface layer, while PSY3 exhibits a salty bias between 0 and 300m.

For the subsurface layers: PSY3 is slightly colder than the observations, mainly between 5 and 800m (0.05°C) while PSY4 appears to warm in the water column (below 0.1°C).

Both systems are more accurate than the WOA09 climatology, for temperature and salinity at all depths except for the mean error in salinity in the 0-100m layer.

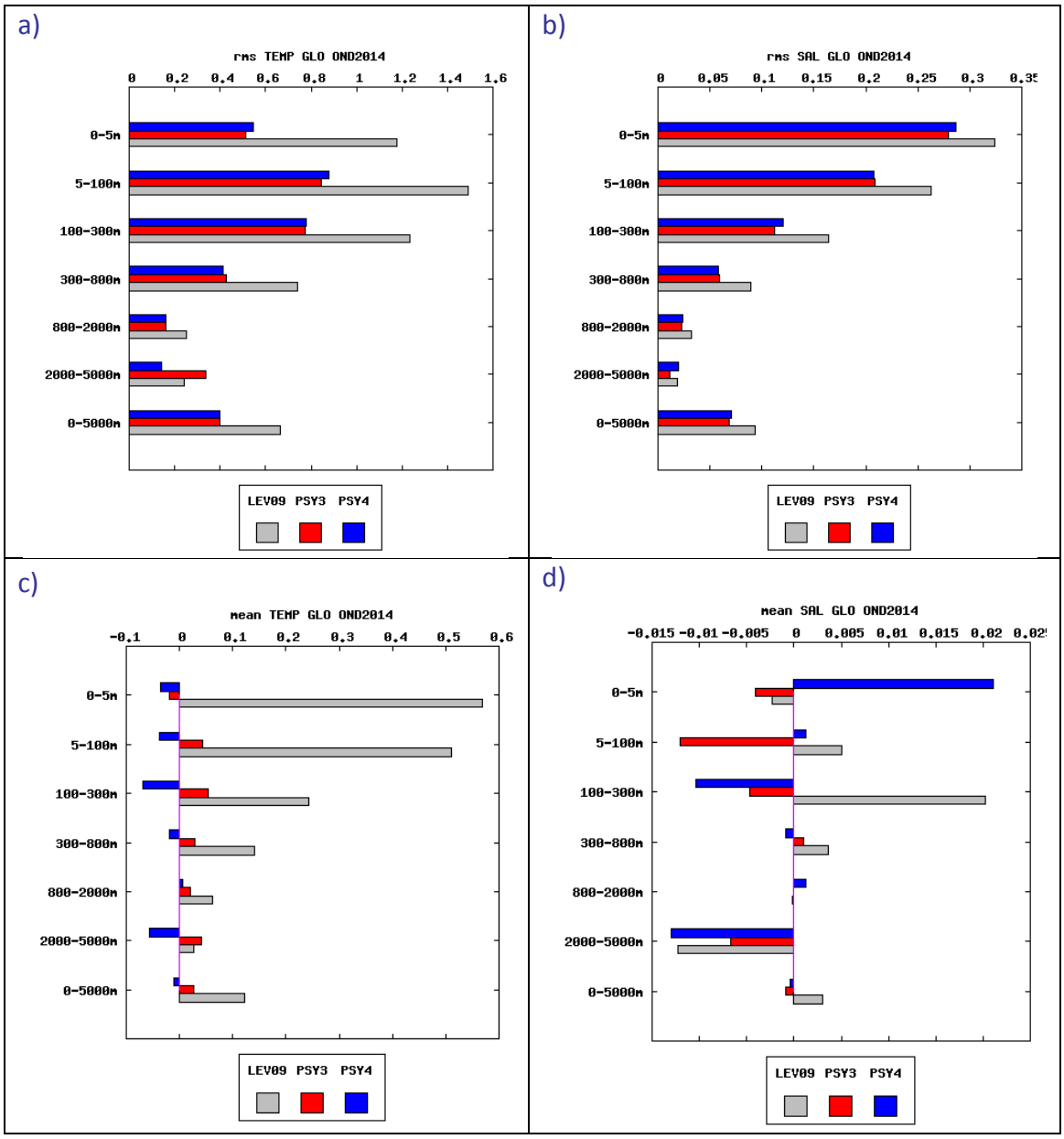

Figure 26 : OND 2014 global statistics of temperature (°C, a and c) and salinity (psu, b and d) averaged in 6 consecutive layers from 0 to 5000m. RMS difference (a and b) and mean difference (observation-model, c and d) between all available T/S observations from the CORIOLIS database and the daily average hindcast products PSY3V3R3 (red), PSY4V2R2 (blue) and WOA09 climatology (grey) colocalised with the observations. NB: average on model levels is performed as an intermediate step which reduces the artefacts of inhomogeneous density of observations on the vertical.

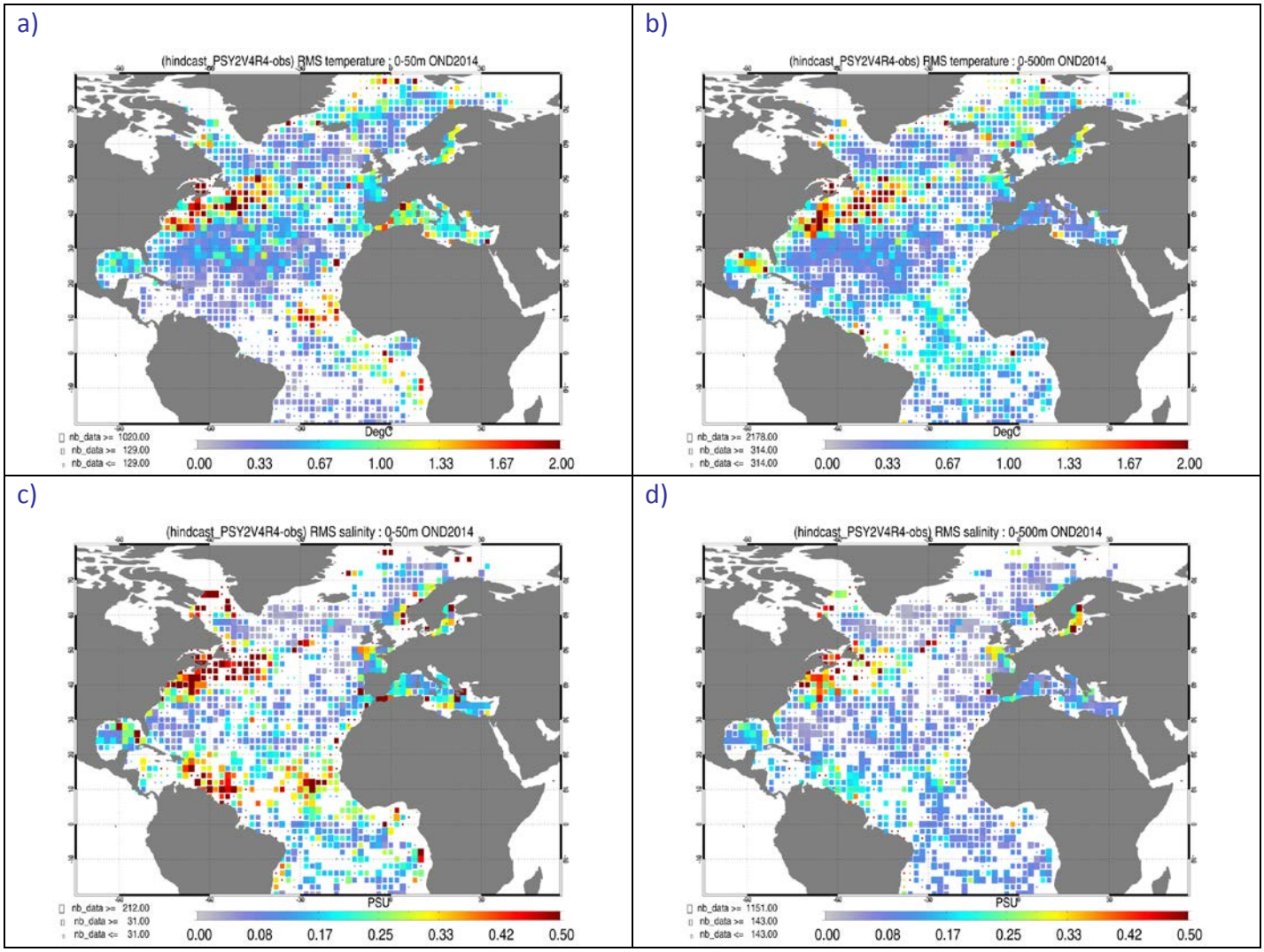

Figure 27: RMS difference (model-observation) of temperature (a and b, °C) and salinity (c and d, psu) in OND 2014 between all available T/S observations from the Coriolis database and the daily average PSY2V4R4 hindcast products colocalised with the observations in the 0-50m layer (a and c) and 0-500m layer (b and d)

The general performance of PSY2 (departures from observations in the 0-500m layer) is less than 0.3°C and 0.05 psu in many regions of the Atlantic and Mediterranean (Figure 27). The strongest departures from temperature and salinity observations are mainly located in the Gulf Stream, the tropical Atlantic and in the Baltic Sea. Near surface salinity biases appear in the Alboran Sea, the Gulf of Guinea, the Caribbean Sea, the Labrador Sea, the Gulf of Mexico (see also Figure 23) , the Baltic Sea and the Gibraltar Strait. In the tropical Atlantic biases concentrate in the 0-50m layer (cold and fresh bias). This is consistent with the bias correction not being at work in the mixed layer.

V.2.1.2. Water masses diagnostics

a)

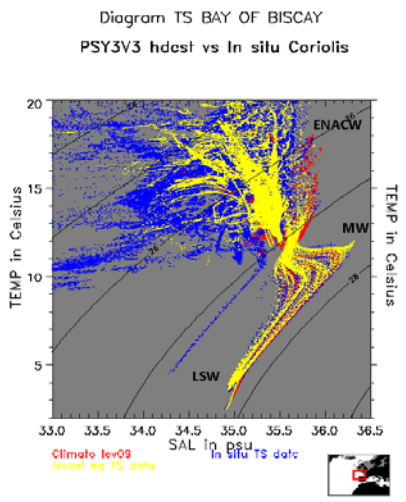

b)

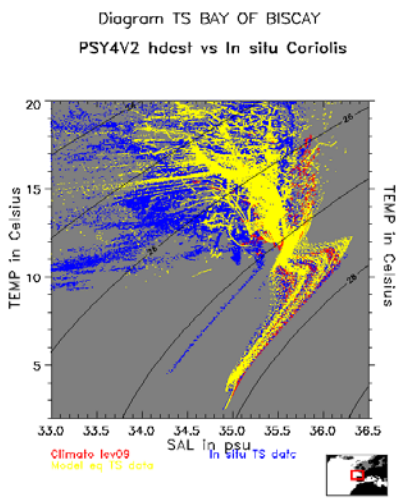

c)

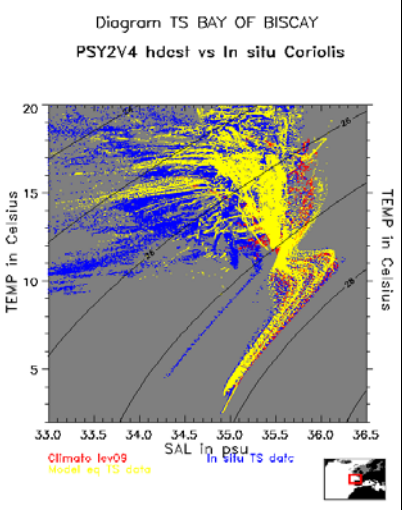

d)

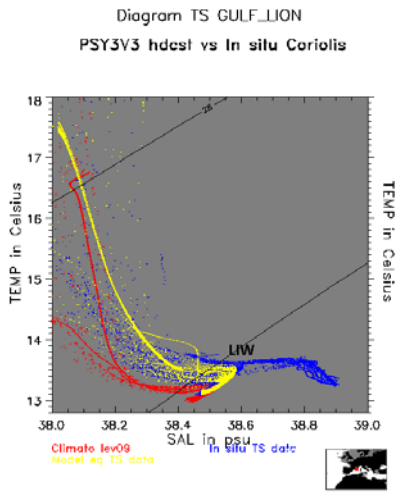

e)
cccc

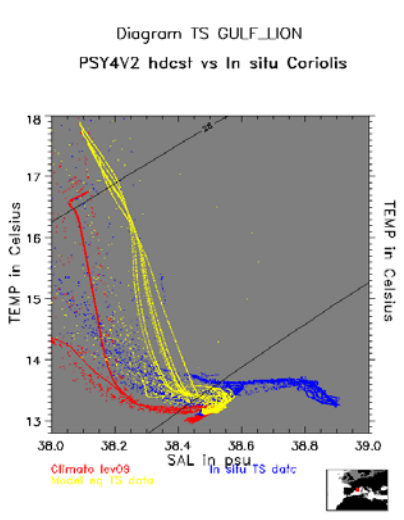

f)

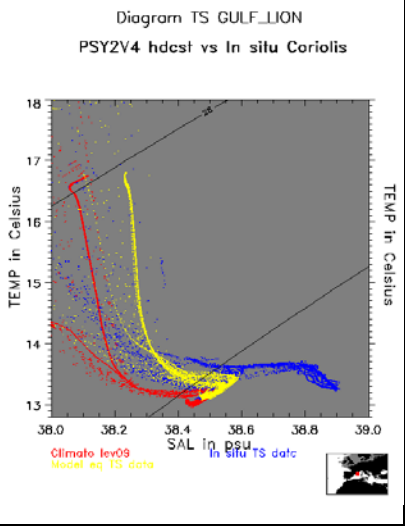

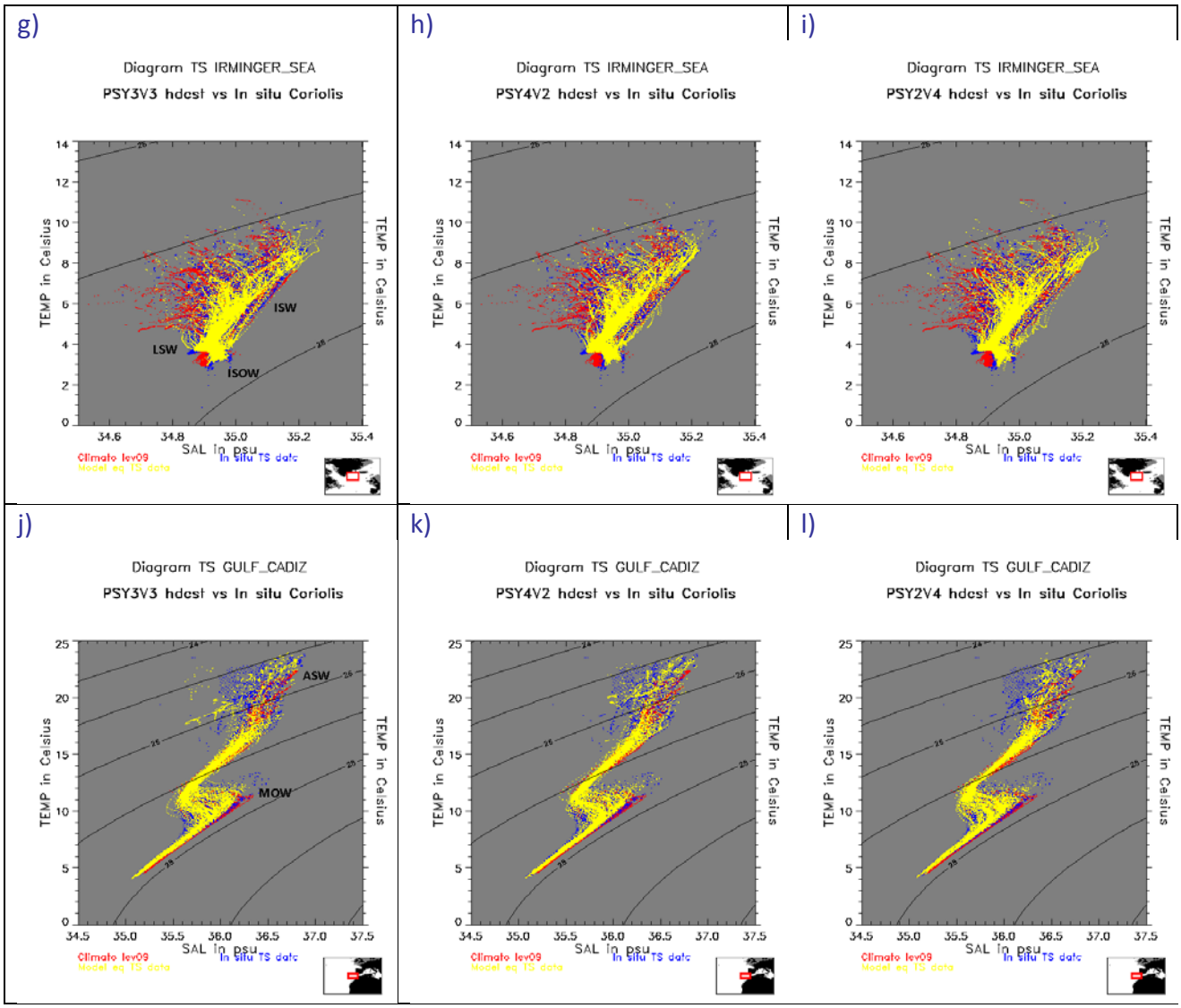

Figure 28: Water masses (Theta, S) diagrams in OND 2014 in the Bay of Biscay (a to c), Gulf of Lion (d to f), Irminger Sea (g to i) and Gulf of Cadiz (j to l), comparison between PSY3V3R3 (a, d, g, j), PSY4V2R2 (b, e, h, k) and PSY2V4R4 (c, f, I, and l) in AMJ 2013. PSY2, PSY3 and PSY4: yellow dots; Levitus WOA09 climatology: red dots; in situ observations: blue dots.

In Figure 28 the daily products (analyses) are collocated with the T/S profiles in order to draw "T, S" diagrams. The water masses characteristics of the three systems are nearly similar, PSY2 being locally slightly better than PSY3 and PSY4 (Mediterranean waters)

In the Bay of Biscay the Eastern North Atlantic Central Water, Mediterranean and Labrador Sea Water can be identified on the diagram.

- Between 15°C and 19°C, 35 and 36.5 psu, warm and relatively salty Eastern North Atlantic Central Water gets mixed with the shelf water masses. The saltiest ENACW waters are well captured by the three systems during this OND 2014 season but PSY2 seems to be the best
- The Mediterranean Waters are characterized by high salinities (Salinities near 36 psu) and relatively high temperatures (Temperatures near 12°C). PSY2 better captures the highest salinities than PSY3 and PSY3 for the main profiles. A few profiles in PSY4 appear much more saltier in the Mercator systems than the *in situ* data.
- The Labrador Sea waters appear between 4°C and 7°C, 35.0 and 35.5 psu and are well represented by the three systems.

In the Gulf of Lion:

- The Levantine Intermediate Water (salinity maximum near 38.6 psu and 13.5°C) is too cold and little fresh and compact in all systems this OND 2014 season.
- The water mass detected near 38.8 psu and 13-13.3°C may correspond to measurements on the shelves made by research vessels.

In the Irminger Sea:

- The Irminger Sea Water (≈ 3°C and 35 psu) and the North Atlantic water (at the surface) are well represented by the systems.
- The Labrador Sea Waters are slightly too salty in all systems.
- Waters colder than 3°C and ≈ 34.9 psu (Iceland Scotland Overflow waters) are presents in all systems but seem too fresh.

In the Gulf of Cadiz:

- The Mediterranean outflow waters (T around 10°C) are well represented but appears too fresh in PSY3. The high resolution systems (PSY2 and PSY4) better capture the spread of temperature and salinity at depth as well as at the surface (Atlantic Surface waters).

In the western tropical Atlantic, all the systems capture the salinity minimum of the Antarctic Intermediate Waters (AIW). The spread of temperature and salinity at surface and sub-surface is well represented too.

In the eastern tropical Atlantic the three systems represent well the water masses. For the high resolution systems, the spread of fresh water near the surface is too extended in comparison with observations.

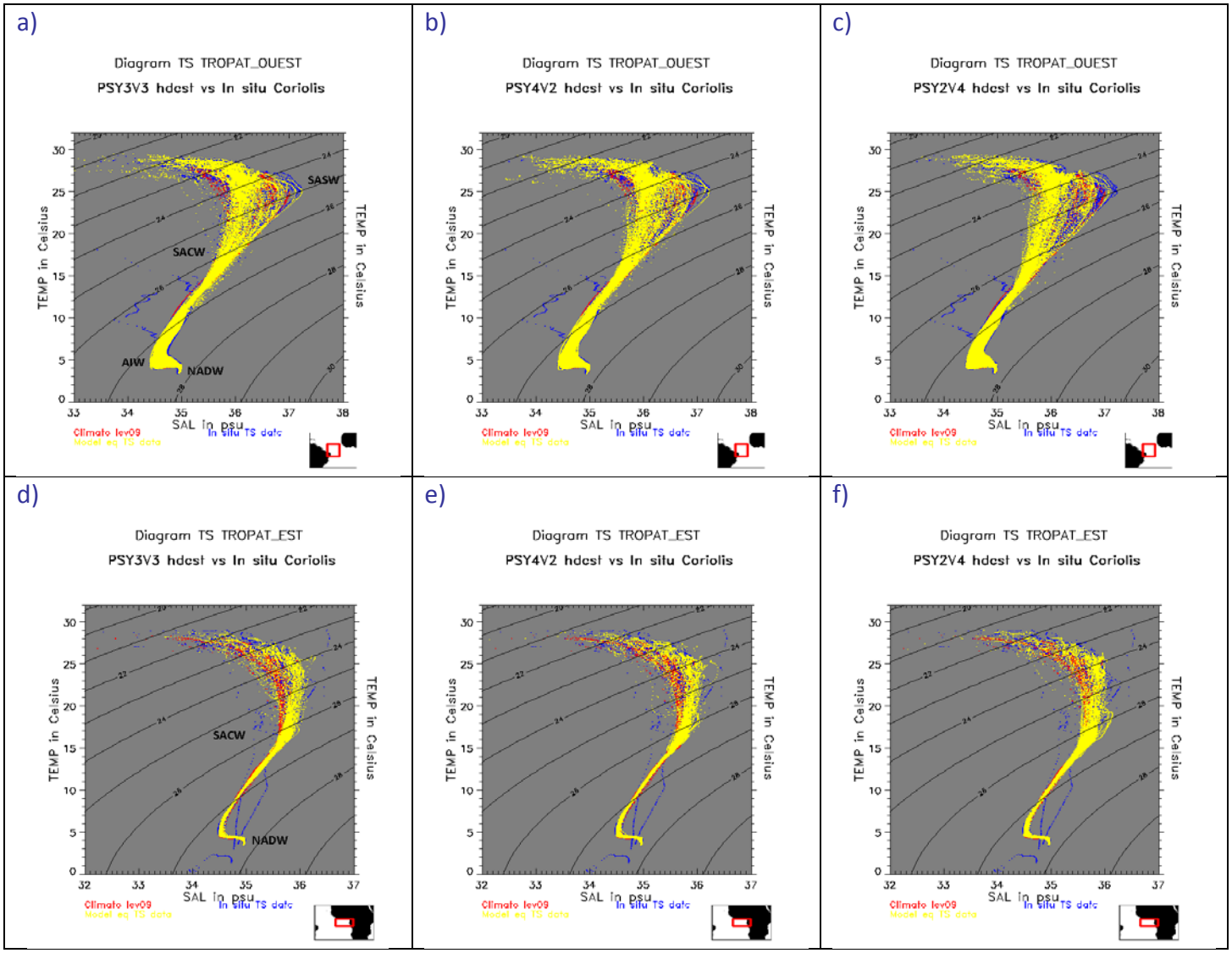

Figure 29 : Water masses (T, S) diagrams in the Western Tropical Atlantic (a to c) and in the Eastern Tropical Atlantic (d to f) in OND 2014: for PSY3V3R3 (a, d); PSY4V2R2 (b, e); and PSY2V4R4 (c, f). PSY2, PSY3 and PSY4: yellow dots; Levitus WOA09 climatology; red dots, in situ observations: blue dots.

In the Agulhas current (Figure 30) PSY3 and PSY4 give a realistic description of water masses. The central and surface waters characteristics are slightly more realistic in PSY4 than in PSY3. In the Kuroshio region the North Pacific Intermediate waters (NPIW) are too salty for the two global systems. At the surface in the highly energetic regions of the Agulhas and of the Gulf Stream, the water masses characteristics display a wider spread in the high resolution 1/12° than in the ¼°, which is more consistent with T and S observations. In the Gulf Stream region, PSY4 is closer to the observations than PSY3 especially in the North Atlantic Central Waters (NACW) where PSY3 is too fresh. The saltiest waters near the surface (North Atlantic Subtropical Waters, NASW) are only captured by PSY4. The two systems are very close in this region.

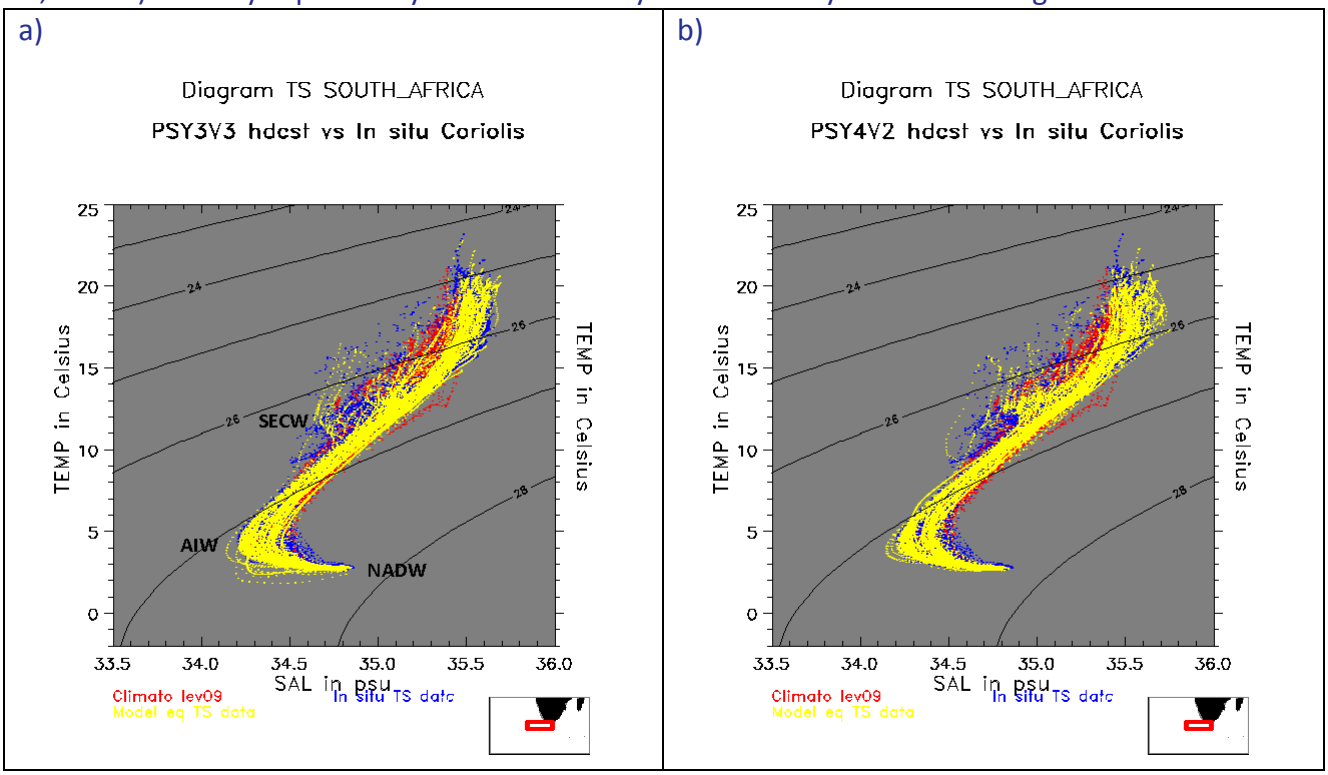

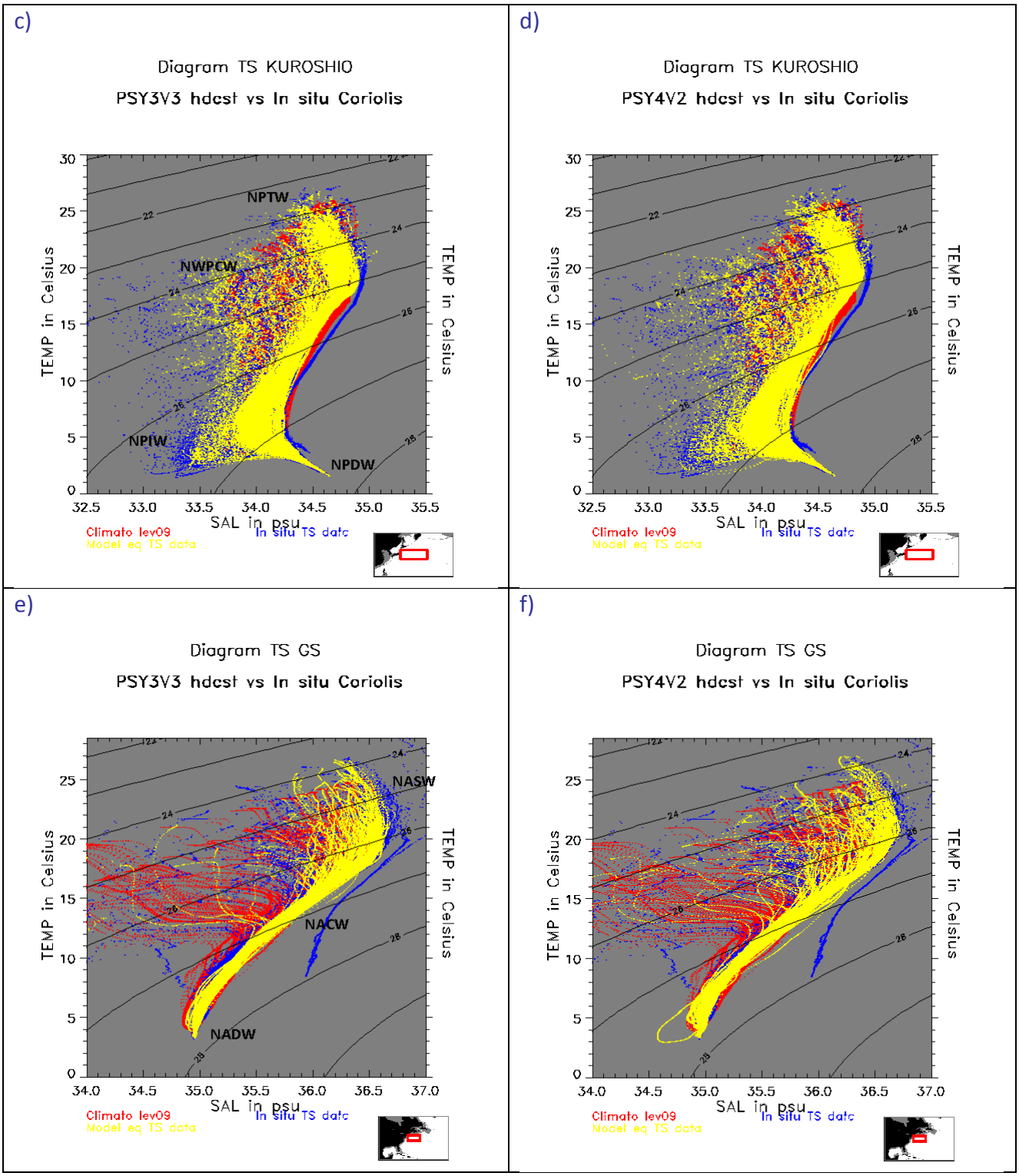

Figure 30: Water masses (T, S) diagrams in South Africa (a and b), Kuroshio (c and d), and Gulf Stream region (e and f): for PSY3V3R1 (a, c and e); PSY4V1R3 (b, d and f) in OND 2014. PSY3 and PSY4: yellow dots; Levitus WOA09 climatology: red dots; in situ observations: blue dots.

V.2.1.2.1. Focus on Beaufort Sea

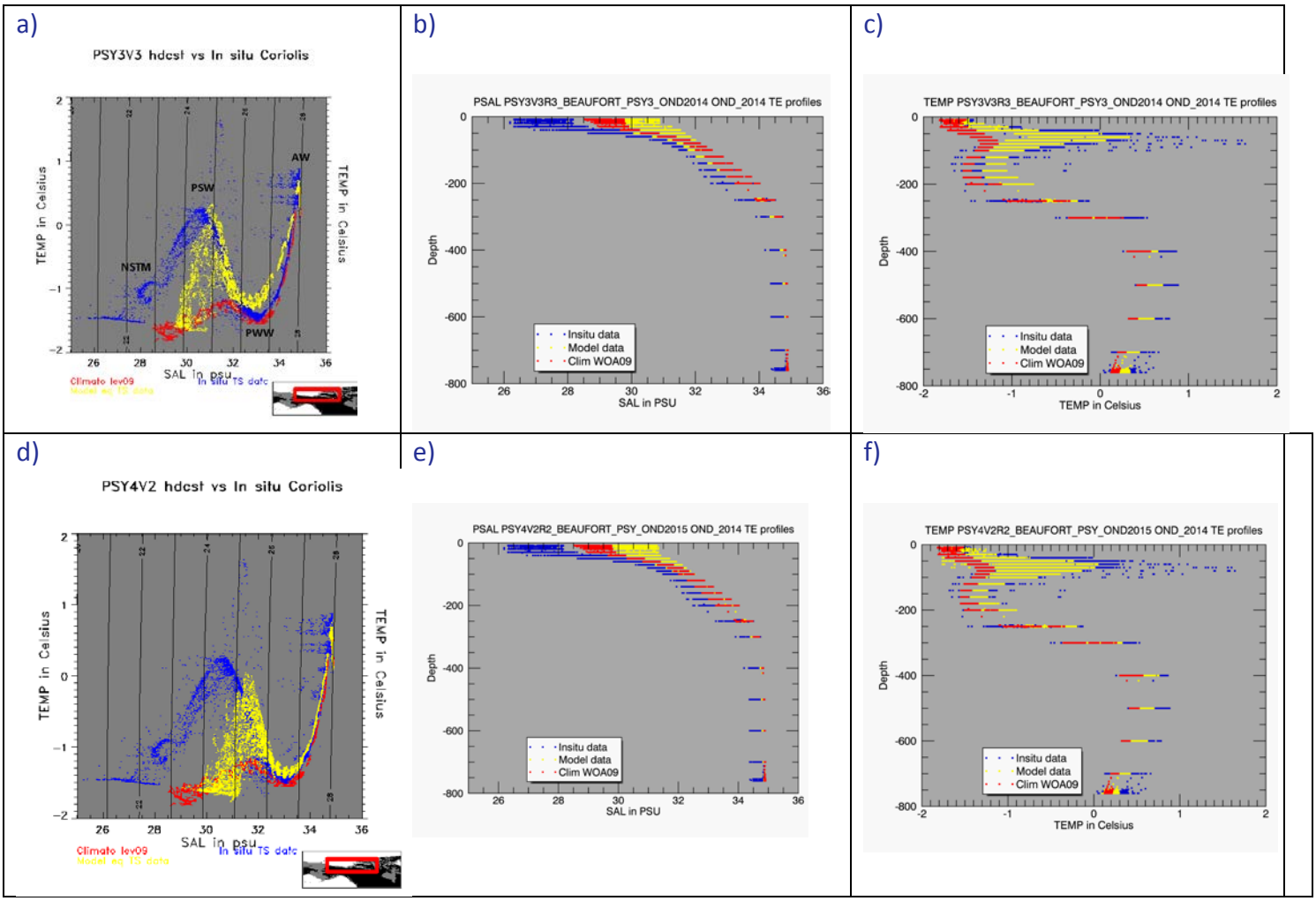

Figure 31 : Water masses (T, S) diagrams in Beaufort Sea for PSY3 (a) and PSY4 (d), salinity profiles in this region for PSY3 b) and PSY4 e), and the same for the temperature profiles : PSY3 (c) and PSY4(f). Symbology : yellow dots; Levitus WOA09 climatology: red dots; in situ observations: blue dots.

The T/S diagrams of in situ profiles are showing three temperature maximums: two bigs and a small. The first big maximum situated around 35 psu and near 1°C corresponds to the Atlantic Water (AW). The second maximum (around 31 and 0.5°C) corresponds to the Pacific Summer Water (PSW) (see ref 3-4) and the third small maximum correspond to the Near Sea Surface Temperature Maximum (NSTM around 28 psu and -1°C near 30m). Two temperature minimums are also presents: the Pacific Winter Water (PWW) and the remnant of the previous winter's surface mixed layer (between the NSTM and the PSW)e. Associated with theses minimums and maximums we have three haloclines: the lower halocline between the PWW and AW maximum, the winter halocline around the PSW maximum and the summer halocline near the NSTM water masse.

The both systems well represent the Atlantic Water but are too salty for the summer Pacific Water but PSY3 sticks better to the observations for this water masse. The NSTM waters are not represented by the two systems. When we look at the profiles, we see a strong cold and salty bias in the two systems in the whole water column. This strong bias could be link to a lake of freshwater in the runoffs or too much melting during the summer. We can notice that the bias correction is not as efficient at this latitude and none of these data are assimilated, so we are close to a free-run mode in this region.

V.2.2. SST Comparisons

Quarterly average SST differences with OSTIA analyses show that the systems' SST is very close to OSTIA, with difference values staying below the observation error of 0.5 °C on average. High RMS difference values (Figure 32) are encountered in high spatial and temporal variability regions such as the Gulf Stream or the Kuroshio, Zapiola eddy, Agulhas. The error is also high (more than 2°C locally) in marginal seas of the Antarctic and Arctic Ocean where the sea ice limit increases the SST errors and the SST contrasts. Small features in the RMS difference appear in PSY3 that are not found in the higher resolution systems PSY4 and PSY2 (for instance this quarter in the Labrador Sea). High RMS differences also appear in the upper part of the Circumpolar current, the main features are located in the South of Indian and Pacific Ocean. A dipole of discrepancies appears in the Tropical Pacific probably link to the positive phase of the North Atlantic Oscillation (see Information on the large scale climatic conditions).

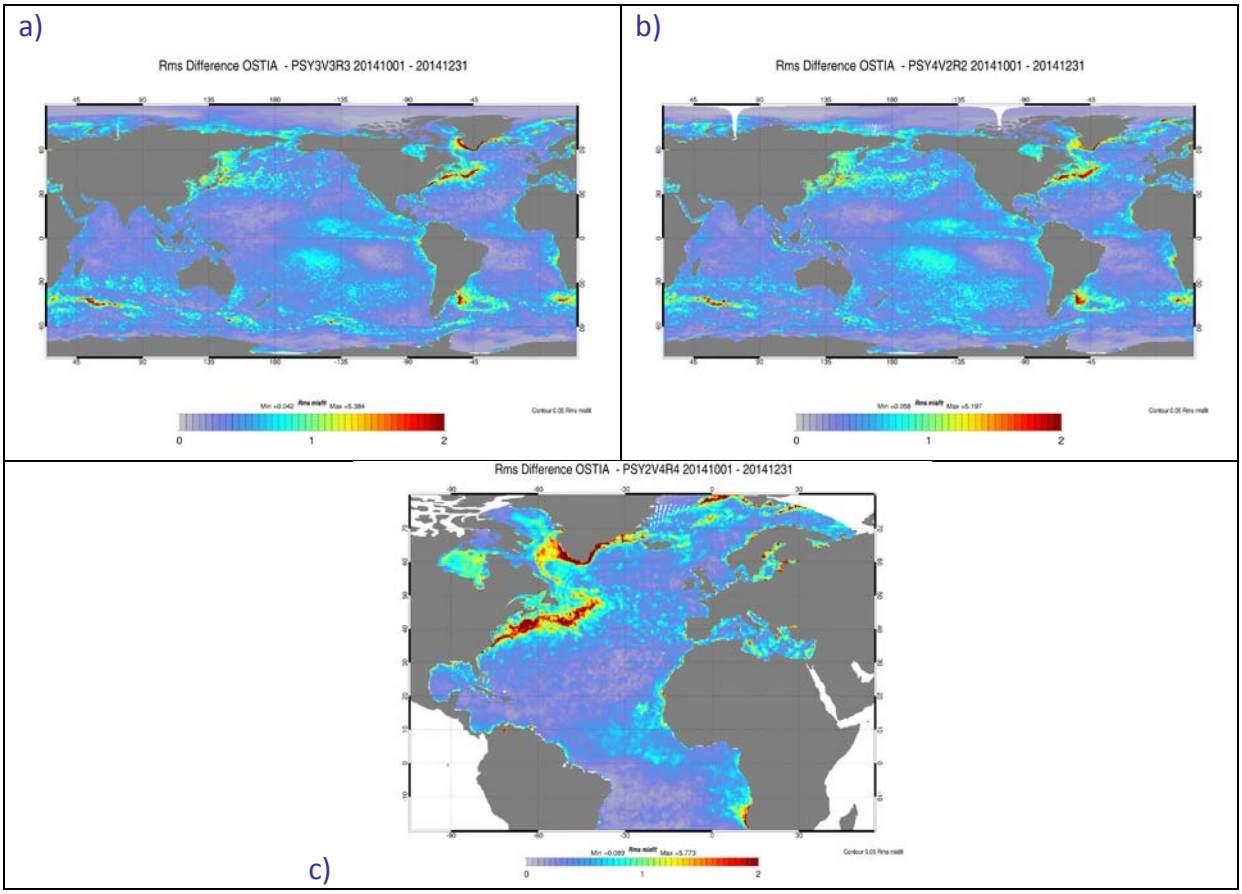

Figure 32 : RMS temperature (°C) differences between OSTIA daily analyses and PSY3V3R3 daily analyses (a); between OSTIA and PSY4V2R2 (b), between OSTIA and PSY2V4R4 (c) in OND 2014. The Mercator Océan analyses are colocalised with the satellite observations analyses.

The systems' tropical oceans are warmer than OSTIA (Figure 33), as do the high latitudes (especially in the ACC this austral winter). The Pacific subtropical and the Indian Ocean are colder than OSTIA on average like the South Atlantic Ocean, and some closed or semi-enclosed seas: the Gulf of Mexico, Chinea Sea, Ariabian Sea.

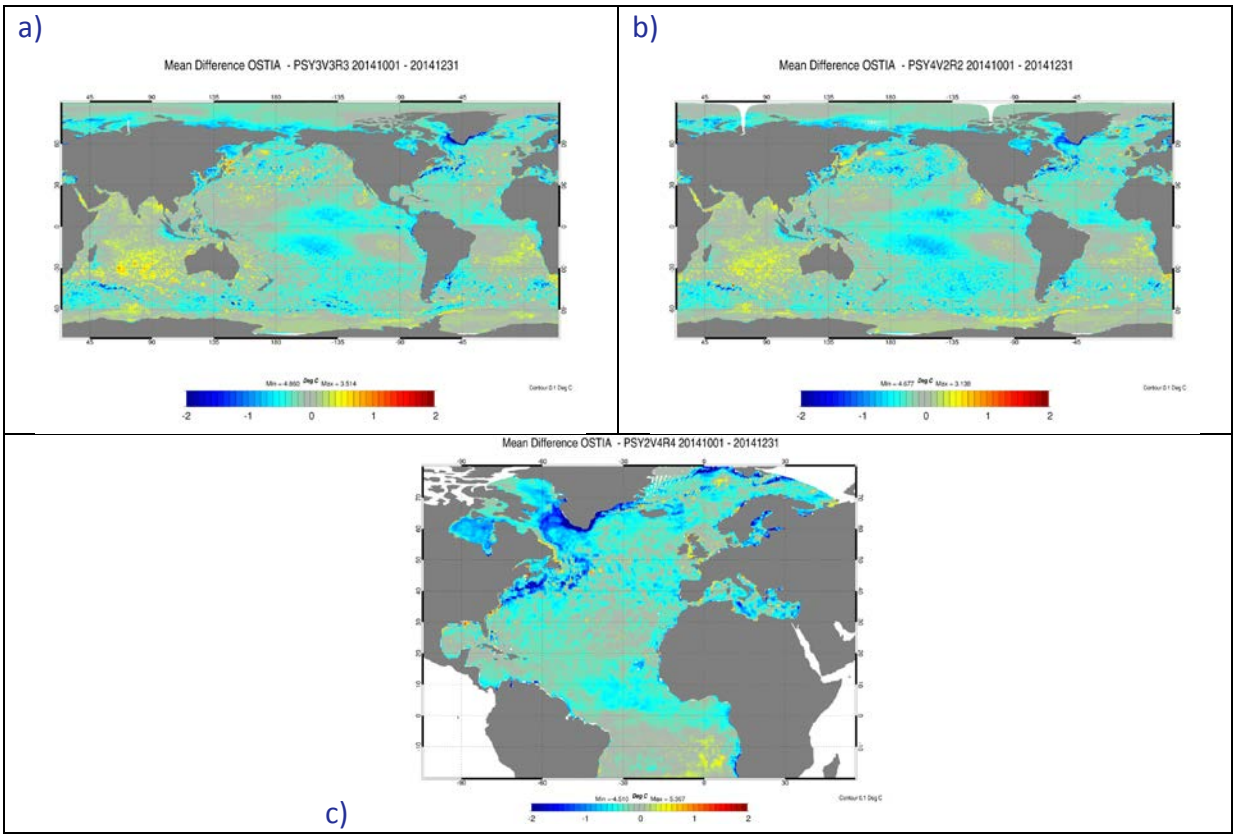

Figure 33: Mean SST (°C) daily differences in OND 2014 between OSTIA daily analyses and PSY3V3R3 daily analyses (a), between OSTIA and PSY4V2R2 (b) and between OSTIA and PSY2V4R4 daily analyses (c).

V.2.3. Drifting buoys velocity measurements

Recent studies (*Law Chune, 2012*[4] , *Drévillon et al, 2012*[5]) - in the context of Search-And-Rescue and drift applications – focus on the need for accurate surface currents in ocean forecasting systems. *In situ* currents are not yet assimilated in the Mercator Ocean operational systems, as this innovation requires a better characterization of the surface currents biases.
The comparison of Mercator analyses and forecast with AOML network drifters velocities combines two methods based on Eulerian and Lagrangian approaches.

V.2.3.1. Eulerian Quality control

[4] Law Chune, 2012 : Apport de l'océanographie opérationnelle à l'amélioration de la prévision de la dérive océanique dans le cadre d'opérations de recherche et de sauvetage en mer et de lutte contre les pollutions marines

[5] Drévillon et al, 2012 : A Strategy for producing refined currents in the Equatorial Atlantic in the context of the search of the AF447 wreckage (Ocean Dynamics, Nov. 2012)

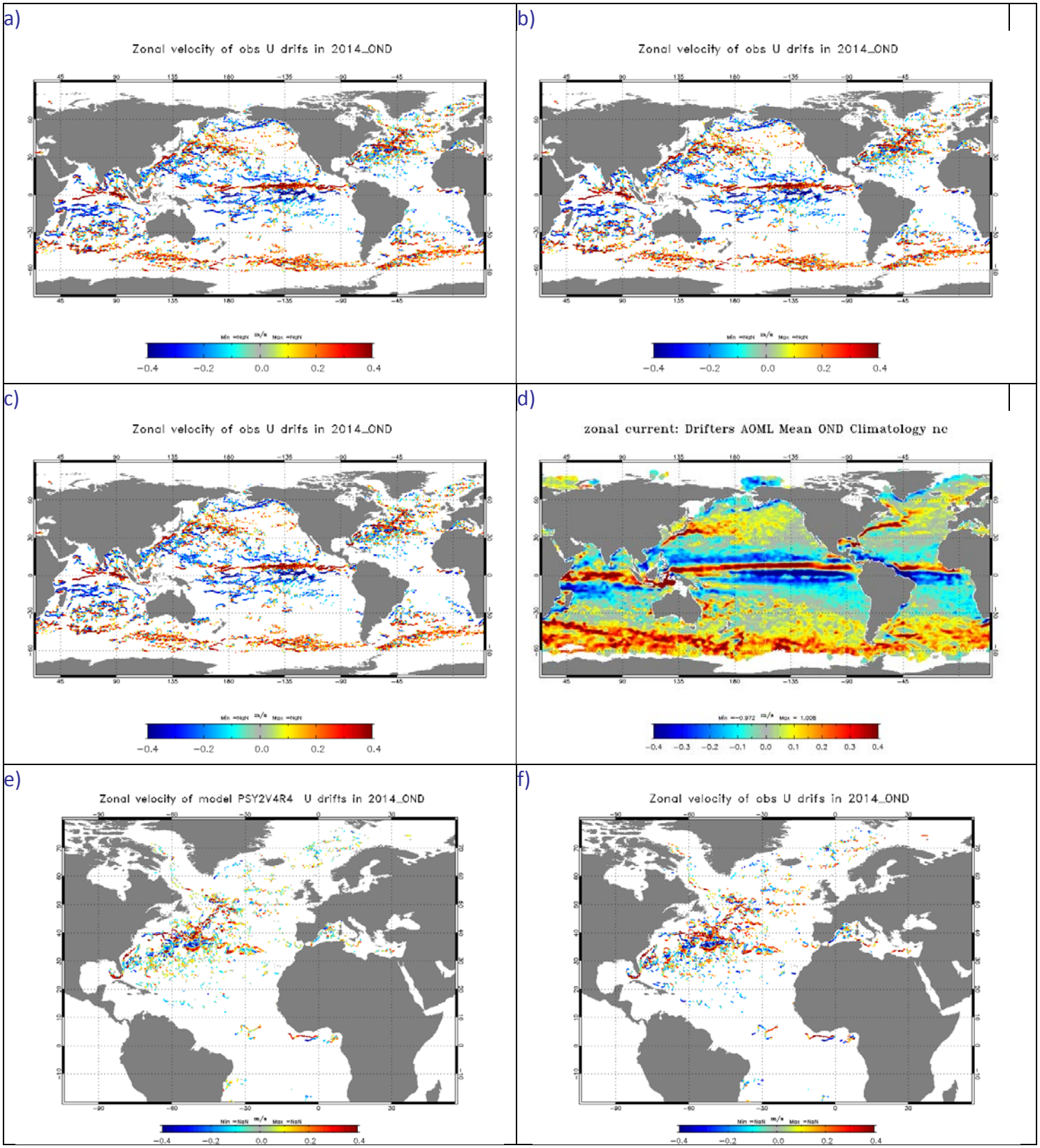

Figure 34: **Near surface (15m) zonal current (m/s) comparison between the Mercator systems analyses and observed velocities from drifters. In the left column: velocities collocated with drifter positions in OND 2014 for PSY3V3R3 (a), PSY4V2R2 (c) and PSY2V4R4 (e). In the right column, zonal current from drifters in OND 2014 (b) at global scale, AOML drifter climatology for OND with new drogue correction from Lumpkin & al, in preparation (d) and observed zonal current in OND 2014 (f) over PSY2's domain.**

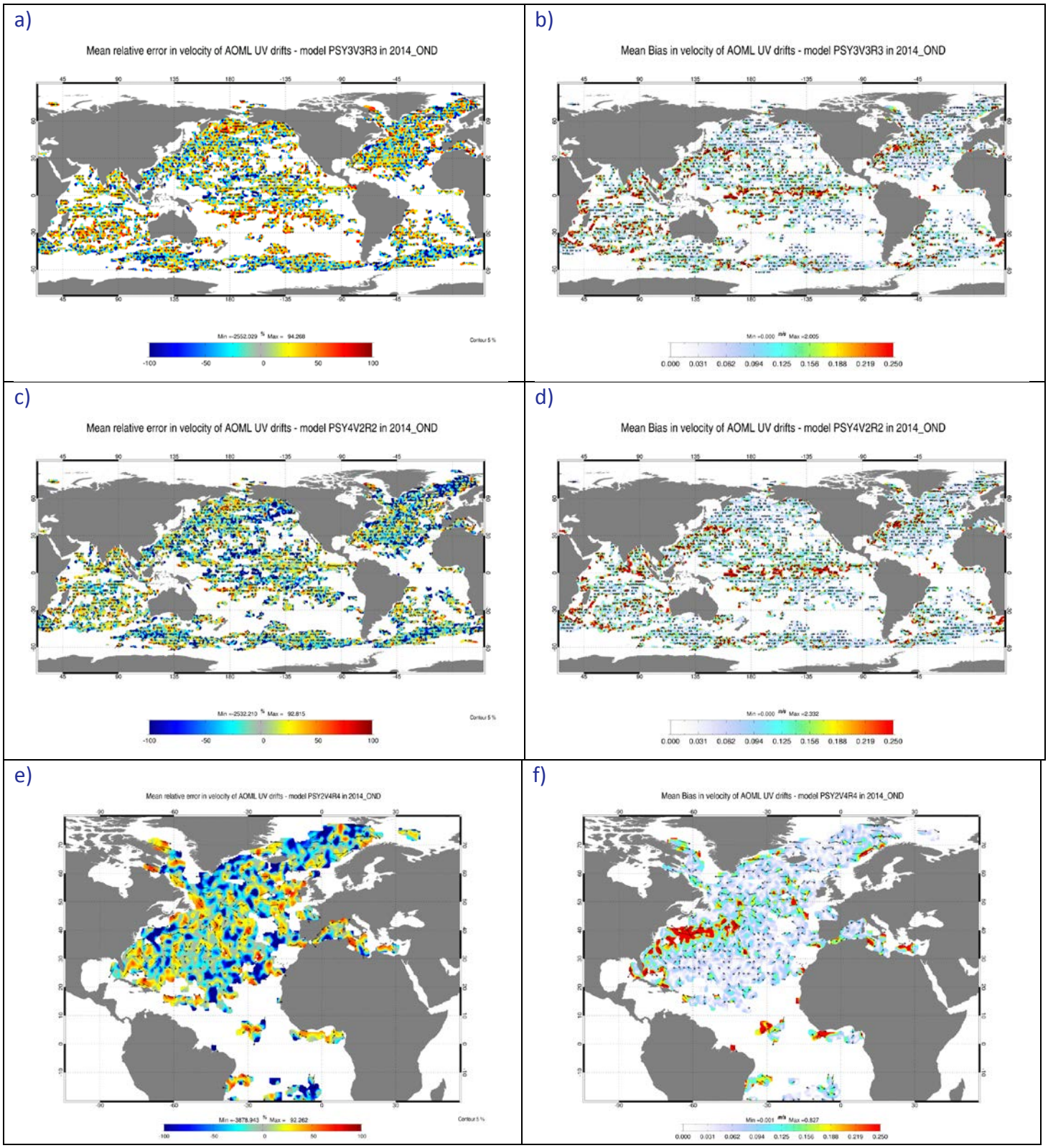

Figure 35 : In OND 2014, comparison of the mean relative velocity error between in situ AOML drifters and model data (a, c and e) and mean zonal velocity bias between in situ AOML drifters with Mercator Ocean correction (see text) and model data (b, d and f). a and b: PSY3V3R3, c and d: PSY4V2R3, e and f: PSY2V4R2. NB: zoom at 500% in order to see the arrows.

The fact that velocities estimated by the drifters happen to be biased towards high velocities is taken into account, applying slippage and windage corrections (cf QuO Va Dis? #5 and Annex C). Once this so called

"Mercator Ocean" correction is applied to the drifter observations, the zonal velocity of the model (Figure 34 and Figure 35) at 15 m depth and the meridional velocity (not shown) is more consistent with the observations for the OND 2014 period.

On average in this OND quarter, the usual behaviour compared to drifters' velocities is that the high resolution system PSY4 overestimates the surface velocity in the mid-latitudes and the low resolution PSY3 underestimates the currents. PSY4 overestimates the Equatorial Pacific currents (South Equatorial Current and North Equatorial Counter Current), the Kuroshio region, the Gulf of Alaska and the Southern Oceans. PSY3 underestimates the Pacific South Equatorial Current, the Western subarctic gyre and the South Indian Ocean and overestimates the Southern oceans and the Gulf Stream region.
For all systems the largest direction errors are local (not shown) and generally correspond to ill positioned strong current structures in high variability regions (Gulf Stream, Kurioshio, North Brazil Current, Zapiola eddy, Agulhas current, Florida current, East African Coast current, Equatorial Pacific Countercurrent).

The differences between the systems mainly appear in the Atlantic and Pacific gyres, in the Western subartic gyre and in the South Indian basin see Figure 35. 50% of the ocean current feedbacks on the wind stress in PSY2 and PSY3, which slows the surface currents with respect to PSY4.

V.2.3.2. Lagrangian Quality control

The aim of the Lagrangian approach is to compare the observed buoy trajectory with virtual trajectories obtained with hindcast velocities, starting from the same observed initial location. The virtual trajectories are computed with the ARIANE software[6] (see annex **Erreur ! Source du renvoi introuvable.**). The metric shown here (Figure 36) is the distance between the trajectories after 1, 3 and 5 days, displayed at each trajectory initial point.

a)

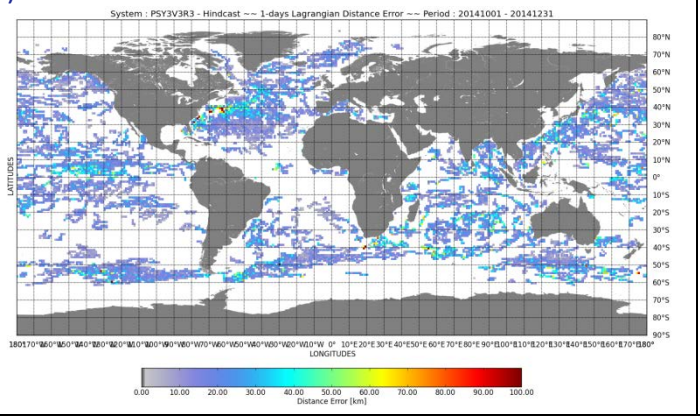

b)

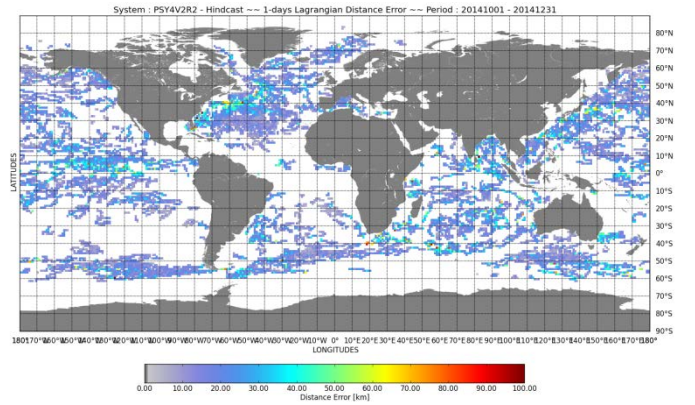

[6] http://stockage.univ-brest.fr/~grima/Ariane/

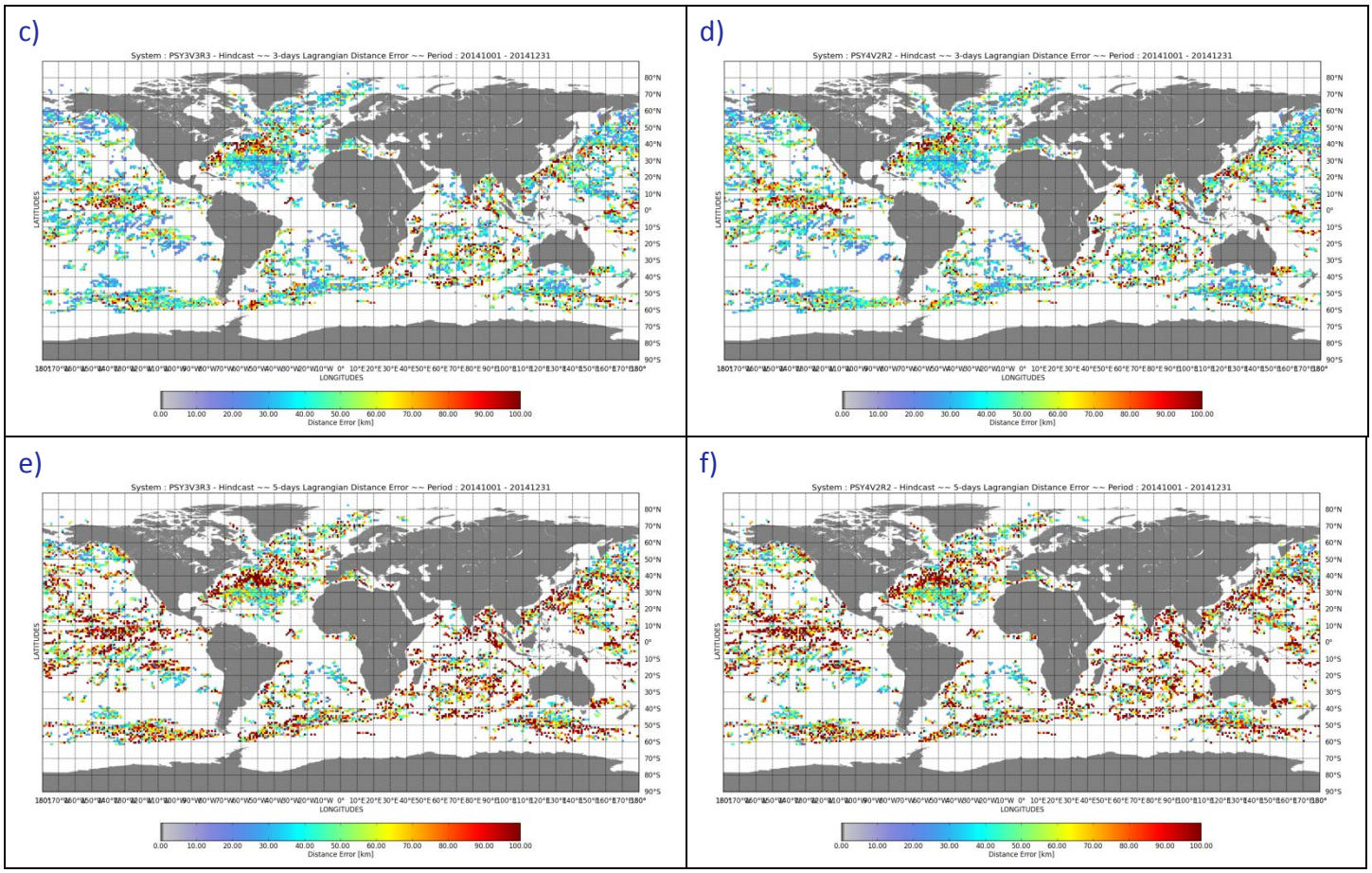

Figure 36: In OND 2014, comparison of the mean distance error in 1°x1° boxes after a 1-day drift (a and b), after a 3-days drift (c and d), and after a 5-days drift (e and f).between AOML drifters' trajectories and PSY3V3R3 trajectories (a, c, and e) and between AOML drifters' trajectories and PSY4V2R2 (b,d, and f).

Few differences appear between the systems and most of the high velocity biases that are diagnosed in Figure 35 imply a large distance error (120 to 180km) after a few days drift in Figure 36. For instance in the Pacific ocean, both PSY3 and PSY4 produce an error larger than 100km after only a 1-day drift near the North Coast of Papua New Guinea.

In the subtropical gyres and in the North Pacific, which are less turbulent regions, the errors rarely exceed 30 km after 5 days.

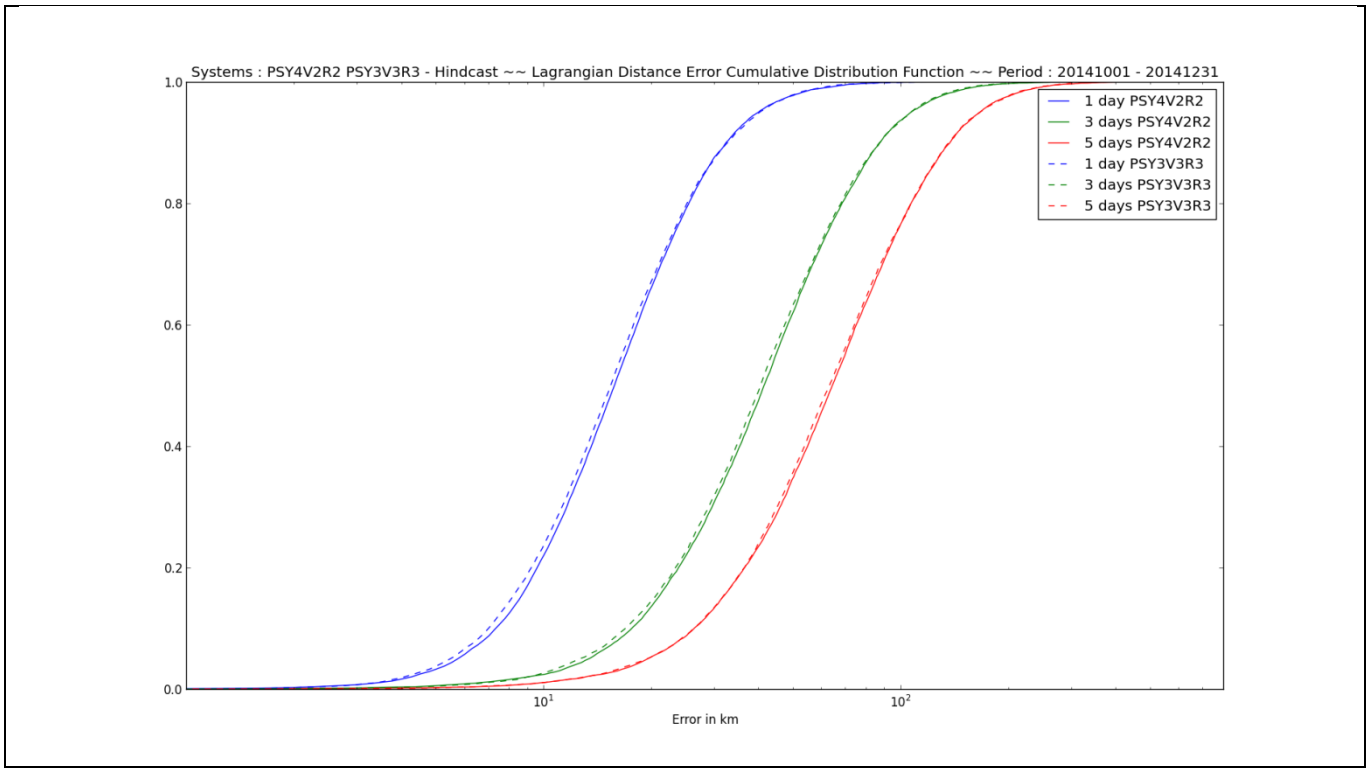

Figure 37:Cumulative Distribution Functions of the distance error (km, on the left) and the direction error (degrees, on the right panel) after 1 day (blue), 3 days (green) and 5 days (red), between PSY4V1R3 forecast trajectories and actual drifters trajectories.

Over the whole domain on a long period, cumulative distribution functions (Figure 37) show that in 80% of cases, PSY3 and PSY4 modelled drifters move away from the real drifters less than : 30km after 1 day, 70km after 3 days, and 100km after 5 days. As explained before, the remaining 20% generally correspond to ill positioned strong current structures in high variability regions. PSY4 currents seem to induce slightly more errors than PSY3 currents essentially for errors below 10-15 km. This is probably related to the high mesoscale activity of the global high resolution model. This may not be systematic at the regional scale (under investigation).

V.2.4. Sea ice concentration

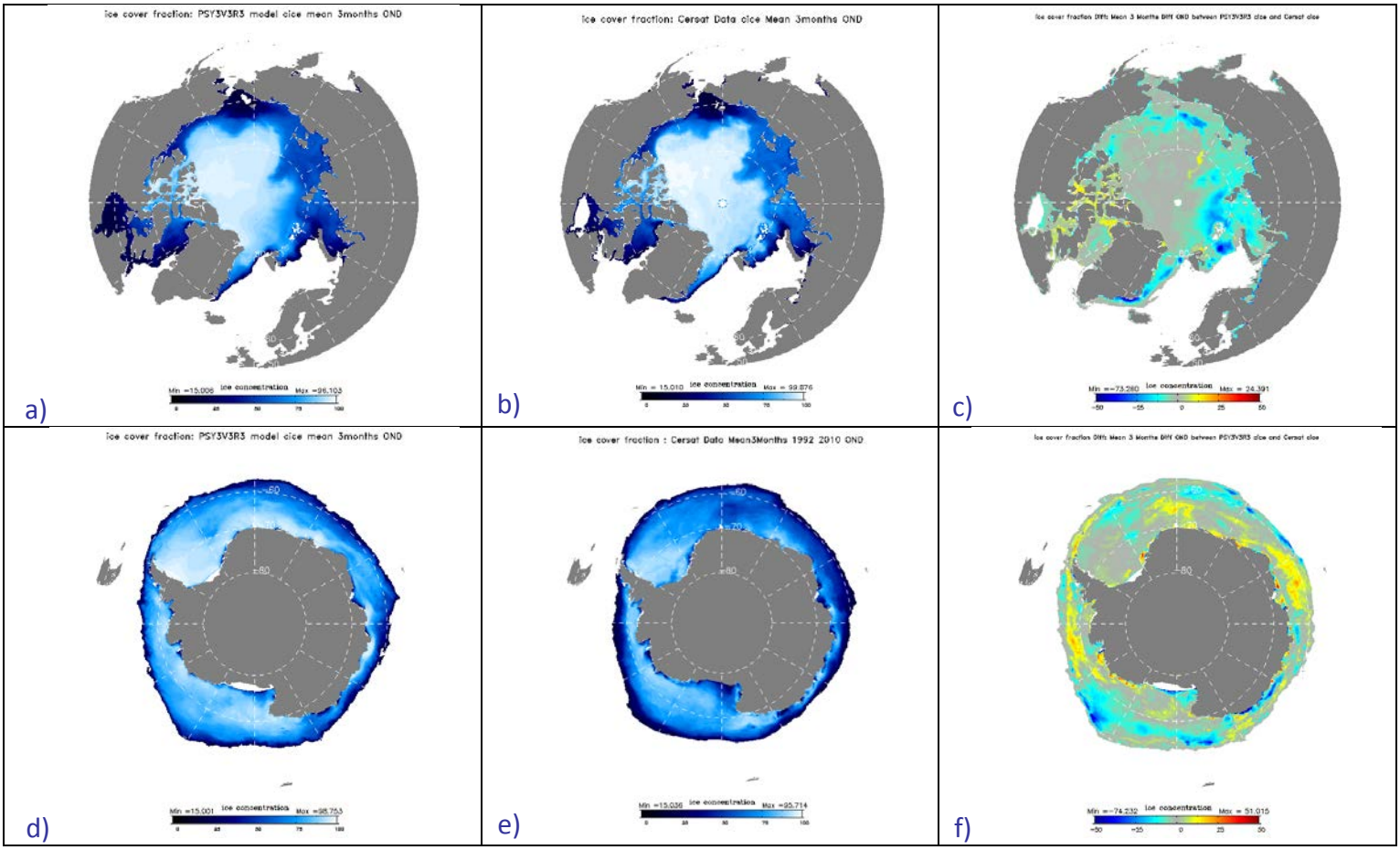

Figure 38: Arctic (a to c) and Antarctic (d to f) OND 2014 Sea ice cover fraction in PSY3V3R3 (a and d), in CERSAT observations (b and e) and difference PSY3 – CERSAT (c and f).

On average over the OND 2014 period, sea ice concentration of the two systems is close to the observations. For both PSY3 and PSY4, underestimations of modelled sea ice concentration with observed sea ice concentration appear near the marginal zones (Greenland Sea, North of Barent Sea, Kara Sea) and in the Canadian basin (Figure 38 and Figure 39). We can notice that the sea ice observations are not yet assimilated by the systems. Even if PSY3 and PSY4 are melting too much ice in the summer, in the beginning of winter the sea ice cover seems to be close to the data. In the Arctic, differences with observations are in the same order for PSY3 and PSY4. Few discrepancies can be distinguished inside the sea ice pack but it will not be considered as significant as the sea ice concentration observations over 95% are not reliable.
Model studies show that the overestimation in the Canadian Archipelago is first due to badly resolved sea ice circulation.
In the Antarctic the summer sea ice concentration is underestimated on average by both PSY3 and PSY4, On the contrary it is overestimated along the sea ice edge in the Bellingshausen Sea and in the South of Kerguelen Island.

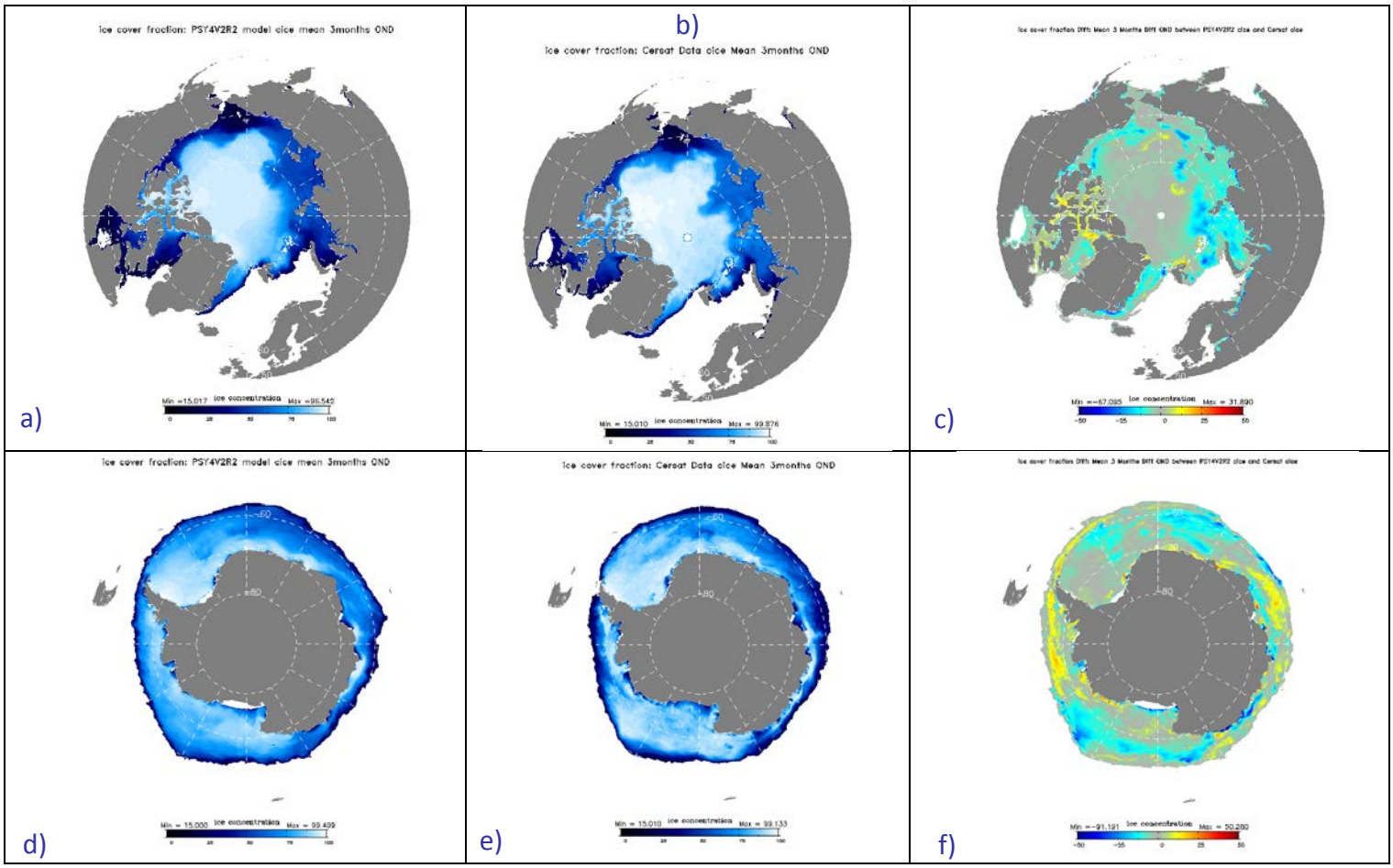

Figure 39: Arctic (a to c) and Antarctic (d to f) OND 2014 Sea ice cover fraction in PSY4V2R2 (a and d), in CERSAT observations (b and e) and difference PSY4 – CERSAT (c and f).

Figure 40 illustrates the fact that in Arctic, the sea ice cover in OND 2014 is less than the past years climatology, especially in the Bering Strait, Greenland Sea, Kara and Barents Sea (see also section IV).
For the Antarctic, the ice cover is greater than the climatology except in the Bellingshausen Sea and in the Southern Indian Ocean. This decrease is due in large part to persistent northerly winds.

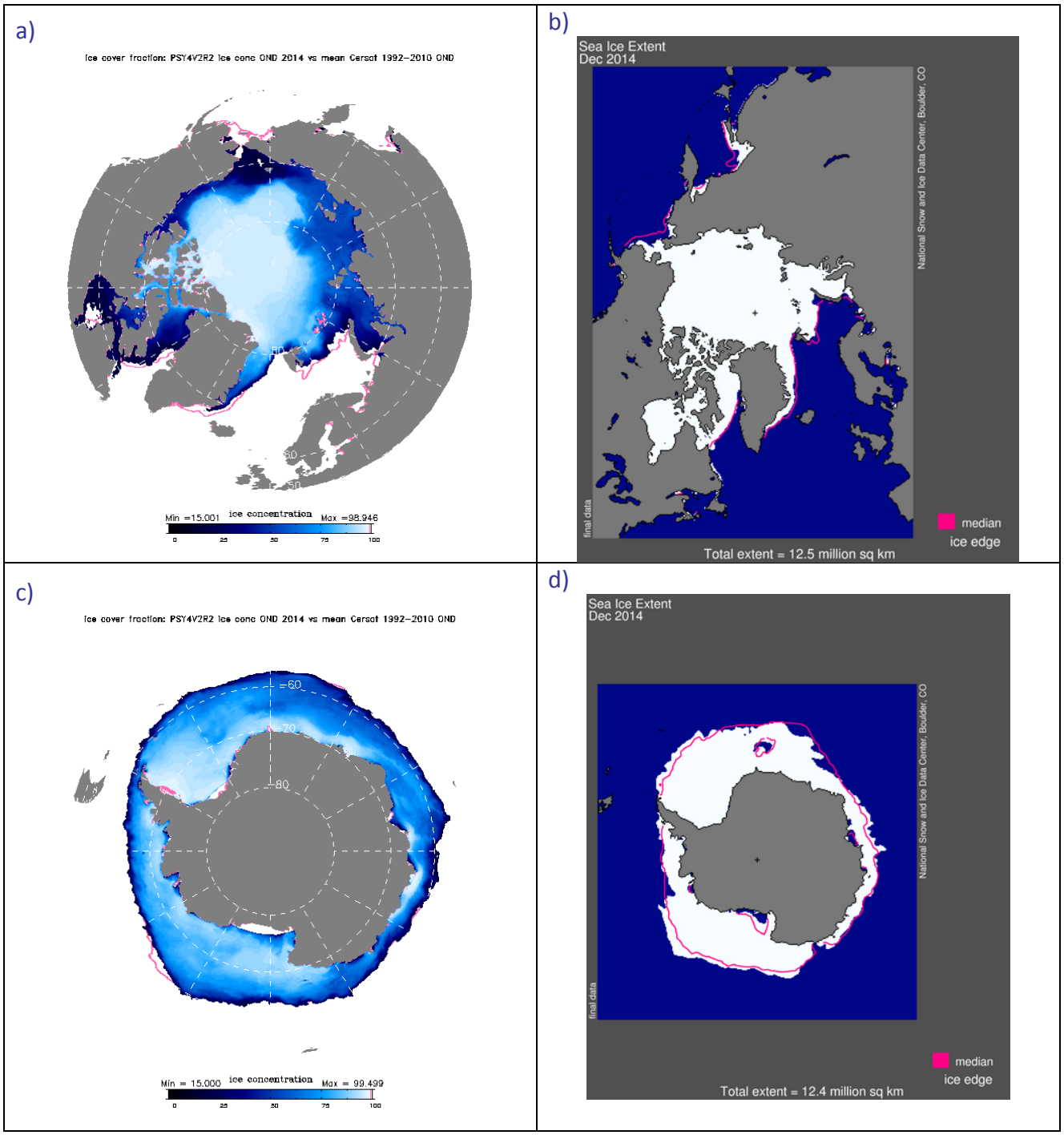

Figure 40: OND 2014 Arctic sea ice extent in PSY4V2R2 with overimposed climatological OND 1992-2010 sea ice fraction (magenta line, > 15% ice concentration) (a) and NSIDC map of the sea ice extent in the Arctic for December 2014 in comparison with a 1979-2000 median extend (b), the same for the Antarctic region for the PSY4V2R2 system c) and the NSIDC estimation d) (ftp://sidads.colorado.edu/DATASETS/NOAA/G02135/Dec/).

V.2.5. Closer to the coast with the IBI36V2 system: multiple comparisons

V.2.5.1. Comparisons with SST from CMS

The bias, RMS error and correlation calculated from comparisons with SST measured by satellite in OND 2014 (Météo-France CMS high resolution SST at 0.02°) are displayed in Figure 41. The cold bias in the North Sea present in JAS 2014 has almost vanished. A cold bias is still present in the Irish Sea and in the Alboran Sea. A warm bias is present along the south Moroccan coast and Canary Islands, and in a large area west of the Iberian Peninsula between 35°N and 50°N. This last warm bias was present in OND 2013 but not so extended (not shown). In the Mediterranean Sea a warm bias can be noticed in the south-west corner of Spain between the coast and the Baleares Islands. Low correlations can be noticed (<0.4) in the northern part of the domain, associated with a warm bias. PSY2 and PSY4 systems show similar results but the biases are generally smaller (especially the cold biases in the Irish Sea and in the Alboran Sea).
Note that the number of observations in the Mediterranean Sea is very good for OND 2014 compared to previous years.

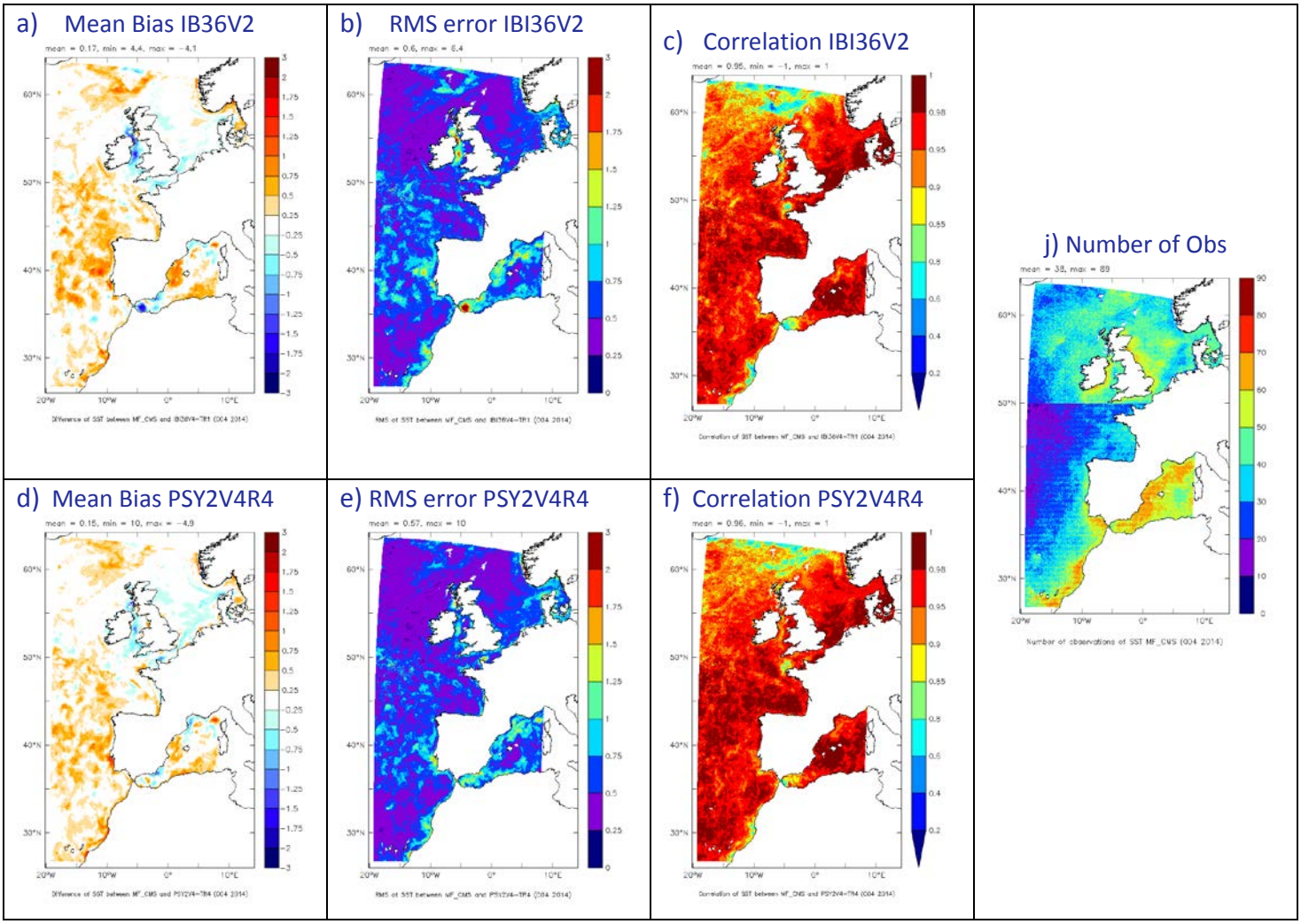

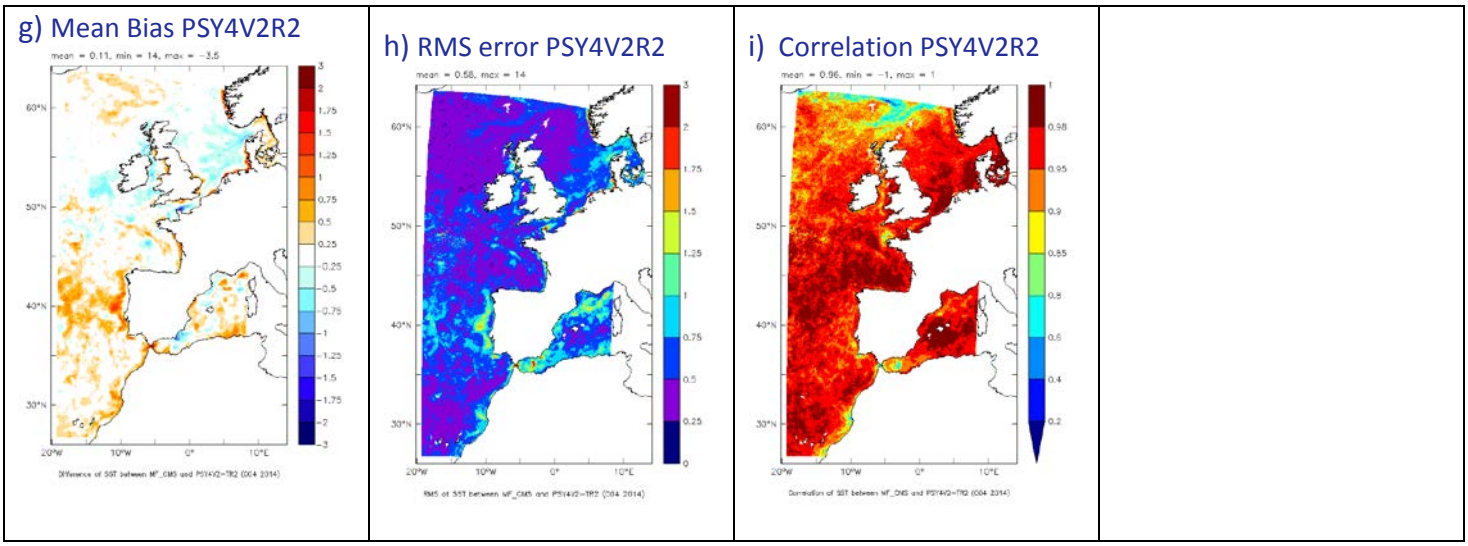

Figure 41 : Mean bias (observation-model) (a), RMS error (b), correlation (c) between IBI36V2 and analysed L3 SST from Météo-France CMS for the OND 2014 quarter. Same diagnostics for PSY2V4R4 (d,e,f) and PSY4V2R2 (g,h,i). Number of Météo-France CMS observations for the OND 2014 quarter (j).

V.2.5.2. Comparisons with in situ data from EN3/ENSEMBLE for OND 2014

Averaged temperature profiles (**Figure 42**) show that the strongest mean bias and RMS error (more than 2°C) are observed between surface and 100 m depth, and around 500 m depth, as in OND and JAS 2014. Below the thermocline, the mean bias is almost zero. In the Bay of Biscay, the bias and RMS error are also maximum near the surface and at the Mediterranean water level. As shown by the mean temperature profiles, IBI36 and PSY2 are very close.

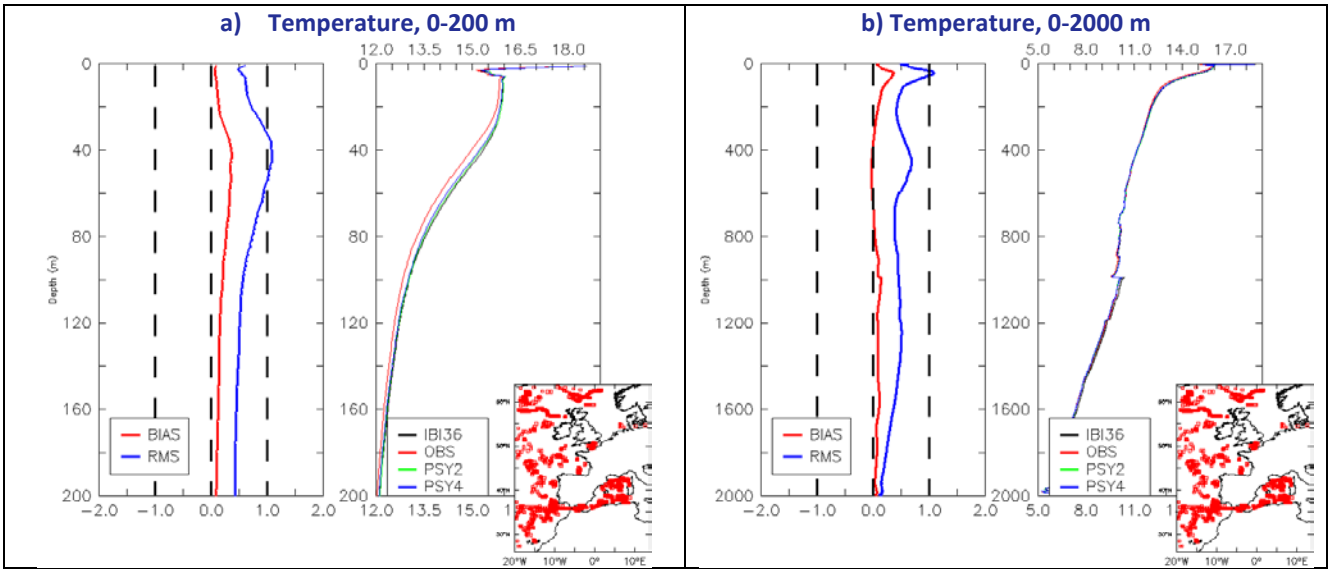

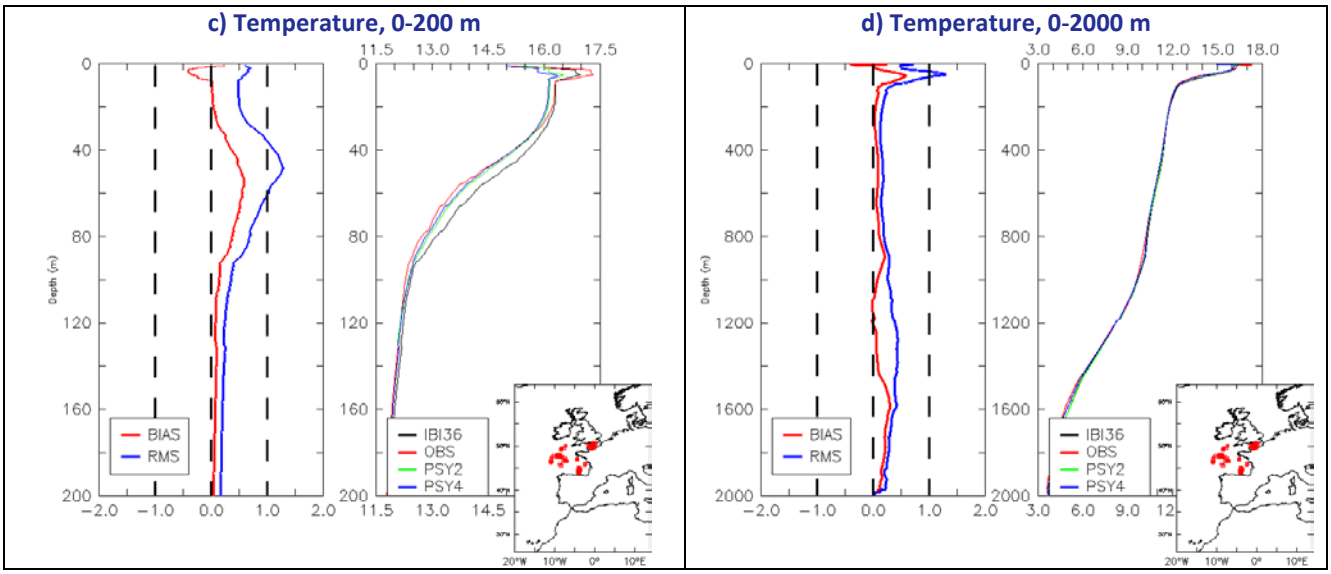

Figure 42 : Over the whole IBI36V4 domain (a and b) and over the Bay of Biscay (c and d): mean "IBI36V4 - observation" salinity (psu) bias (red) and RMS error (blue) in OND 2014 (a and c), and mean profile from IBI36V4 (black), PSY2V4R4 (green) and from the observations (red) in OND 2014 (b and d). In the lower right corner of each plot: position of the individual profiles.

The maximum salinity bias and RMS error (Figure 43) occur near the surface. The model is too fresh between the surface and 120 m depth, with PSY2 closer to the observations than IBI36. The RMS error is slightly stronger at the Mediterranean Sea Water level. In the Bay of Biscay the Mediterranean waters are too salty. Note: averaged profiles are discontinuous because the number of observations varies with depth.

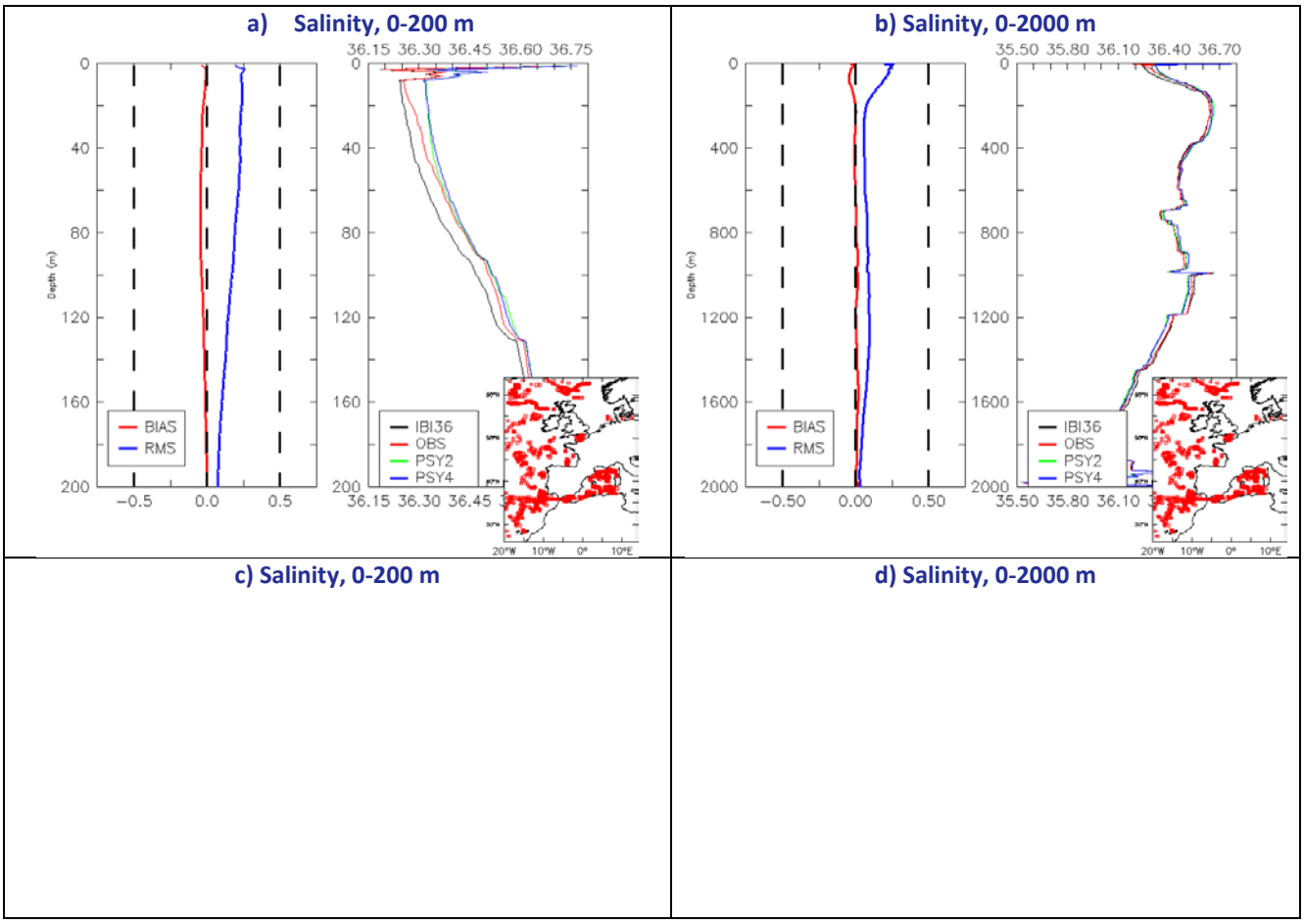

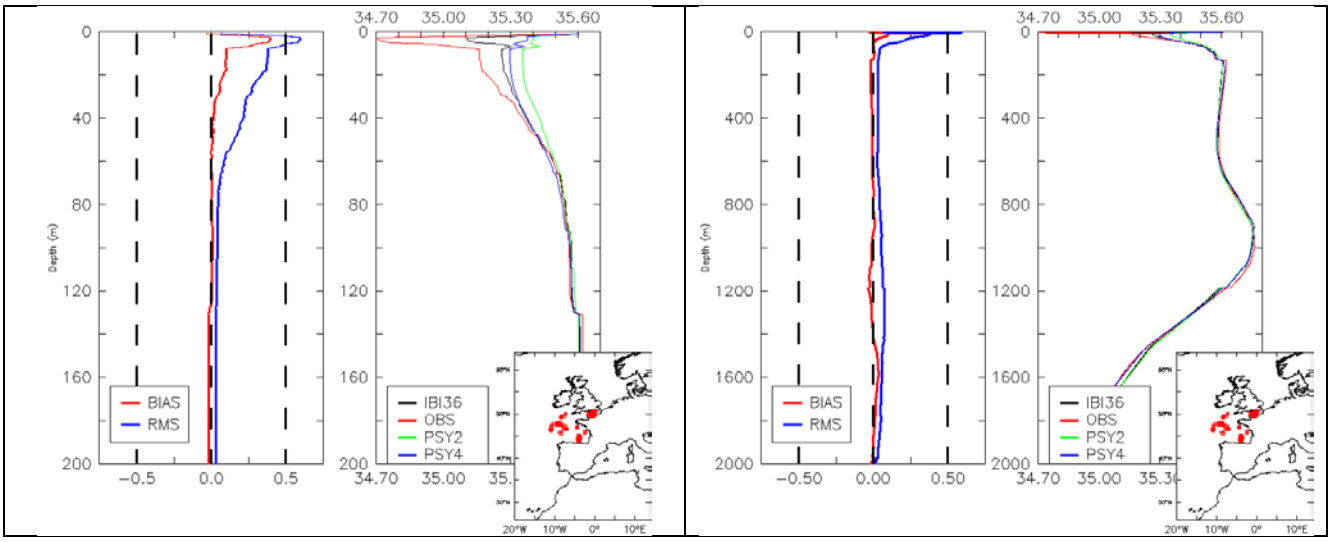

Figure 43: Over the whole IBI36V4 domain (a and b) and over the Bay of Biscay (c and d): mean "IBI36V4 - observation" salinity (psu) bias (red) and RMS error (blue) in OND 2014 (a and c), and mean profile from IBI36V4 (black), PSY2V4R4 (green) and from the observations (red) in OND 2014 (b and d). In the lower right corner of each plot: position of the individual profiles.

V.2.5.3. MLD Comparisons with in situ data

Figure 44 shows that the distribution of modeled mixed layer depths among the available profiles is comparable to the observed distribution for both PSY2 and IBI over the whole IBI domain. Values of the mixed layer depth between 50 m and 70 m occur too often in the systems compared with the observations (especially for PSY2). In the Bay of Biscay, IBI36 over-estimates the values between 15 m and 35 m, and under-estimates the values between 35 m and 60 m.

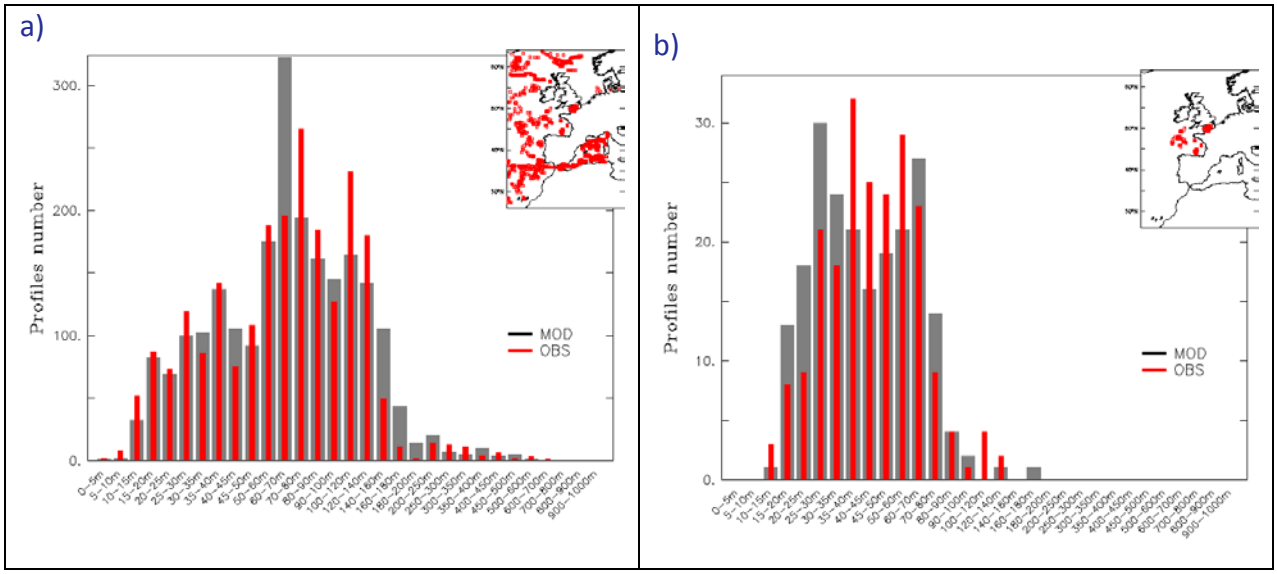

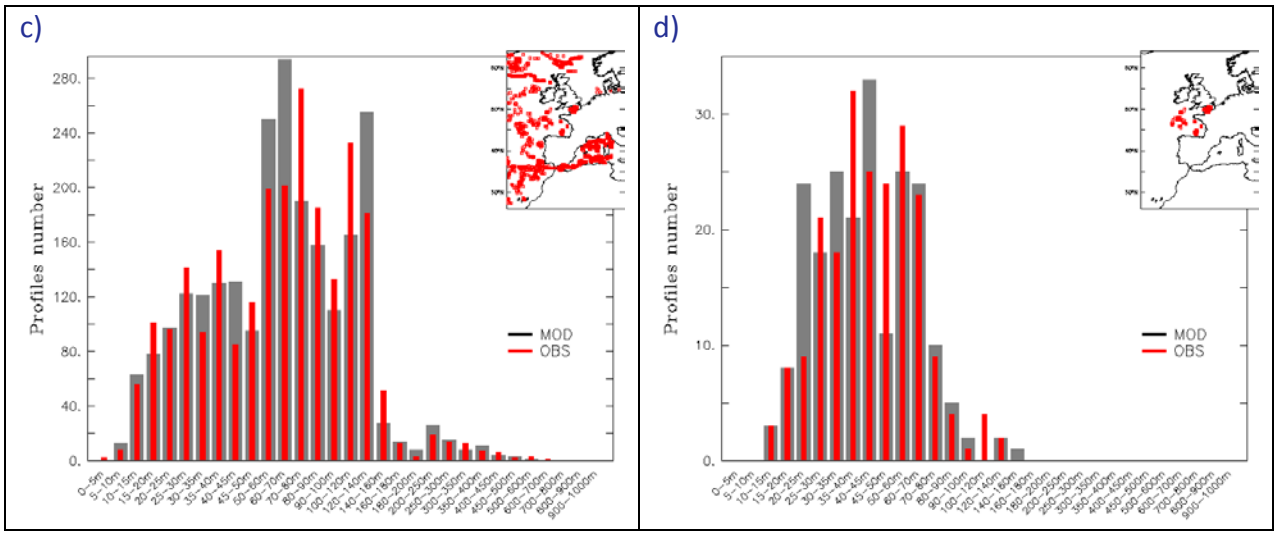

Figure 44 : Mixed Layer Depth distribution in OND 2014 in IBI36V4 (a and b) and PSY2V4R4 (c and d), calculated from profiles with the temperature criteria (difference of 0.2°C with the surface); the models are in grey, the observations in red. a and c: classification for the whole IBI domain, b and d: classification for the Bay of Biscay

V.2.5.4. Comparisons with moorings and tide gauges

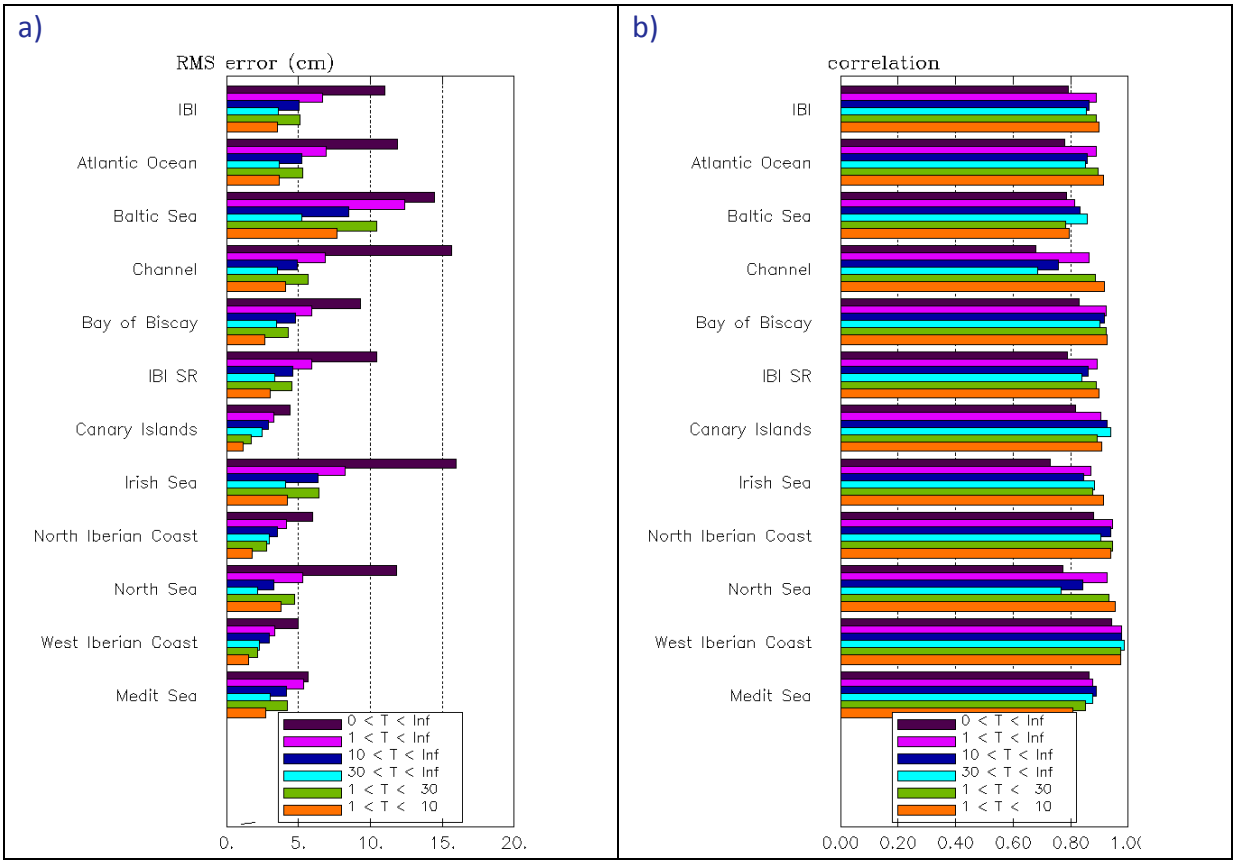

Figure 45 : For IBI36V4: RMS error (a, in cm) and correlation (b) for the non-tidal Sea Surface Elevation at tide gauges in OND 2014, for different regions and frequencies.

The RMS error of the residual (non tidal) elevation of sea surface (Figure 45) computed with harmonic decomposition (Foreman 1977) and Loess low-pass filtering is between 5 and 16 cm. It is close to 5 cm in the Canary Islands, Mediterranean Sea and Iberian Coast. The RMS decreases for some frequency bands, and the

smallest values occur in the 1-10-day band. The correlation is significant at all frequencies, and reaches high values for periods lower than 30 days (at high frequencies).

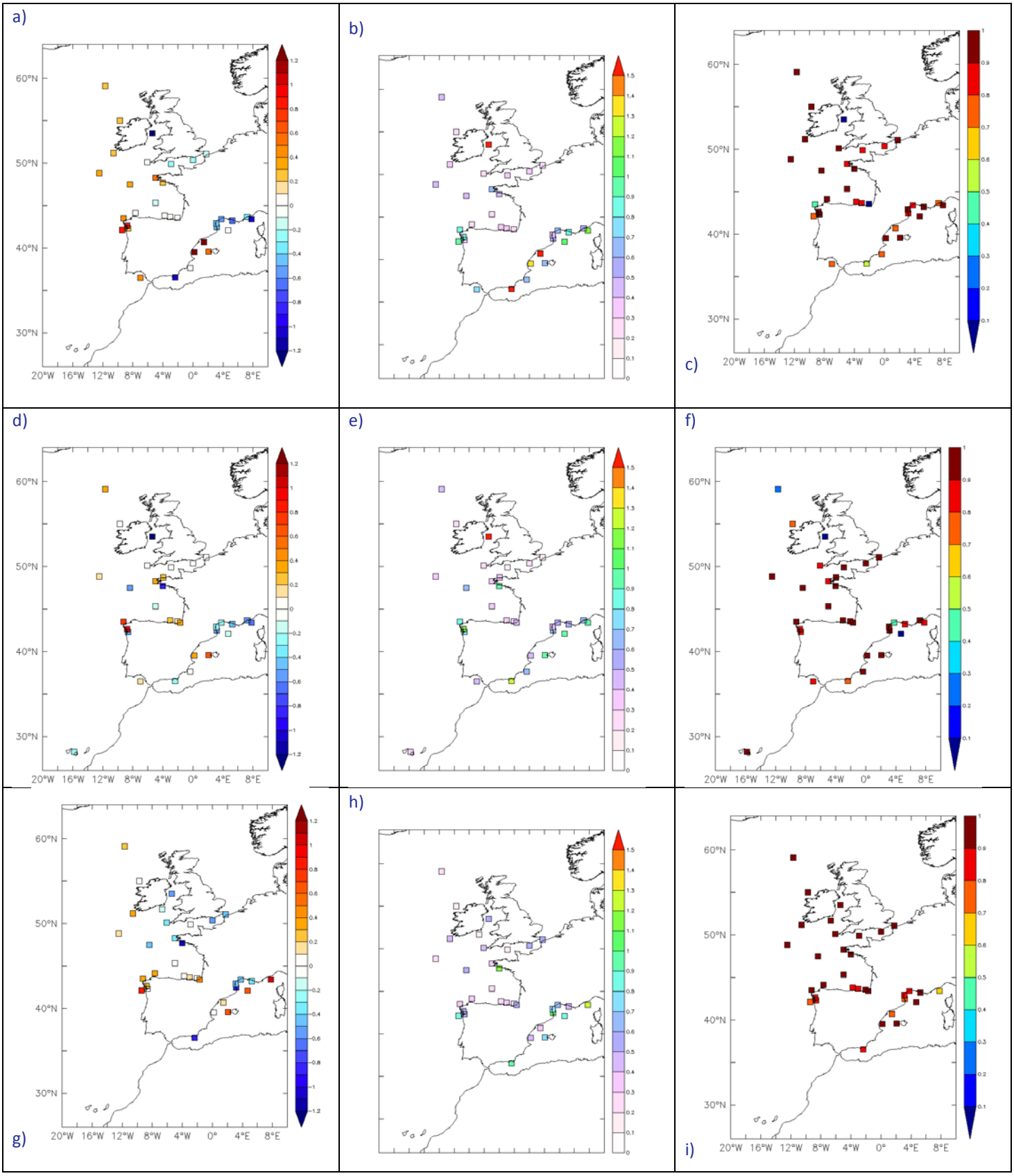

Figure 46 : For IBI36V4: Bias (observation-model) (a, d and g), RMS error (°C) (b, e and h) and correlation (c, f and i) of the Sea Surface Temperature between IBI36 and moorings measurements in October (a to c), November (d to f) and December 2014 (g to i).

In Figure 47 we can see that the SST correlations between the coastal moorings and the IBI model are generally good for the three months. In December the model is colder than the observations in the Irish Sea, Celtic Sea and English Channel. Along the coast of the Gulf of Lions, the model is colder than the observations for the three months.

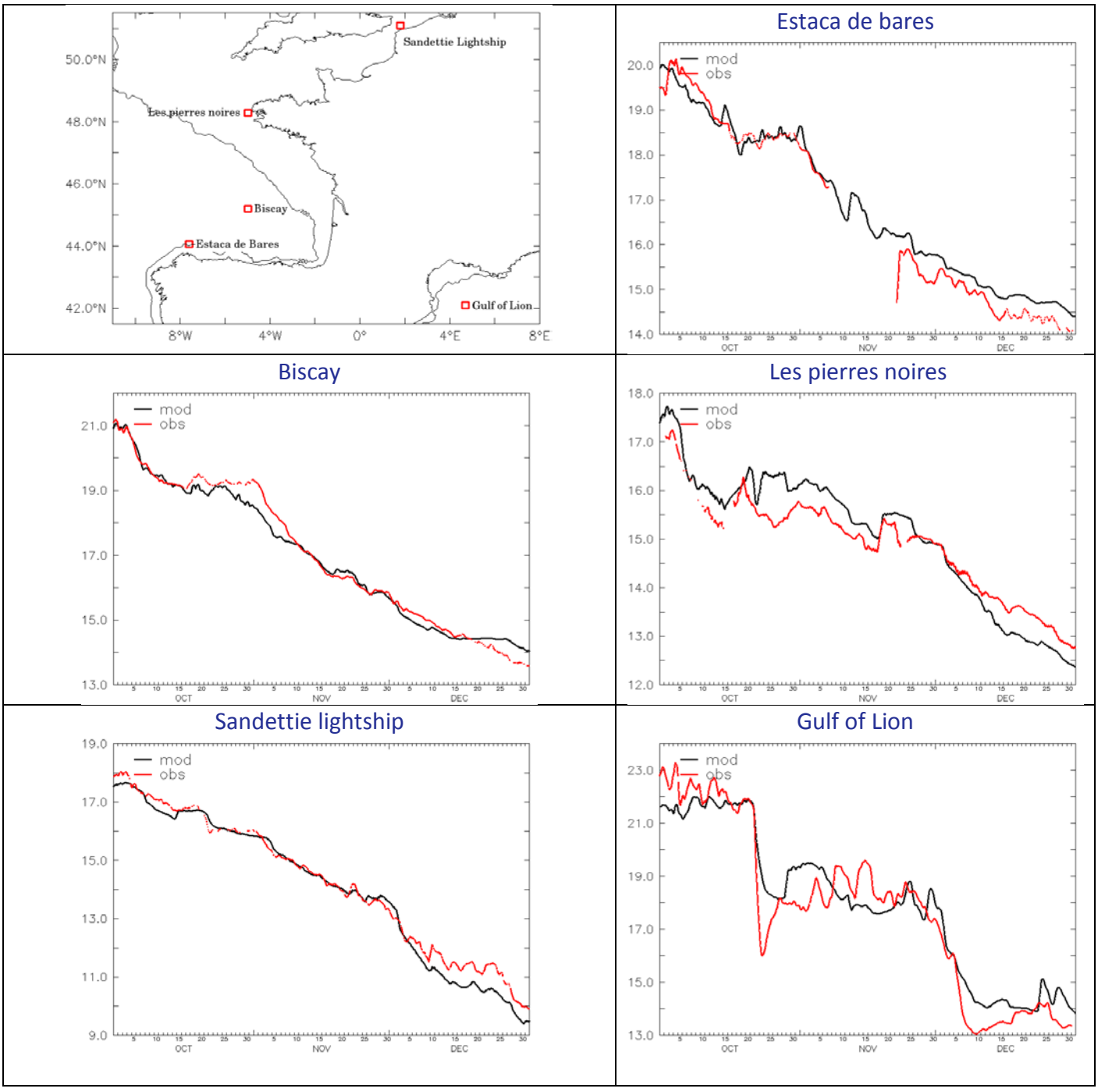

Figure 47 : Surface temperature (°C) time series at a selection of moorings which locations are shown on the upper left panel (no observation for Gulf of Lion).

V.2.6. Biogeochemistry validation: ocean colour maps

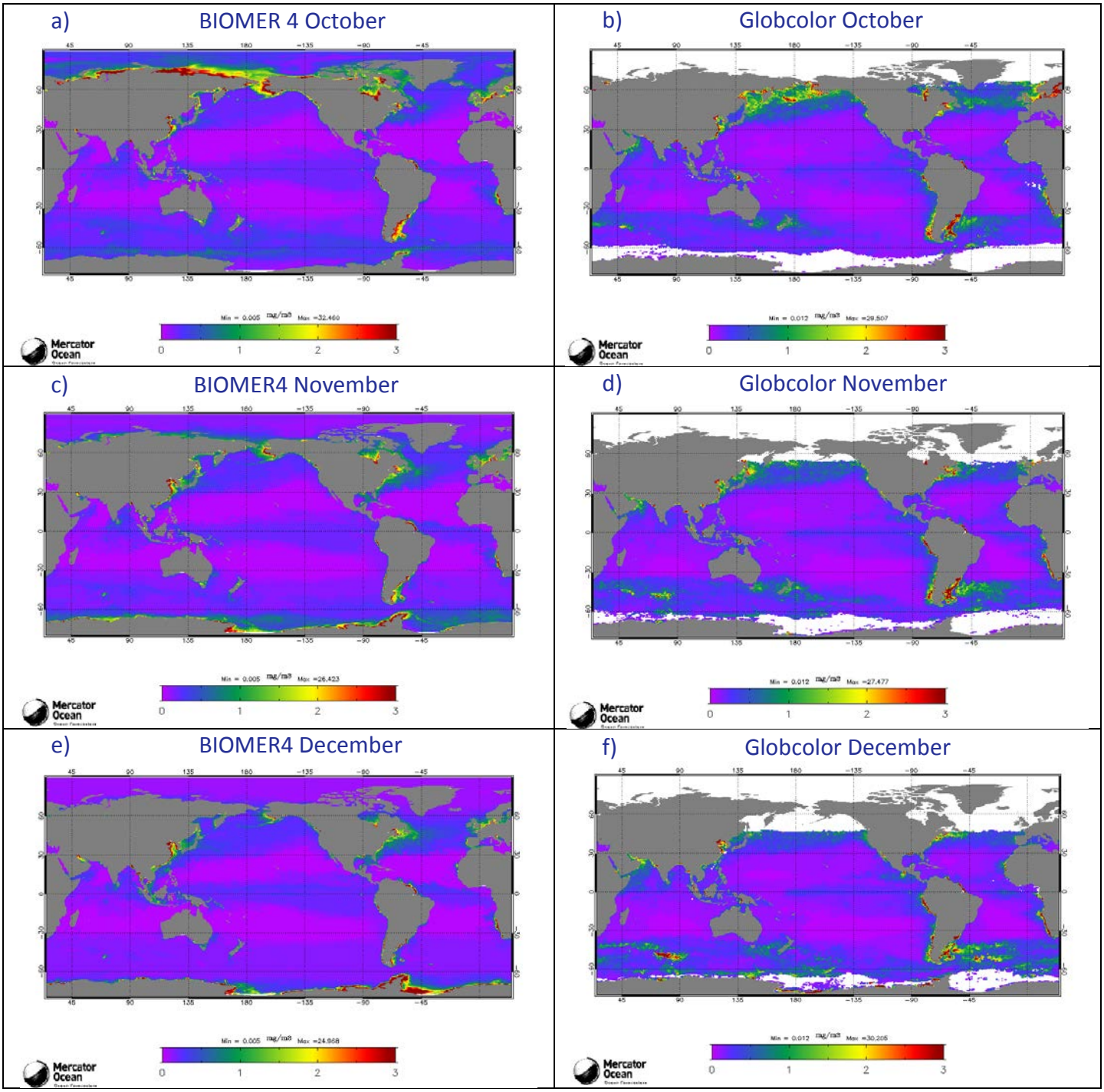

Figure 48 : Chlorophyll-a concentration (mg/m^3) in October(a and b), November (c and d) and December 2014 (e and f) for the Mercator system BIOMER4 (a, c, and e) and Chlorophyll-a concentration from Globcolour (b, d and f).

As can be seen on Figure 48, the surface chlorophyll-a concentration by the new version of BIOMER (BIOMER4 see Quovadis #18 for a complete description) is in a good agreement with observations on average over the globe. Discrepancies remain anyway: along the Argentina's coast, near Bering Strait, or in the subpolar gyres. For the distribution of Chlorophyll-a concentration errors in Figure 49 , the shape of BIOMER4's distribution is Gaussian but the mean bias remains still important.

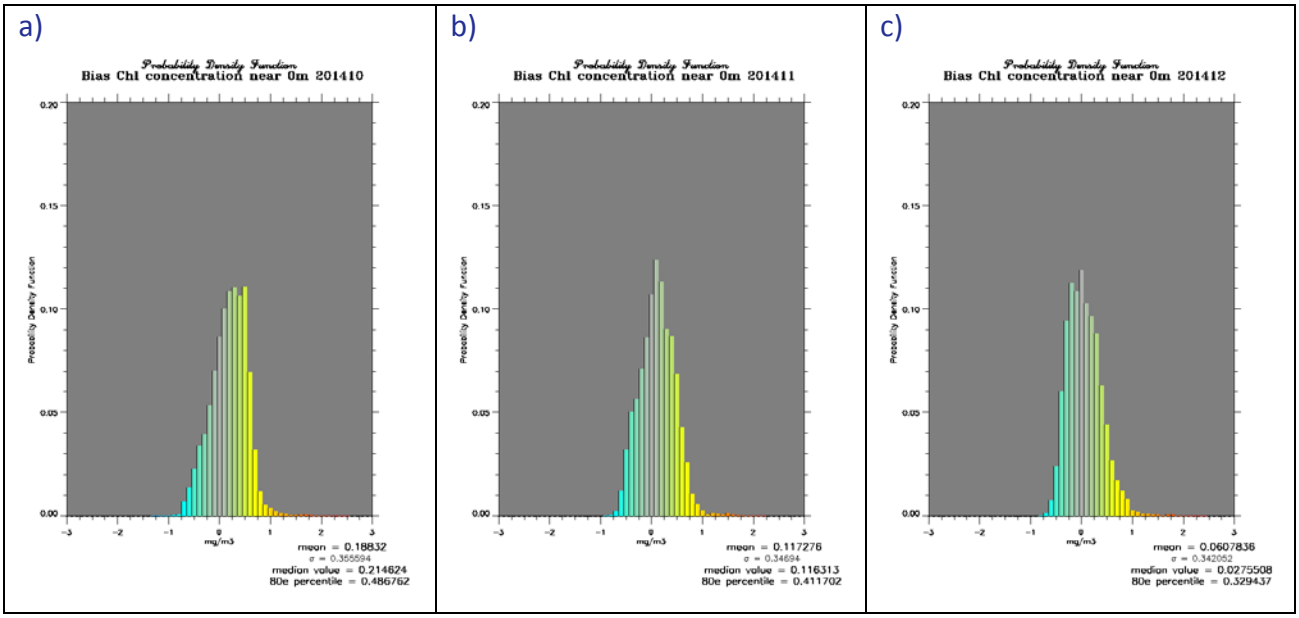

Figure 49 : Probability Density Function (PDF) of Chl-a bias in log scale (log10(obs)-log10(model)) in the North Atlantic (30-70N; 80W:20E) for October (a), November (b) and December (c) 2014.

The discrepancies at the global scale appear in the RMS differences for the mean OND 2014 season (Figure 50) especially in the Zapiola region, near the Peru-Chili coast (upwelling region), in the South of Indian Basin near Kerguelen Islands.

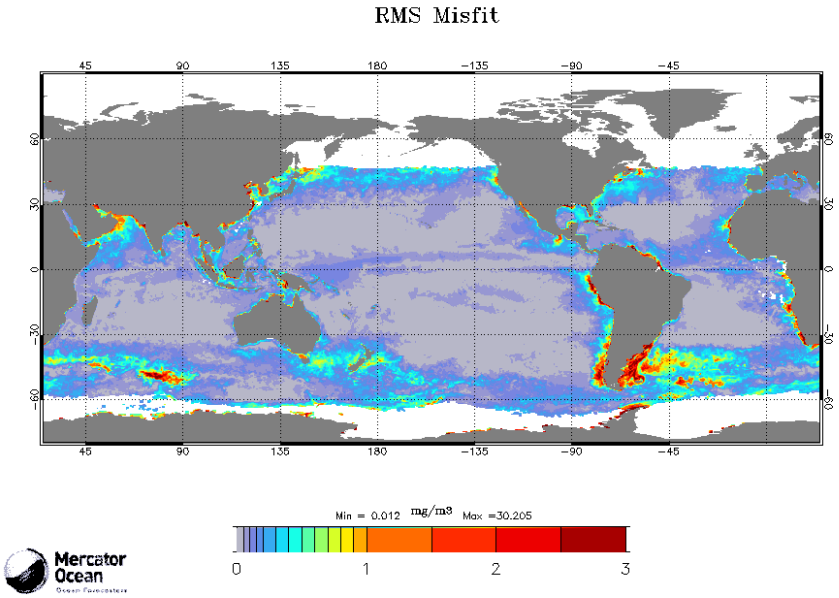

Figure 50 : RMS difference between BIOMER and Globcolour Chl-a concentrations (mg/m^3) in OND 2014.

VI Forecast error statistics

VI.1. General considerations

The daily forecasts (with updated atmospheric forcings) are validated in collaboration with SHOM/CFUD. This collaboration has been leading us to observe the degradation of the forecast quality depending on the forecast range. When the forecast range increases the quality of the ocean forecast decreases as the initialization errors propagate and the quality of the atmospheric forcing decreases. Additionally the atmospheric forcing frequency also changes (see Figure 51). The 5-day forecast quality is optimal; starting from the 6th day a drop in quality can be observed which is linked with the use of 6-hourly atmospheric fields instead of 3-hourly; and starting from the 10th day the quality is strongly degraded due to the use of persisting atmospheric forcings (but not constant from the 10th to the 14th day as they are relaxed towards a 10-day running mean).

Figure 51: Schematic of the change in atmospheric forcings applied along the 14-day ocean forecast.

VI.2. Forecast accuracy: comparisons with T and S observations when and where available

VI.2.1. North Atlantic region

As can be seen in Figure 52 the PSY2 temperature products have a better accuracy than the climatology in the North Atlantic region in OND 2014 (note that in the 2000-5000m layer, the statistics are performed on a very small sample of observations, and thus are not really representative of the region or layer. In general the analysis is more accurate than the 3-day and 6-day forecast for both temperature and salinity. The RMS error thus increases with the forecast range (shown for NAT region Figure 52 and MED region Figure 53). The biases in temperature are generally small (of the order of 0.2 °C) compared to the climatology's biases (of the order of 0.8 °C) while the salinity biases are significant (0.12 psu at the surface while the climatology bias is only 0.05 psu). The whole water column is too salty and warm (0.1°C and 0.1 PSU at the surface).

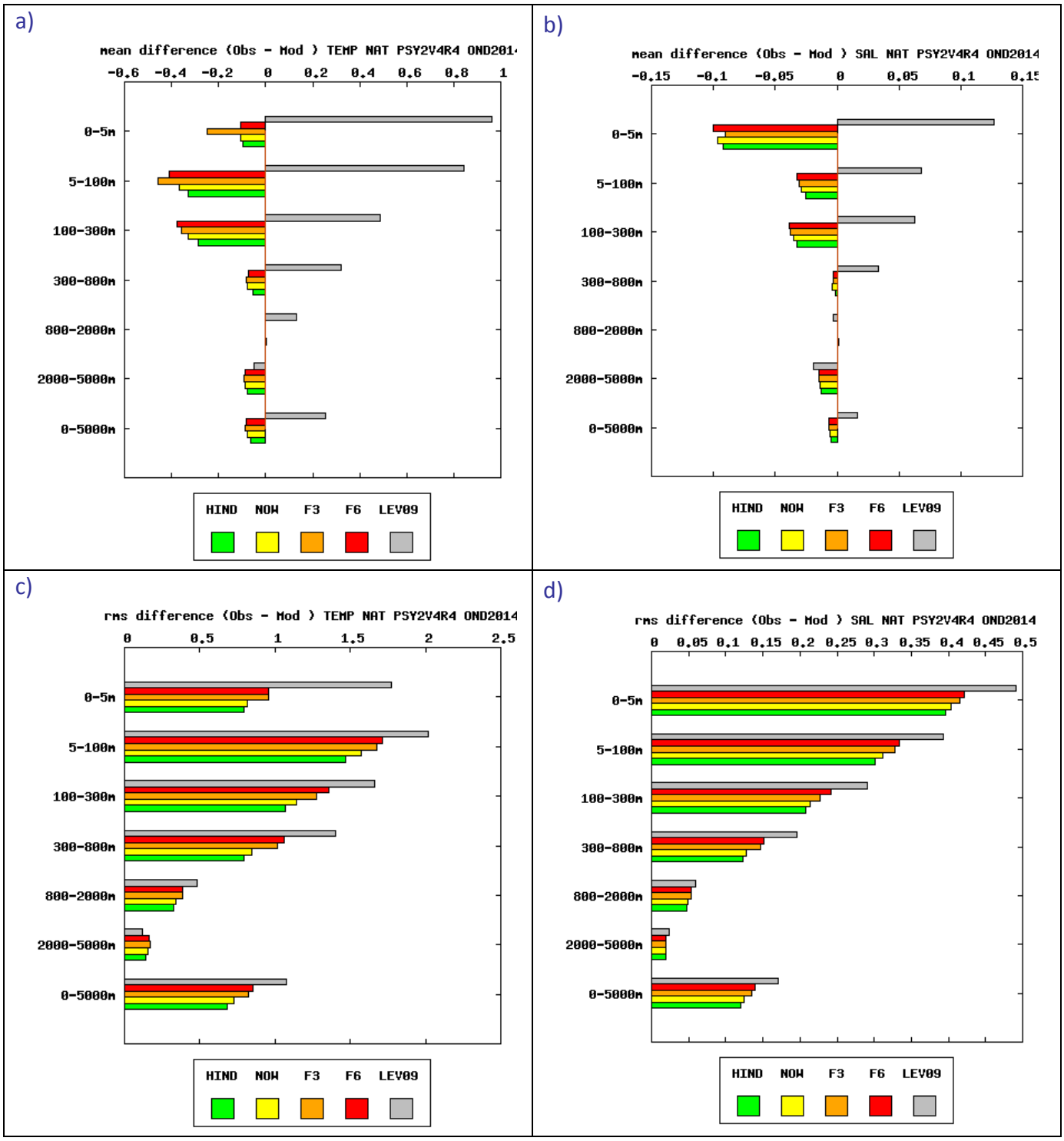

Figure 52: Accuracy intercomparison in the North Atlantic region for PSY2V4R4 in temperature (a and c) and salinity (b and dl) between hindcast (green), nowcast (yellow), 3-day (orange) and 6-day (red) forecast and WO09 climatology (grey). Accuracy is measured by a mean difference (a and b) and by a rms difference (c and d) of temperature and salinity with respect to all available observations from the CORIOLIS database averaged in 6 consecutive layers from 0 to 5000m. All statistics are performed for the OND 2014 period. NB: average on model levels is performed as an intermediate step which reduces the artefacts of inhomogeneous density of observations on the vertical.

VI.2.2. Mediterranean Sea

In the Mediterranean Sea in OND 2014 (Figure 53) the PSY2 products are more accurate than the climatology on average. PSY2 is too salty at the surface (0.03 psu) and too warm and fresh between 5-100m (up to 0.04 psu and 0.2°C).

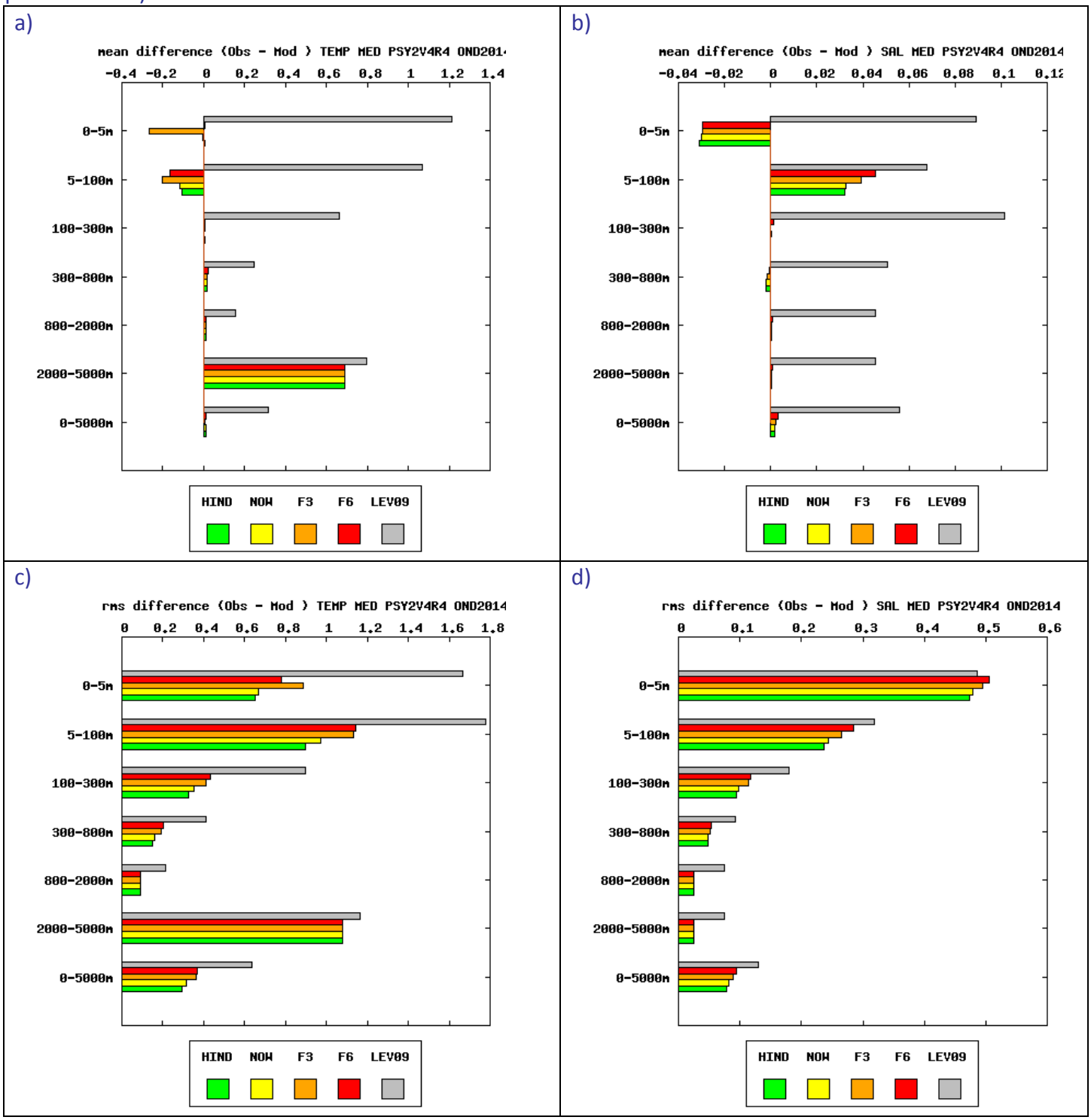

Figure 53: Accuracy intercomparison in the Mediterranean Sea region for PSY2V4R4 in temperature (°C, a and c) and salinity (psu, b and d) between hindcast, nowcast, 3-day and 6-day forecast and WO09 climatology. Accuracy is measured by a rms difference (c and d) and by a mean difference (a and b) with respect to all available observations from the CORIOLIS database averaged in 6 consecutive layers from 0 to 5000m. All statistics are performed for the OND 2014 period. NB: average on model levels is performed as an intermediate step which reduces the artefacts of inhomogeneous density of observations on the vertical.

VI.2.3. Tropical Oceans and global

Results already described in previous sections are confirmed by the profiles shown in Figure 54. PSY4 and PSY2 are usually warmer (less cold) than PSY3 and the observations in common regions especially in the 0-800m layer. PSY2 and PSY4 suffer from a fresh bias in the Tropical oceans, especially in the Tropical Atlantic (up to 0.15 psu in the surface layer). In the other tropical basins PSY3 is less biased than PSY4 in terms of salinity but suffer from a slightly salty bias in the 0-300m layer.

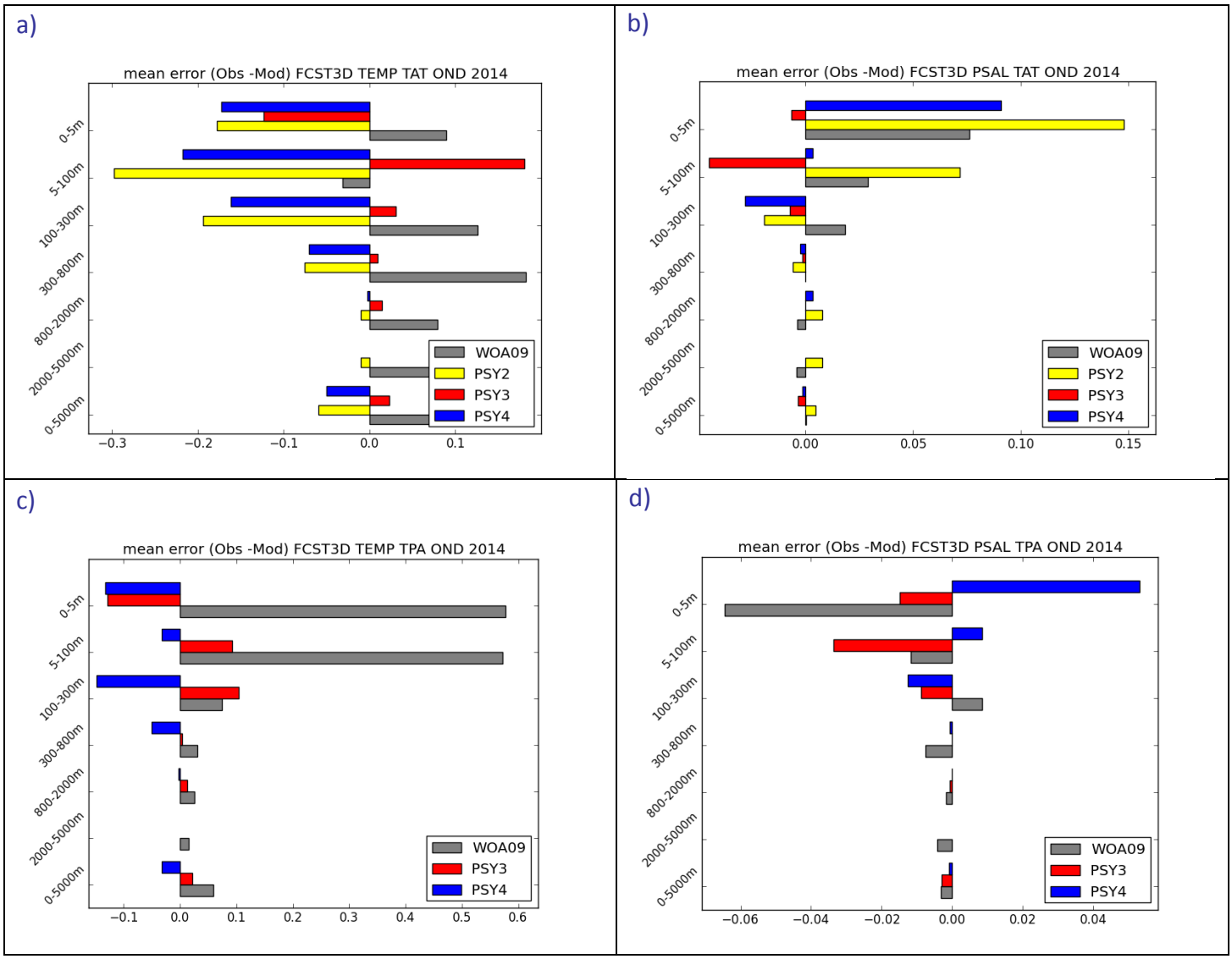

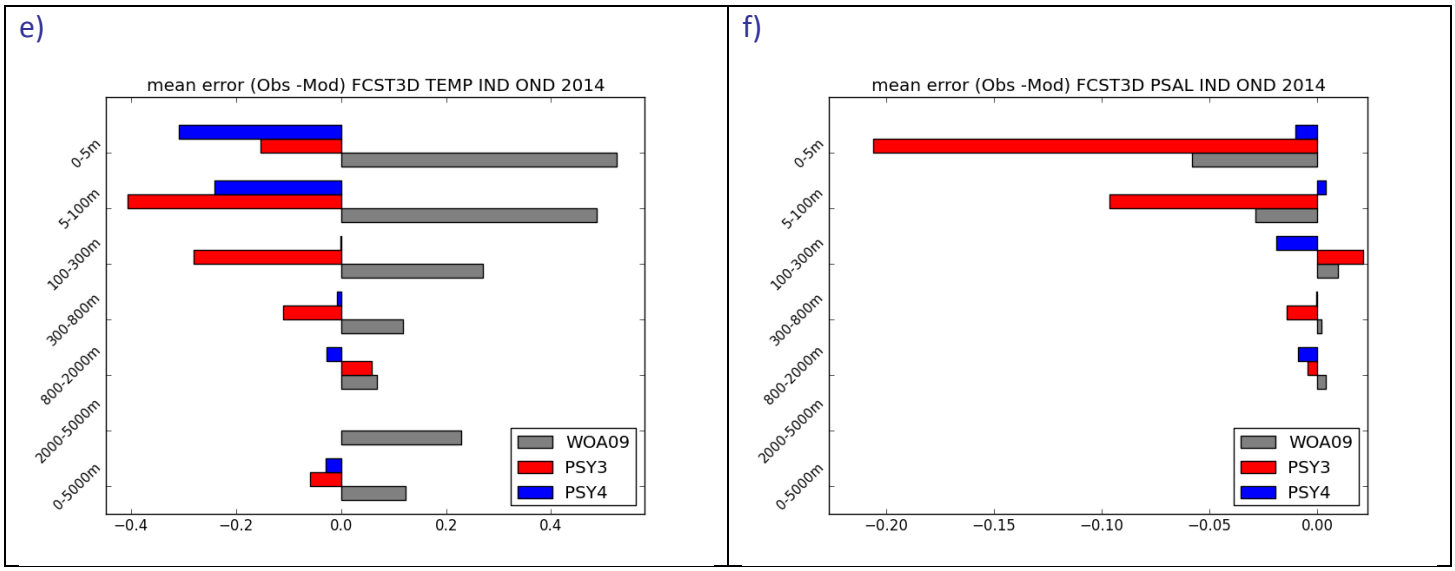

Figure 54: (Obs-model) mean differences in temperature (°C, a, c, and e) and salinity (psu, b, d, and f) for PSY3V3R3 (red), PSY2V4R4 (yellow) and PSY4V2R2 (blue) systems in the Tropical Atlantic (a and b), the Tropical Pacific (c and d) and the Indian Ocean (e and f) in OND 2014.

At the surface, PSY4 is too fresh for the Tropical Pacific and PSY3 is too salty in the Indian Ocean; PSY3 beats PSY4 in Tropical Atlantic and Pacific but not in the Indian Ocean where PSY3 exhibits a strong salty bias between 0-100m (up to 0.2).

PSY3, PSY4 and PSY2 display similar accuracy levels in terms of temperature RMS error in the Tropical Oceans. At the surface, PSY3's salinity slightly outperforms PSY4 on average over the globe. RMS error increases with forecast range (shown here for PSY3), as could be expected, and that the 5-day forecast always beats the climatology (except for global mean salinity). Eventually this OND 2014 quarter, we would suggest choosing PSY3 for Atlantic and Pacific Tropical Ocean and PSY4 for Indian Ocean.

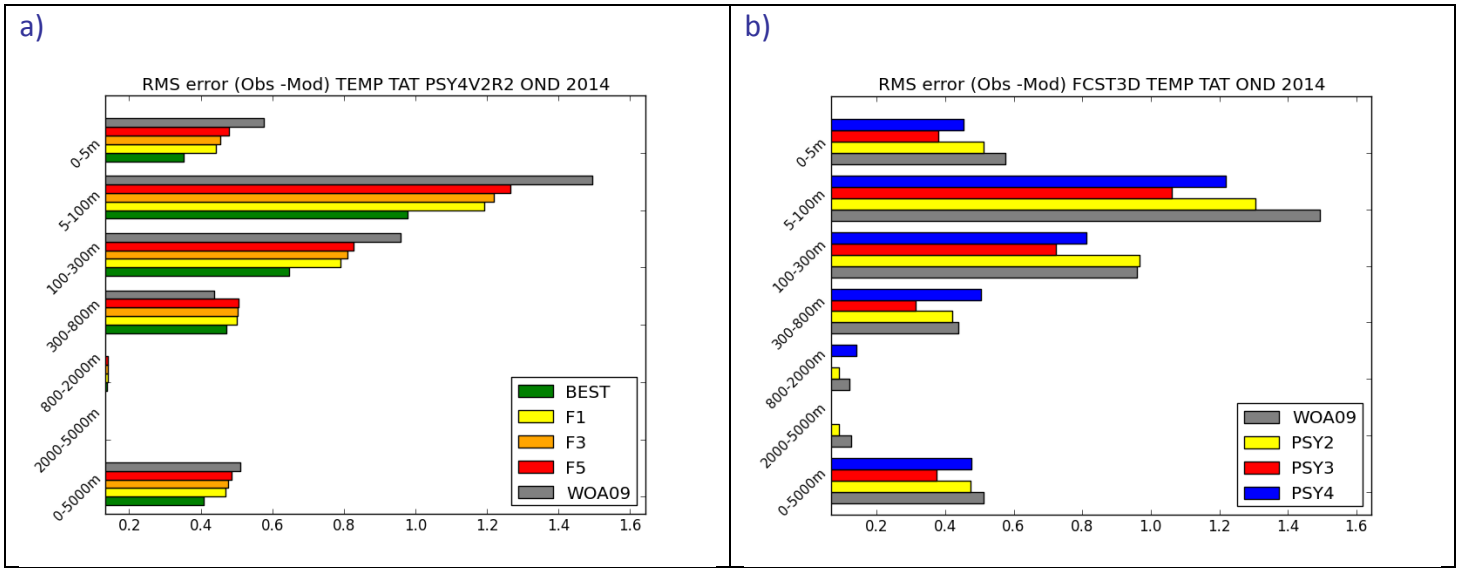

c)

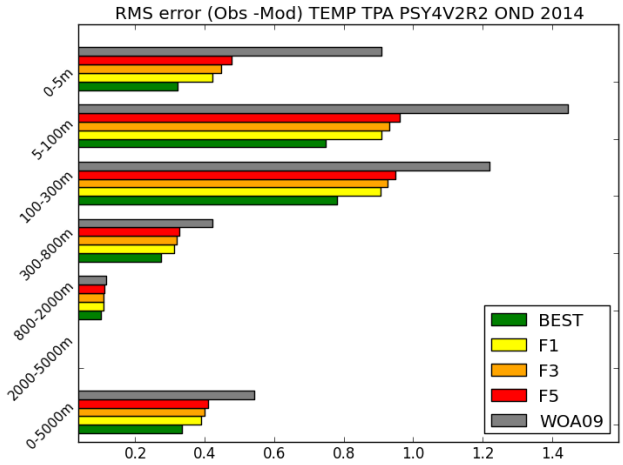
RMS error (Obs -Mod) TEMP TPA PSY4V2R2 OND 2014
0-5m
5-100m
100-300m
300-800m
800-2000m
2000-5000m
0-5000m
0.2
0.4
0.6
0.8
1.0
1.2
1.4
BEST
F1
F3
F5
WOA09

d)

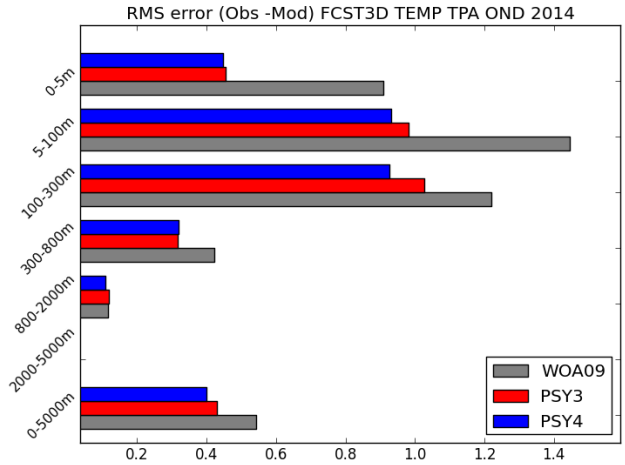
RMS error (Obs -Mod) FCST3D TEMP TPA OND 2014
0-5m
5-100m
100-300m
300-800m
800-2000m
2000-5000m
0-5000m
0.2
0.4
0.6
0.8
1.0
1.2
1.4
WOA09
PSY3
PSY4

e)

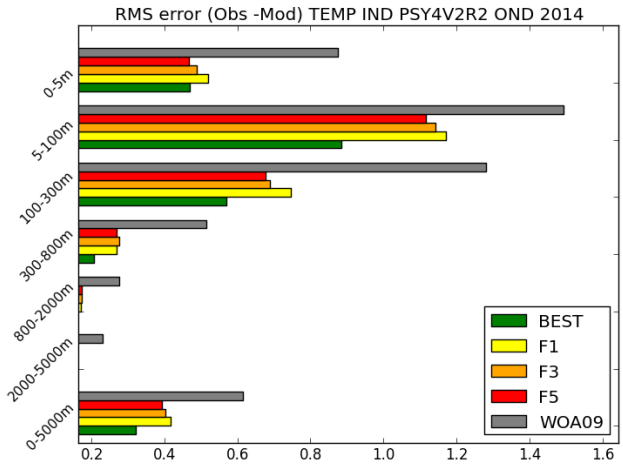
RMS error (Obs -Mod) TEMP IND PSY4V2R2 OND 2014
0-5m
5-100m
100-300m
300-800m
800-2000m
2000-5000m
0-5000m
0.2
0.4
0.6
0.8
1.0
1.2
1.4
1.6
BEST
F1
F3
F5
WOA09

f)

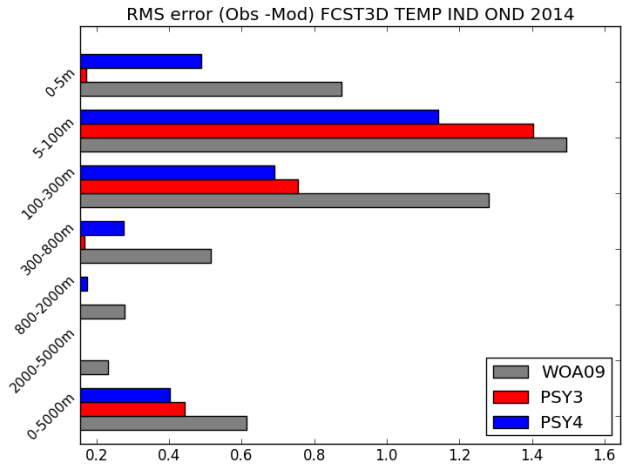
RMS error (Obs -Mod) FCST3D TEMP IND OND 2014
0-5m
5-100m
100-300m
300-800m
800-2000m
2000-5000m
0-5000m
0.2
0.4
0.6
0.8
1.0
1.2
1.4
1.6
WOA09
PSY3
PSY4

g)

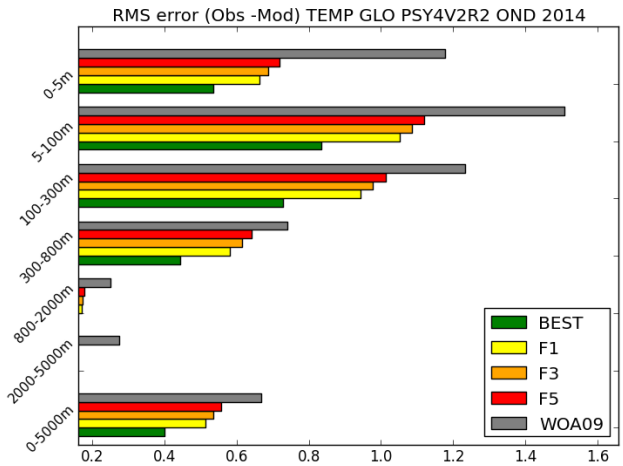
RMS error (Obs -Mod) TEMP GLO PSY4V2R2 OND 2014
0-5m
5-100m
100-300m
300-800m
800-2000m
2000-5000m
0-5000m
0.2
0.4
0.6
0.8
1.0
1.2
1.4
1.6
BEST
F1
F3
F5
WOA09

h)

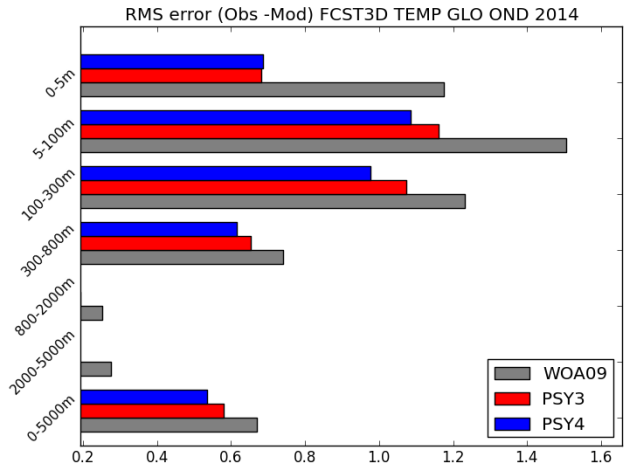
RMS error (Obs -Mod) FCST3D TEMP GLO OND 2014
0-5m
5-100m
100-300m
300-800m
800-2000m
2000-5000m
0-5000m
0.2
0.4
0.6
0.8
1.0
1.2
1.4
1.6
WOA09
PSY3
PSY4

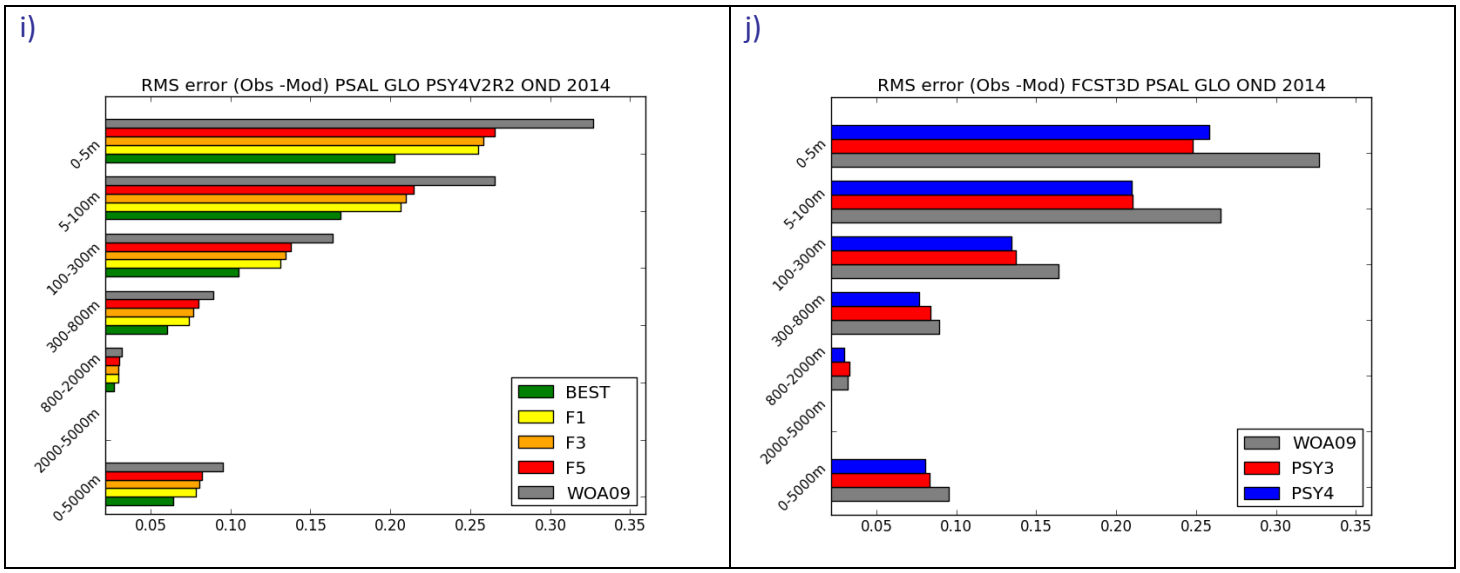

Figure 55: same as Figure 52 but for RMS statistics and for temperature (°C), PSY3V3R3 and PSY4V2R2 systems and the Tropical Atlantic (a and b), the Tropical Pacific (c and d) and the Indian Ocean (e and f). The global statistics are also shown for temperature (°C, g and h) and salinity (psu, I and j). The right column compares the analysis of the global ¼° PSY3V3R3 (red) with the analysis of the global 1/12° PSY4V2R2 (blue).

VI.3. Forecast accuracy: skill scores for T and S

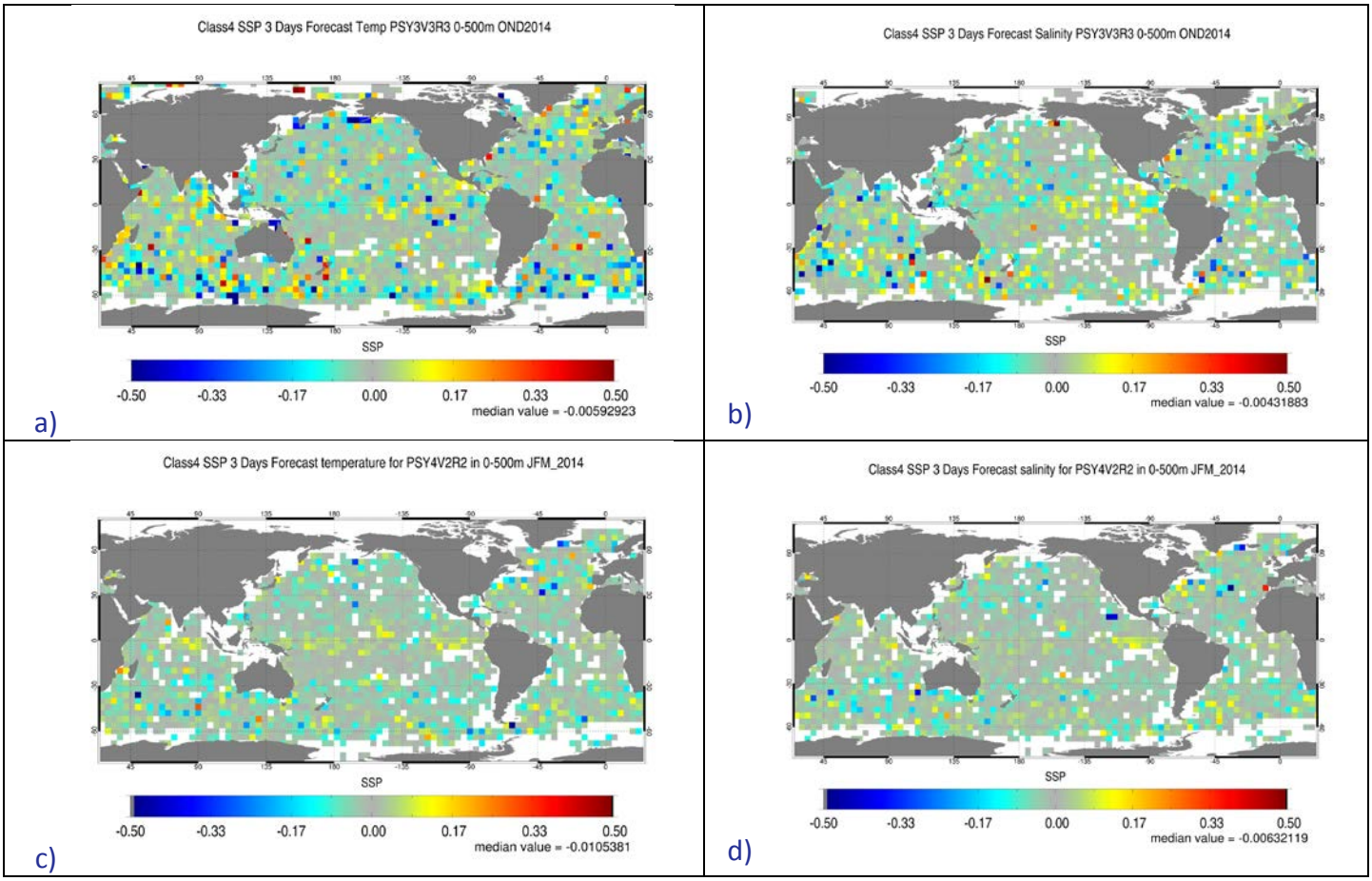

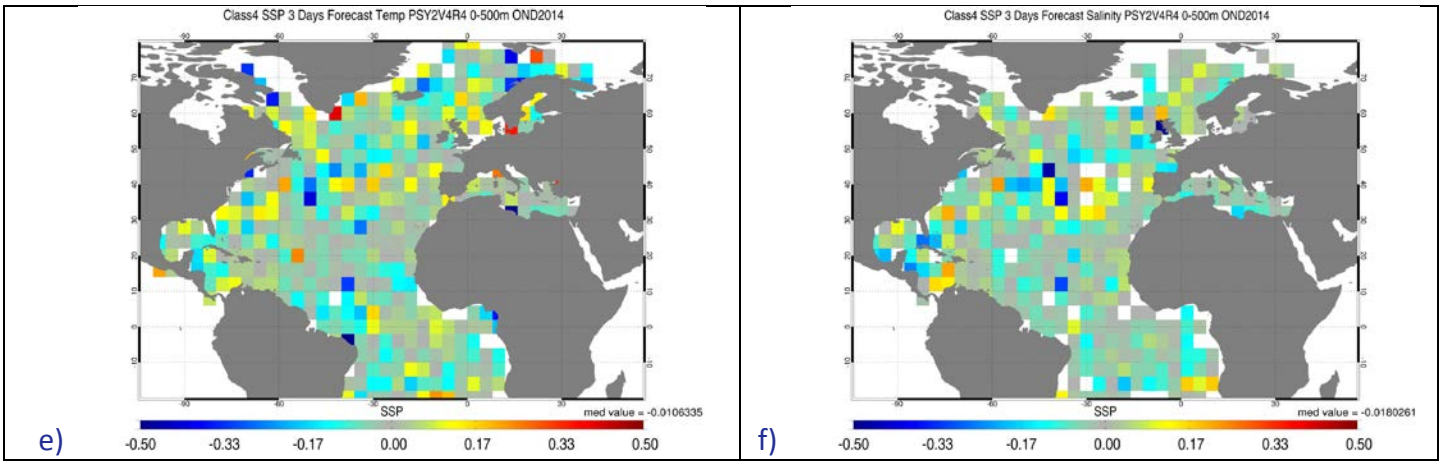

Figure 56: Temperature (left) and salinity (right) skill scores in 4°x4° bins and in the 0-500m layer in OND 2014 in PSY3V3R3 (a and b) , PSY4V2R2 (c and d) and PSY2V4R4 (e and f). The skill illustrates the ability of the 3-days forecast to be closer to in situ observations than the persistence of the analysis, see Equation 1. Yellow to red values indicate that the forecast is more accurate than the persistence.

The Murphy Skill Score (see Equation 1) is described by Wilks, *Statistical Methods in the Atmospheric Sciences*, Academic Press, 2006. This score is close to 0 if the forecast is equivalent to the reference. It is positive and aims towards 1 if the forecast is more accurate than the reference.

$$SS = 1 - \frac{\sum_{k=1}^{n}\left[\frac{1}{M}\sum_{m=1}^{M}\left(Forecast_m - Obs_m\right)^2\right]}{\sum_{k=1}^{n}\left[\frac{1}{M}\sum_{m=1}^{M}\left(Ref_m - Obs_m\right)^2\right]}$$

Equation 1

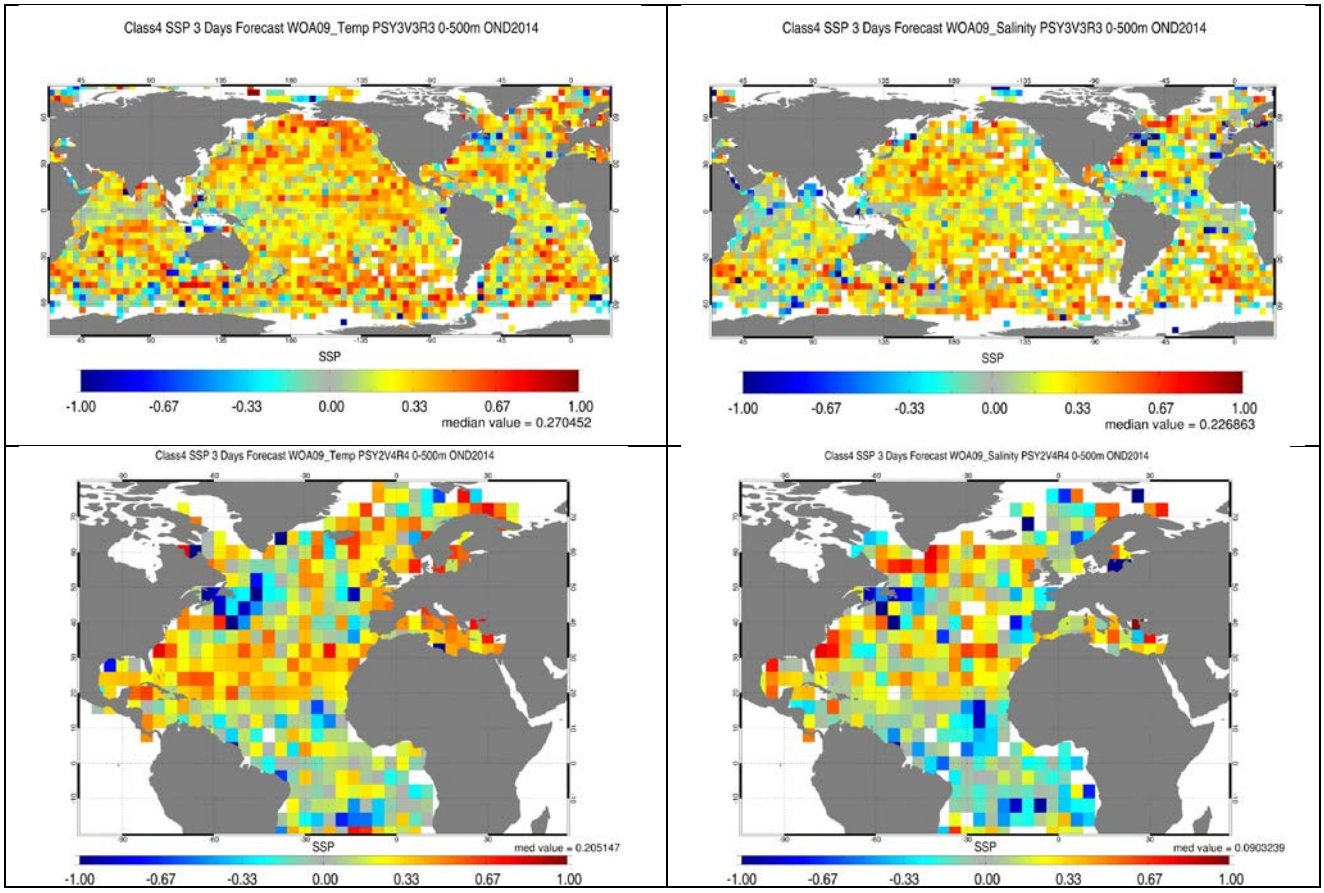

Figure 57 : As Figure 56 but the reference is the WOA 2009 climatology. Temperature (a and c) and salinity (b and d) skill scores are displayed for OND 2014, for PSY3V3R3 (a and b) and for PSY2V4R4 (c and d). The skill illustrates the ability of the 3-days forecast to be closer to in situ observations than the climatology, see Equation 1. Yellow to red values indicate that the forecast is more accurate than the climatology.

The Skill Scores displayed on Figure 56 and Figure 57 show the added value of the PSY3 forecast with respect to the persistence of the analysis (Figure 56) and to climatology (Figure 57). All Mercator Ocean systems have a very good level of performance with respect to the climatology (see previous section). The same diagnostics with climatology for PSY4 are not available for OND 2014. When the reference is the persistence of the last analysis, the result is noisier and the systems 3-day forecast seems to have skill in some regions in particular: North East Atlantic, eastern pacific, Northern Indian basin. In some regions of high variability (for instance in the Antarctic, Gulf Stream, Agulhas Current, Zapiola) the persistence of the previous analysis is locally more accurate than the forecast.

VI.4. Forecast verification: comparison with analysis everywhere

Not available this quarter.

VII Monitoring of ocean and sea ice physics

VII.1. Global mean SST and SSS

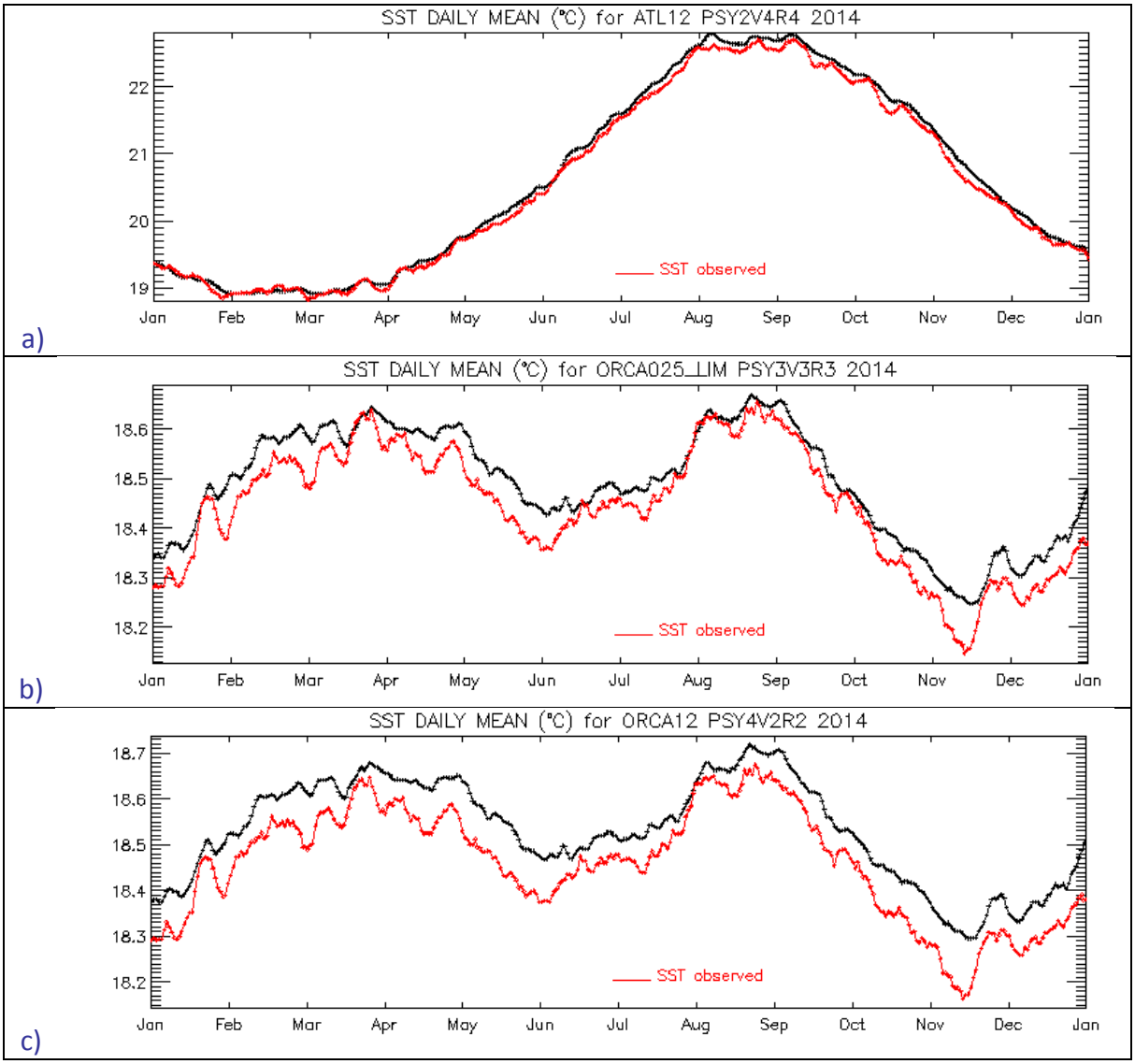

Figure 58: daily SST (°C) spatial mean for a one year period ending in AMJ 2013 for PSY2V4R4 (a), PSY3V3R3 (b), and PSY4V2R1 until 31/10/2012 then PSY4V2R2 (c). Mercator Ocean systems are in black and Reynolds AVHRR ¼° analysis in red.

The spatial mean of SST is computed for each day of the year, for PSY2, PSY3 and PSY4. The mean SST is compared to the mean of Reynolds AVHRR SST on the same domain (Figure 58).
The main feature is the good agreement of PSY2 and PSY3 with the observations all year long and on global average. A warm bias can be diagnosed in PSY3 and PSY4 with respect to the observations.

VII.2. Surface EKE

Regions of high mesoscale activity are diagnosed in Figure 59: Kuroshio, Gulf Stream, Niño 3 region in the eastern Equatorial pacific, Zapiola eddy, Agulhas current. PSY3 at ¼° and PSY4 at 1/12° are in very good agreement. EKE is generally higher in the high resolution PSY4 system, for instance this quarter at the Equator near 120°W.

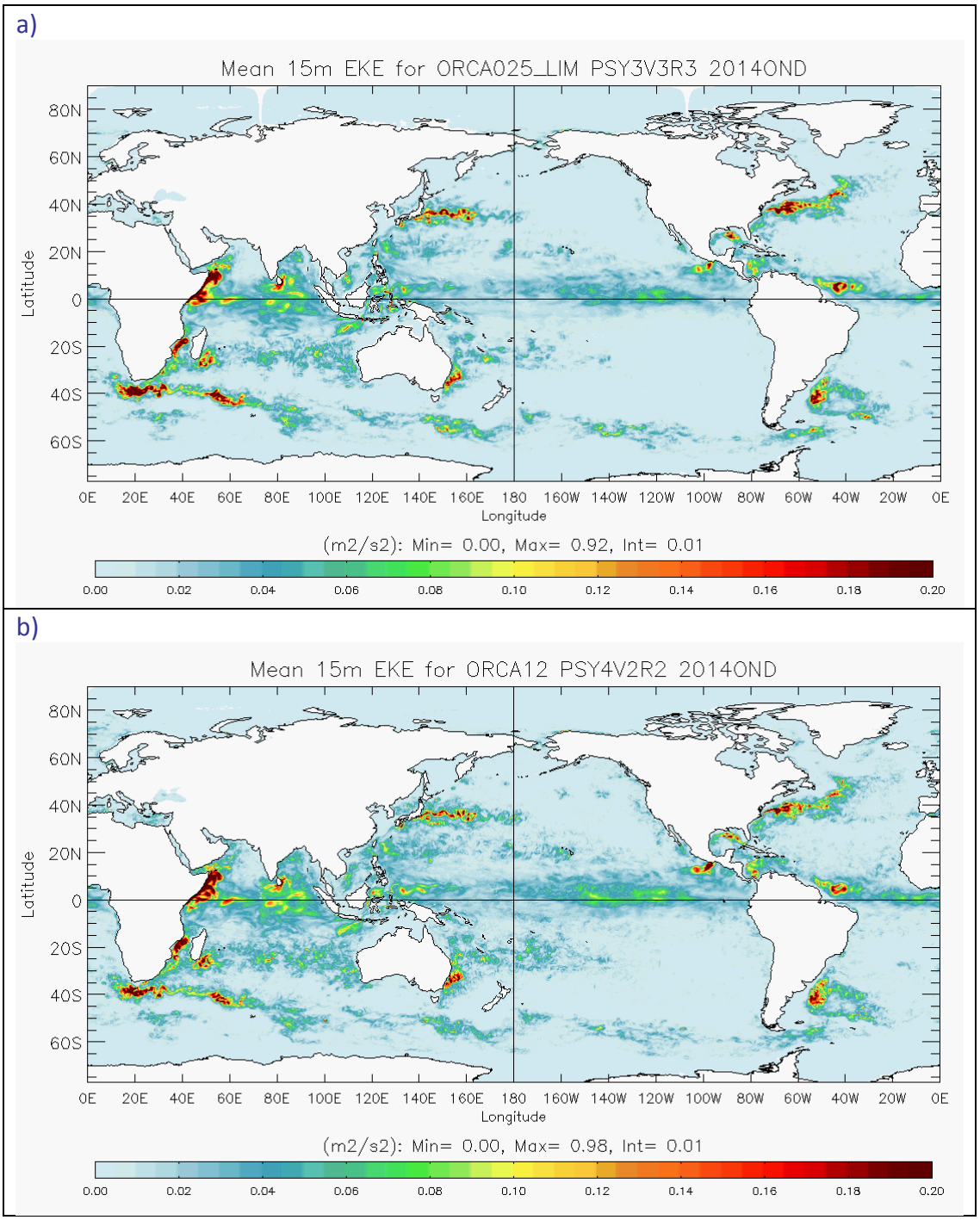

Figure 59: eddy kinetic energy EKE (m^2/s^2) at 15m for PSY3V3R3 (a) and PSY4V2R2 (b) for OND 2014.

VII.3. Mediterranean outflow

The Mediterranean outflow displayed in Figure 60 is more diffuse in all systems than in the climatology of the Gulf of Cadiz. All systems now display similar vertical structure in the region.

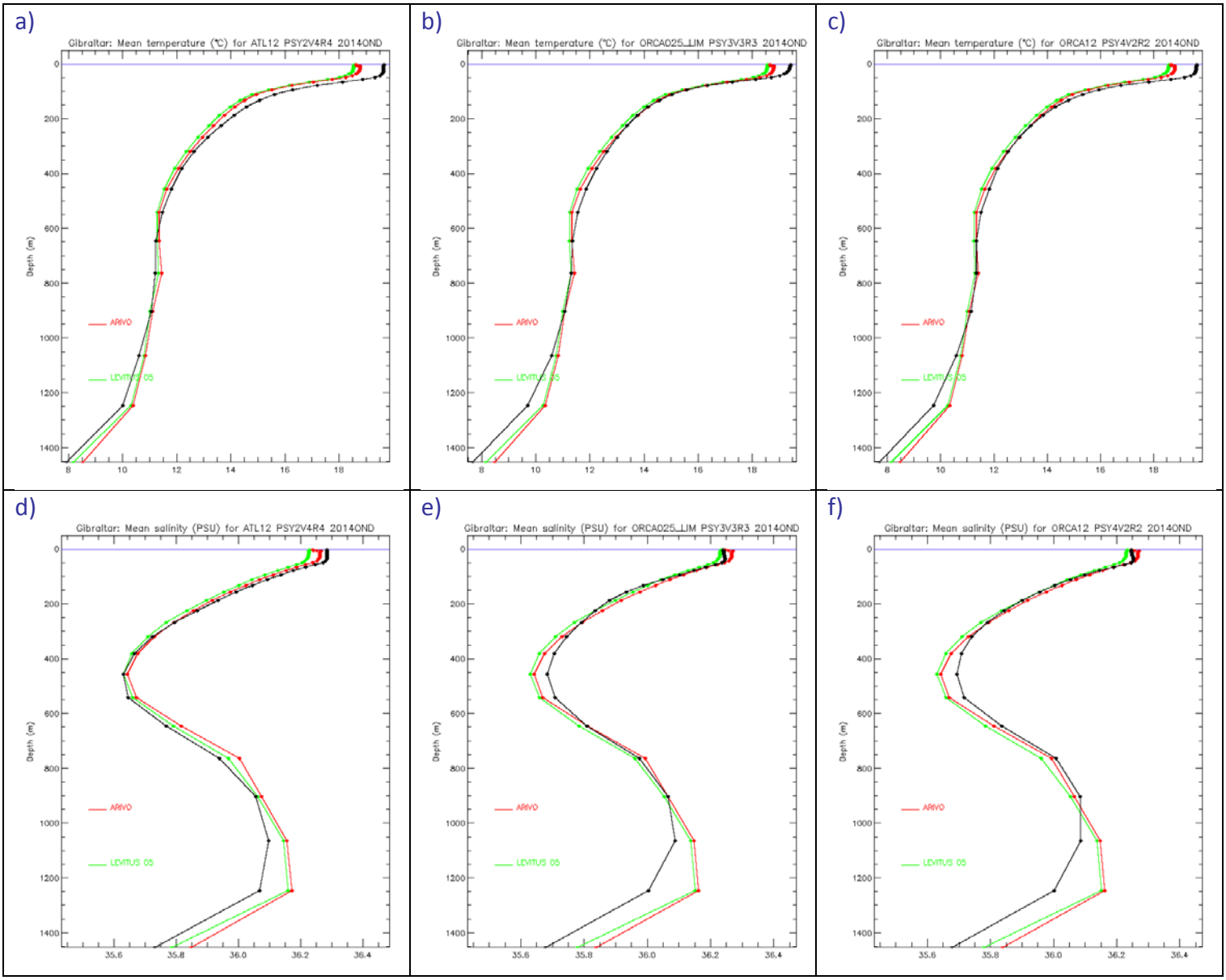

Figure 60: Comparisons between OND 2014 mean temperature (°C, a to c) and salinity (psu, d to f) profiles in Mercator systems (black): PSY2V4R4 (a and d), PSY3V3R3 (b and e) and PSY4V2R2 (c and f), and in the Levitus WOA05 (green) and ARIVO (red) monthly climatologies.

VII.4. Sea Ice extent and area

The time series of monthly means of sea ice area and sea ice extent (area of ocean with at least 15% sea ice) are displayed in Figure 61 and compared to SSM/I microwave observations. Both ice extent and area include

the area near the pole not imaged by the sensor. NSIDC web site specifies that it is assumed to be entirely ice covered with at least 15% concentration. This area is 0.31 million square kilometres for SSM/I.

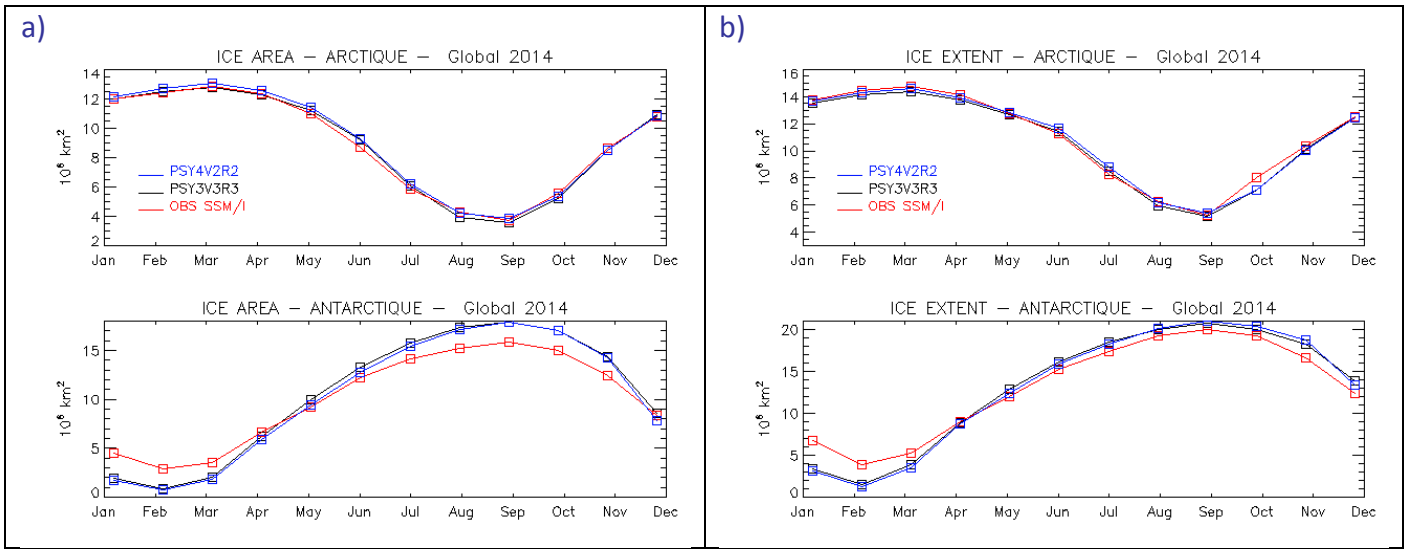

Figure 61: Sea ice area (a, 10^6 km2) and extent (b, 10^6 km2) in PSY3V3R3 (blue line), PSY4V1R3 until October then PSY4V2R2 (black line) and SSM/I observations (red line) for a one year period ending in OND 2014, in the Arctic (upper panel) and Antarctic (lower panel).

These time series indicate that sea ice products from PSY4 and PSY3 are now very similar on average over the polar domains. In the Arctic both systems perform very well in terms of average quantities. In the Antarctic the seasonal cycle of the sea ice area is overestimated, with an overestimated sea ice area this austral Spring in both systems (while the extent is better captured), and too much melting in summer for both systems.

I Annex A

I.1. Table of figures

Figure 1: schematic of the operational forecast scenario for IBI36Q (green) and PSY2Q (blue). Solid lines are the PSY2 weekly hindcast and nowcast experiments, and the IBI36 spin up. Dotted lines are the weekly 14-day forecast, dashed lines are daily updates of the ocean forecast forced with the latest ECMWF atmospheric analysis and forecast. The operational scenario of PSY3, PSY4 and PSY3Q, PSY4Q is similar to PSY2's scenario. In the case of PSY4, only weekly hindcast, nowcast and 7-day forecast are performed. 7
Figure 2: Seasonal OND 2014 temperature anomalies with respect to GLORYS2V3 climatology (1993-2011). (a): SST anomaly (°C) at the global scale from the 1/4° ocean monitoring and forecasting system PSY3V3R3. (b): heat content anomaly ($\rho_0 C_p \Delta T$, with constant ρ_0=1020 kg/m3) from the surface to 300m. 12
Figure 3: Seasonal OND 2014 temperature anomaly (°C) with respect to GLORYS2V3 climatology (1993-2011), vertical section 2°S-2°N mean, Pacific Ocean, PSY3V3R3. 12
Figure 4 : Arctic sea ice extent from the NSIDC, available at http://nsidc.org/arcticseaicenews..... 13
Figure 5 : Comparison between SLA data assimilation scores (a: average misfit in cm, b: RMS misfit in cm, c: number of observations) for all available Mercator Ocean systems in OND 2014. The scores are averaged for all available satellite along track data (Saral/altiKa, Jason 2, Cryosat 2). For each region the bars refer to PSY2V4R4 (yellow), PSY3V3R3 (red), PSY4V2R2 (blue). 14
Figure 6: Comparison between SLA data assimilation scores (a: average misfit in cm, b: RMS misfit in cm, c: number of observations) for all available Mercator Ocean systems in OND 2014 in sub-regions of the Tropical Atlantic (TAT) and North Atlantic (NAT). The scores are averaged for all available satellite along track data (Jason 1 G, Jason 2, Cryosat 2). For each region the bars refer respectively to PSY2V4R4 (yellow), PSY3V3R3 (red), and PSY4V2R2 (blue).15
Figure 7: Comparison between SLA data assimilation scores (a: average misfit in cm, b: RMS misfit in cm, c: number of observations) for all available Mercator Ocean systems in OND 2014 in the Mediterranean Sea MED sub-regions: PSY2V4R4 (yellow), PSY3V3R3 (red) and PSY4V2R2 (blue). The scores are averaged for all available satellite along track data (Jason 1 G, Jason 2, Cryosat 2). See annex B for geographical location of regions. 16
Figure 8: Comparison between SLA data assimilation scores (a: average misfit in cm, b: RMS misfit in cm, c: number of observations) for all available global Mercator Ocean systems in OND 2014 in sub-regions of the SAT, IND, NPA, SPA, TPA, and ACC basins: PSY3V3R3 (red) and PSY4V2R2 (blue). The scores are averaged for all available along track satellite data (Jason 1 G, Jason 2, Cryosat 2). The geographical location of regions is displayed in annex B. 17
Figure 9: Comparison between Reynolds ¼°AVHRR-data assimilation scores (a: average misfit in °C, b: RMS misfit in °C, c: number of observations) for all available Mercator Ocean systems in OND 2014: PSY4V2R2 (blue), PSY3V3R3 (red), and PSY2V4R4 (yellow)..... 18
Figure 10: Comparison between Reynolds ¼°AVHRR SST data assimilation scores (a: average misfit in °C, b: RMS misfit in °C, c: number of observations) for all available Mercator Ocean systems in OND 2014 in sub-regions of the Tropical Atlantic (TAT) and of the North Atlantic (NAT): PSY4V2R2 (blue), PSY3V3R3 (red) and PSY2V4R4 (yellow). The geographical location of regions is displayed in annex B..... 19
Figure 11: Comparison between Reynolds ¼° AVHRR SST data assimilation scores (a: average misfit in °C, b: RMS misfit in °C, c: number of observations) for all available Mercator Ocean systems in OND 2014 in the Mediterranean Sea: PSY4V2R2 (blue), PSY3V3R3 (red) and PSY2V4R4 (yellow). The geographical location of regions is displayed in annex B. 20
Figure 12: Comparison between Reynolds ¼° AVHRR SST data assimilation scores (a: average misfit in °C, b: RMS misfit in °C, c: number of observations) for all available global Mercator Ocean systems in OND 2014 in the SAT, NPA, TPA, SPA, IND and ACC basins: PSY3V3R3 (red) and PSY4V2R2 (blue). See annex B for geographical location of regions.21
Figure 13: Profiles of OND 2014 innovations of temperature (°C, left column) and salinity (psu, right column), mean (solid line) and RMS (dashed line) for PSY3V3R3 (red), PSY2V4R4 (yellow) and PSY4V1R3 (blue) in the North Atlantic NAT (a and b), Mediterranean Sea MED (c and d) and Arctic Ocean ARC (e an fl, the region starts of north of 67°N). Basin masks are applied to keep only the main basin of interest (no Mediterranean in the Altantic NAT, no Black Sea in the Mediterranean MED, etc…). 23
Figure 14: As Figure 13 in the Tropical Atlantic TAT (a and b), South Atlantic SAT (c and d) and Indian IND (e and f) basins. 25
Figure 15: As Figure 13 in the North Pacific NPA (a and b), Tropical Pacific TPA (c and d) and South Pacific SPA (e and f). 27
Figure 16: As Figure 13 in the ACC Southern Ocean basin (from 35°S). 28
Figure 17: As Figure 13 in the North East Atlantic (IBI) and the North Madeira XBT regions. 29

Figure 18: As Figure 13 in the Dakar region. 30
Figure 19: As Figure 13 in the Ascension tide (a and b), the Gulf of Mexico (c and d) and the Gulf Stream 1 regions (e and f) 31
Figure 20 : number of observations of T (a) and S (b) assimilated in PSY4V2R2 in the Gulf Stream 1 region during the OND 2014 quarter. 32
Figure 21: As Figure 13 in the Algerian (a and b), the gulf of Lion (c and d), the Ionian (e and f) and the Mersa Matruh (g and h) regions. 34
Figure 22: As Figure 13 in the North West Indian (a and b), the South West Indian (c and d) and the East Indian (e and f) regions 36
Figure 23: Average difference MODEL-OBSERVATION of temperature (a, c, and e, in °C) and salinity (b, d, and f, in psu) in OND 2014 between the daily average hindcast PSY4V2R2 (a and b), PSY3V3R3 (c and d) and PSY2V4R4 (e and f) hindcast products and all available T/S observations from the Coriolis database. The Mercator hindcast products are taken at the time and location of the observations. Averages are performed in the 0-50m layer. The size of the pixel is proportional to the number of observations used to compute the RMS in 2°x2° boxes. 38
Figure 24: RMS temperature (°C) difference (model-observation) in OND 2014 between all available T/S observations from the Coriolis database and the daily average hindcast PSY3V3R3 products on the left and hindcast PSY4V2R2 on the right column colocalised with the observations. Averages are performed in the 0-50m layer (a and b) and in the 0-500m layer (c and d). The size of the pixel is proportional to the number of observations used to compute the RMS in 2°x2° boxes. 39
Figure 25: RMS salinity (psu) difference (model-observation) in OND 2014 between all available T/S observations from the Coriolis database and the daily average hindcast PSY3V3R3 products (a and c) and hindcast PSY4V2R2 (b and d), colocalised with the observations. Averages are performed in the 0-50m layer (a and b) and in the 0-500m layer (c and d). The size of the pixel is proportional to the number of observations used to compute the RMS in 2°x2° boxes. 40
Figure 26 : OND 2014 global statistics of temperature (°C, a and c) and salinity (psu, b and d) averaged in 6 consecutive layers from 0 to 5000m. RMS difference (a and b) and mean difference (observation-model, c and d) between all available T/S observations from the CORIOLIS database and the daily average hindcast products PSY3V3R3 (red), PSY4V2R2 (blue) and WOA09 climatology (grey) colocalised with the observations. NB: average on model levels is performed as an intermediate step which reduces the artefacts of inhomogeneous density of observations on the vertical. 41
Figure 27: RMS difference (model-observation) of temperature (a and b, °C) and salinity (c and d, psu) in OND 2014 between all available T/S observations from the Coriolis database and the daily average PSY2V4R4 hindcast products colocalised with the observations in the 0-50m layer (a and c) and 0-500m layer (b and d) 42
Figure 28: Water masses (Theta, S) diagrams in OND 2014 in the Bay of Biscay (a to c), Gulf of Lion (d to f), Irminger Sea (g to i) and Gulf of Cadiz (j to l), comparison between PSY3V3R3 (a, d, g, j), PSY4V2R2 (b, e, h, k) and PSY2V4R4 (c, f, I, and l) in AMJ 2013. PSY2, PSY3 and PSY4: yellow dots; Levitus WOA09 climatology: red dots; in situ observations: blue dots. 44
Figure 29 : Water masses (T, S) diagrams in the Western Tropical Atlantic (a to c) and in the Eastern Tropical Atlantic (d to f) in OND 2014: for PSY3V3R3 (a, d); PSY4V2R2 (b, e); and PSY2V4R4 (c, f). PSY2, PSY3 and PSY4: yellow dots; Levitus WOA09 climatology; red dots, in situ observations: blue dots. 46
Figure 30: Water masses (T, S) diagrams in South Africa (a and b), Kuroshio (c and d), and Gulf Stream region (e and f): for PSY3V3R1 (a, c and e); PSY4V1R3 (b, d and f) in OND 2014. PSY3 and PSY4: yellow dots; Levitus WOA09 climatology: red dots; in situ observations: blue dots. 47
Figure 31 : Water masses (T, S) diagrams in Beaufort Sea for PSY3 (a) and PSY4 (d), salinity profiles in this region for PSY3 b) and PSY4 e), and the same for the temperature profiles : PSY3 (c) and PSY4(f). Symbology : yellow dots; Levitus WOA09 climatology: red dots; in situ observations: blue dots. 48
Figure 32 : RMS temperature (°C) differences between OSTIA daily analyses and PSY3V3R3 daily analyses (a); between OSTIA and PSY4V2R2 (b), between OSTIA and PSY2V4R4 (c) in OND 2014. The Mercator Océan analyses are colocalised with the satellite observations analyses. 49
Figure 33: Mean SST (°C) daily differences in OND 2014 between OSTIA daily analyses and PSY3V3R3 daily analyses (a), between OSTIA and PSY4V2R2 (b) and between OSTIA and PSY2V4R4 daily analyses (c)..... 50
Figure 34: Near surface (15m) zonal current (m/s) comparison between the Mercator systems analyses and observed velocities from drifters. In the left column: velocities collocated with drifter positions in OND 2014 for PSY3V3R3 (a), PSY4V2R2 (c) and PSY2V4R4 (e). In the right column, zonal current from drifters in OND 2014 (b) at global scale, AOML drifter climatology for OND with new drogue correction from Lumpkin & al, in preparation (d) and observed zonal current in OND 2014 (f) over PSY2's domain. 51
Figure 35 : In OND 2014, comparison of the mean relative velocity error between in situ AOML drifters and model data (a, c and e) and mean zonal velocity bias between in situ AOML drifters with Mercator Ocean correction (see text) and model data (b, d and f). a and b: PSY3V3R3, c and d: PSY4V2R3, e and f: PSY2V4R2. NB: zoom at 500% in order to see the arrows. 52

Figure 36: In OND 2014, comparison of the mean distance error in 1°x1° boxes after a 1-day drift (a and b), after a 3-days drift (c and d), and after a 5-days drift (e and f).between AOML drifters' trajectories and PSY3V3R3 trajectories (a, c, and e) and between AOML drifters' trajectories and PSY4V2R2 (b,d, and f). 54
Figure 37:Cumulative Distribution Functions of the distance error (km, on the left) and the direction error (degrees, on the right panel) after 1 day (blue), 3 days (green) and 5 days (red), between PSY4V1R3 forecast trajectories and actual drifters trajectories..... 55
Figure 38: Arctic (a to c) and Antarctic (d to f) OND 2014 Sea ice cover fraction in PSY3V3R3 (a and d), in CERSAT observations (b and e) and difference PSY3 – CERSAT (c and f). 56
Figure 39: Arctic (a to c) and Antarctic (d to f) OND 2014 Sea ice cover fraction in PSY4V2R2 (a and d), in CERSAT observations (b and e) and difference PSY4 – CERSAT (c and f). 57
Figure 40: OND 2014 Arctic sea ice extent in PSY4V2R2 with overimposed climatological OND 1992-2010 sea ice fraction (magenta line, > 15% ice concentration) (a) and NSIDC map of the sea ice extent in the Arctic for December 2014 in comparison with a 1979-2000 median extend (b), the same for the Antarctic region for the PSY4V2R2 system c) and the NSIDC estimation d) (ftp://sidads.colorado.edu/DATASETS/NOAA/G02135/Dec/). 58
Figure 41 : Mean bias (observation-model) (a), RMS error (b), correlation (c) between IBI36V2 and analysed L3 SST from Météo-France CMS for the OND 2014 quarter. Same diagnostics for PSY2V4R4 (d,e,f) and PSY4V2R2 (g,h,i). Number of Météo-France CMS observations for the OND 2014 quarter (j). 60
Figure 42 : Over the whole IBI36V4 domain (a and b) and over the Bay of Biscay (c and d): mean "IBI36V4 - observation" salinity (psu) bias (red) and RMS error (blue) in OND 2014 (a and c), and mean profile from IBI36V4 (black), PSY2V4R4 (green) and from the observations (red) in OND 2014 (b and d). In the lower right corner of each plot: position of the individual profiles. 61
Figure 43: Over the whole IBI36V4 domain (a and b) and over the Bay of Biscay (c and d): mean "IBI36V4 - observation" salinity (psu) bias (red) and RMS error (blue) in OND 2014 (a and c), and mean profile from IBI36V4 (black), PSY2V4R4 (green) and from the observations (red) in OND 2014 (b and d). In the lower right corner of each plot: position of the individual profiles. 62
Figure 44 : Mixed Layer Depth distribution in OND 2014 in IBI36V4 (a and b) and PSY2V4R4 (c and d), calculated from profiles with the temperature criteria (difference of 0.2°C with the surface); the models are in grey, the observations in red. a and c: classification for the whole IBI domain, b and d: classification for the Bay of Biscay 63
Figure 45 : For IBI36V4: RMS error (a, in cm) and correlation (b) for the non-tidal Sea Surface Elevation at tide gauges in OND 2014, for different regions and frequencies..... 63
Figure 46 : For IBI36V4: Bias (observation-model) (a, d and g), RMS error (°C) (b, e and h) and correlation (c, f and i) of the Sea Surface Temperature between IBI36 and moorings measurements in October (a to c), November (d to f) and December 2014 (g to i). 65
Figure 47 : Surface temperature (°C) time series at a selection of moorings which locations are shown on the upper left panel (no observation for Gulf of Lion). 65
Figure 48 : Chlorophyll-a concentration (mg/m^3) in October(a and b), November (c and d) and December 2014 (e and f) for the Mercator system BIOMER4 (a, c, and e) and Chlorophyll-a concentration from Globcolour (b, d and f). 66
Figure 49 : Probability Density Function (PDF) of Chl-a bias in log scale (log10(obs)-log10(model)) in the North Atlantic (30-70N; 80W:20E) for October (a), November (b) and December (c) 2014..... 67
Figure 50 : RMS difference between BIOMER and Globcolour Chl-a concentrations (mg/m^3) in OND 2014..... 67
Figure 51: Schematic of the change in atmospheric forcings applied along the 14-day ocean forecast..... 68
Figure 52: Accuracy intercomparison in the North Atlantic region for PSY2V4R4 in temperature (a and c) and salinity (b and dl) between hindcast (green), nowcast (yellow), 3-day (orange) and 6-day (red) forecast and WO09 climatology (grey). Accuracy is measured by a mean difference (a and b) and by a rms difference (c and d) of temperature and salinity with respect to all available observations from the CORIOLIS database averaged in 6 consecutive layers from 0 to 5000m. All statistics are performed for the OND 2014 period. NB: average on model levels is performed as an intermediate step which reduces the artefacts of inhomogeneous density of observations on the vertical. 69
Figure 53: Accuracy intercomparison in the Mediterranean Sea region for PSY2V4R4 in temperature (°C, a and c) and salinity (psu, b and d) between hindcast, nowcast, 3-day and 6-day forecast and WO09 climatology. Accuracy is measured by a rms difference (c and d) and by a mean difference (a and b) with respect to all available observations from the CORIOLIS database averaged in 6 consecutive layers from 0 to 5000m. All statistics are performed for the OND 2014 period. NB: average on model levels is performed as an intermediate step which reduces the artefacts of inhomogeneous density of observations on the vertical. 70
Figure 54: (Obs-model) mean differences in temperature (°C, a, c, and e) and salinity (psu, b, d, and f) for PSY3V3R3 (red), PSY2V4R4 (yellow) and PSY4V2R2 (blue) systems in the Tropical Atlantic (a and b), the Tropical Pacific (c and d) and the Indian Ocean (e and f) in OND 2014. 72

Figure 55: same as Figure 52 but for RMS statistics and for temperature (°C), PSY3V3R3 and PSY4V2R2 systems and the Tropical Atlantic (a and b), the Tropical Pacific (c and d) and the Indian Ocean (e and f). The global statistics are also shown for temperature (°C, g and h) and salinity (psu, I and j). The right column compares the analysis of the global ¼° PSY3V3R3 (red) with the analysis of the global 1/12° PSY4V2R2 (blue). 74
Figure 56: Temperature (left) and salinity (right) skill scores in 4°x4° bins and in the 0-500m layer in OND 2014 in PSY3V3R3 (a and b) , PSY4V2R2 (c and d) and PSY2V4R4 (e and f). The skill illustrates the ability of the 3-days forecast to be closer to in situ observations than the persistence of the analysis, see Equation 1. Yellow to red values indicate that the forecast is more accurate than the persistence. 75
Figure 57 : As Figure 56 but the reference is the WOA 2009 climatology. Temperature (a and c) and salinity (b and d) skill scores are displayed for OND 2014, for PSY3V3R3 (a and b) and for PSY2V4R4 (c and d). The skill illustrates the ability of the 3-days forecast to be closer to in situ observations than the climatology, see Equation 1. Yellow to red values indicate that the forecast is more accurate than the climatology. 76
Figure 58: daily SST (°C) spatial mean for a one year period ending in AMJ 2013 for PSY2V4R4 (a), PSY3V3R3 (b), and PSY4V2R1 until 31/10/2012 then PSY4V2R2 (c). Mercator Ocean systems are in black and Reynolds AVHRR ¼° analysis in red. 77
Figure 59: eddy kinetic energy EKE (m^2/s^2) at 15m for PSY3V3R3 (a) and PSY4V2R2 (b) for OND 2014. 78
Figure 60: Comparisons between OND 2014 mean temperature (°C, a to c) and salinity (psu, d to f) profiles in Mercator systems (black): PSY2V4R4 (a and d), PSY3V3R3 (b and e) and PSY4V2R2 (c and f), and in the Levitus WOA05 (green) and ARIVO (red) monthly climatologies. 79
Figure 61: Sea ice area (a, 10^6 km2) and extent (b, 10^6 km2) in PSY3V3R3 (blue line), PSY4V1R3 until October then PSY4V2R2 (black line) and SSM/I observations (red line) for a one year period ending in OND 2014, in the Arctic (upper panel) and Antarctic (lower panel). 80
Figure 62 : illustration of QC: Quality test example chosen for windage (eg. 1%) we reject or correct a drift that differs little from the windage (less than 70% of the drift angle <40 °) 88
Figure 63: Example of the surface currents Lagrangian quality control algorithm on a global map (bottom panel) and zooms (upper panels). 89
Figure 64: Illustration of the surface currents Lagrangian quality control algorithm. 90

II Annex B

II.1. Maps of regions for data assimilation statistics

II.1.1. Tropical and North Atlantic

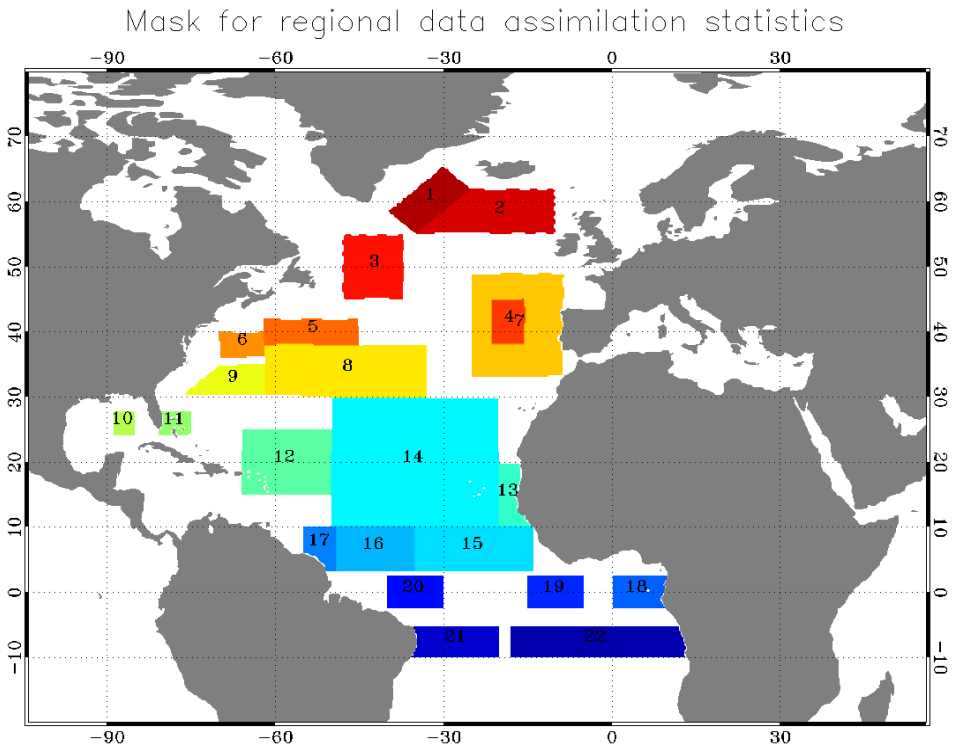

1	Irminger Sea	12	Puerto Rico XBT
2	Iceland Basin	13	Dakar
3	Newfoundland-Iceland	14	Cape Verde XBT
4	Yoyo Pomme	15	Rio-La Coruna Woce
5	Gulf Stream2	16	Belem XBT
6	Gulf Stream1 XBT	17	Cayenne tide
7	North Medeira XBT	18	Sao Tome tide
8	Charleston tide	19	XBT - central SEC
9	Bermuda tide	20	Pirata
10	Gulf of Mexico	21	Rio-La Coruna
11	Florida Straits XBT	22	Ascension tide

I.1.1. Mediterranean Sea

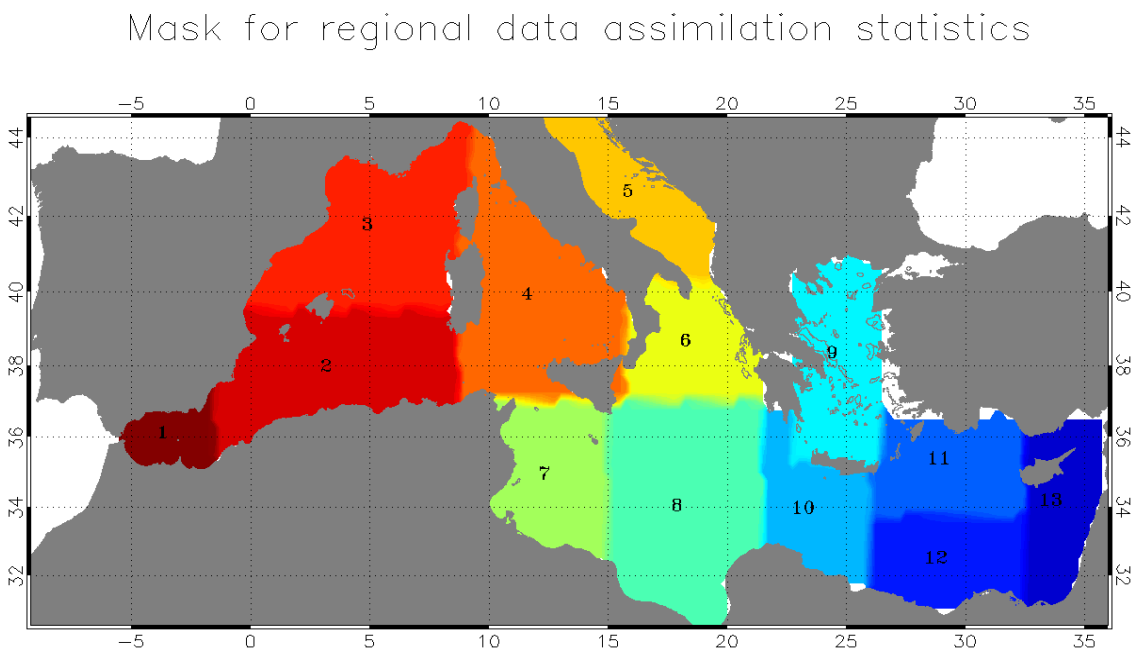

1	Alboran	8	Ionian
2	Algerian	9	Egee
3	Lion	10	Ierepetra
4	Thyrrhenian	11	Rhodes
5	Adriatic	12	MersaMatruh
6	Otranto	13	Asia Minor
7	Sicily		

I.1.2. Global ocean

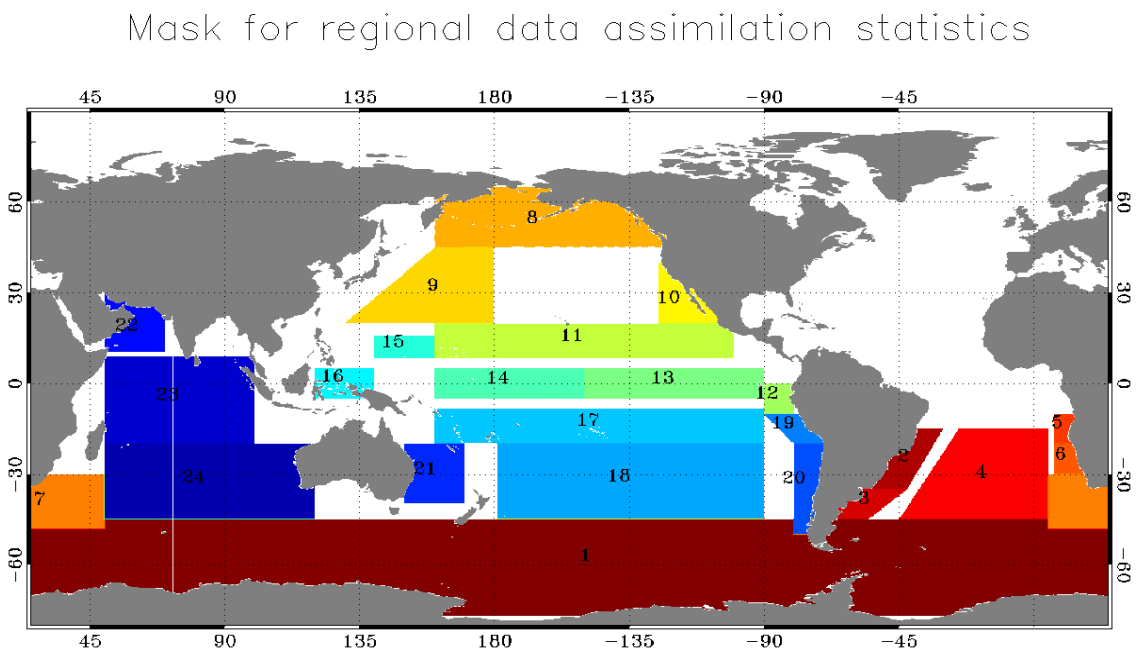

1	Antarctic Circumpolar Current	13	Nino3
2	South Atlantic	14	Nino4
3	Falkland current	15	Nino6
4	South Atl. gyre	16	Nino5
5	Angola	17	South tropical Pacific
6	Benguela current	18	South Pacific Gyre
7	Aghulas region	19	Peru coast
8	Pacific Region	20	Chile coast
9	North Pacific gyre	21	Eastern Australia
10	California current	22	Indian Ocean
11	North Tropical Pacific	23	Tropical indian ocean
12	Nino1+2	24	South indian ocean

III Annex C

III.1. Quality control algorithm for the Mercator Ocean drifter data correction (Eric Greiner)

Before estimating the bias, it is essential to conduct a quality control. We must consider an individual monitoring of buoys, and a comparison with the geostrophy and windage. In real time, this is not possible, and I propose below a simple test developed by position (date by date) which involves only the mean wind (2 days) and the buoy drift. Basically, we found drifters where drift is close to argue between 0.2 and 3% of the wind (almost the same direction with a drag corresponding to a loss of drogue). For these buoys, if the contamination is real, then the error due to the wind is important with respect to current real at 15m depth. We test different values of windage (wind effect for a fraction of a given wind between 0.2% and 3%). If a questionable observation is found for a given windage, we estimate a correction. We apply at the end an average correction QC (windage among all acceptable). We although increase the error of observation. Note that in delayed time, we could correct all the data from the buoy, at least in a 10-day window. **Note however that a buoy that has lost its drogue can give a good measure if the wind is low**

- **No anomaly : slippage correction of 0.07% of the 10m wind speed**
- **Windage > 0.2% or < 3% correction of 1% of windage**

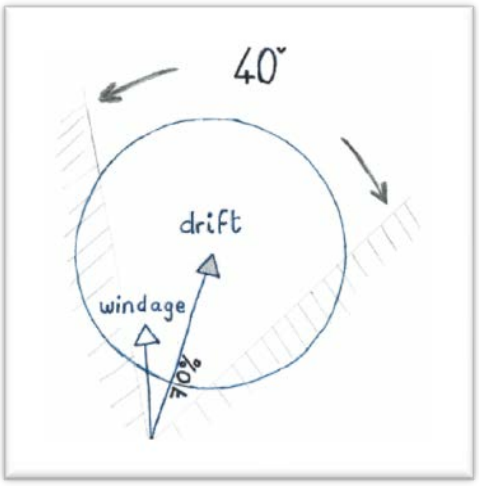

Figure 62 : illustration of QC: Quality test example chosen for windage (eg. 1%) we reject or correct a drift that differs little from the windage (less than 70% of the drift angle <40 °)

Note that a correction of more than 3% is not normally possible (construction of the buoy). This may correspond to breaking waves and swell. Between 2% and 3%, there is ambiguity between Stokes and windage. In other words, it is likely that beyond 2%, we eliminate all or part of the effect of waves and swell. If waves and swell are not aligned with the mean wind (swell remote for example), then the correction will be approximate. Ideally, you should use the Stokes drift from a wave model like Wavewatch3.
When calculating the equivalent models with AOML positions, which were filtered to remove 36h gravity waves and reduce positioning errors, we must :

- **add 0.07% wind averaged over 48h 10m : slippage correction**
- **windage correction and modify the error**

III.2. Algorithm of the Lagrangian verification of the Mercator Ocean surface currents forecast

Algorithm of the Lagrangian verification of the Mercator Océan surface currents forecast. The Mercator Océan surface currents quality control now combines two methods based on Eulerian and Lagrangian approaches using the AOML drifters network.
The Lagrangian approach is slightly different from the Eulerian approach. In the Eulerian approach, the consecutive positions of a drifter are considered as independent buoys recording velocity observations. Then, these observations are compared to the modeled velocity.

We aim here at studying the trajectory of the buoy along with the trajectory of a modeled buoy which would drift from the same starting point. The computation of the trajectory of the modeled drifter is made possible by ARIANE (see ref 1 above)
The algorithm aims at producing the maps on Figure 63. It shows the mean 1-to-5-days distance error –that is the distance between the modeled trajectory and the observed trajectory- in 1°x1° boxes. The mean D-days distance error is computed by averaging the D-days distance errors computed for all the drifters that crossed the box.
The individual points of a trajectory are not independent, merely because the location of a drifter is to a large extent determined by its former location.

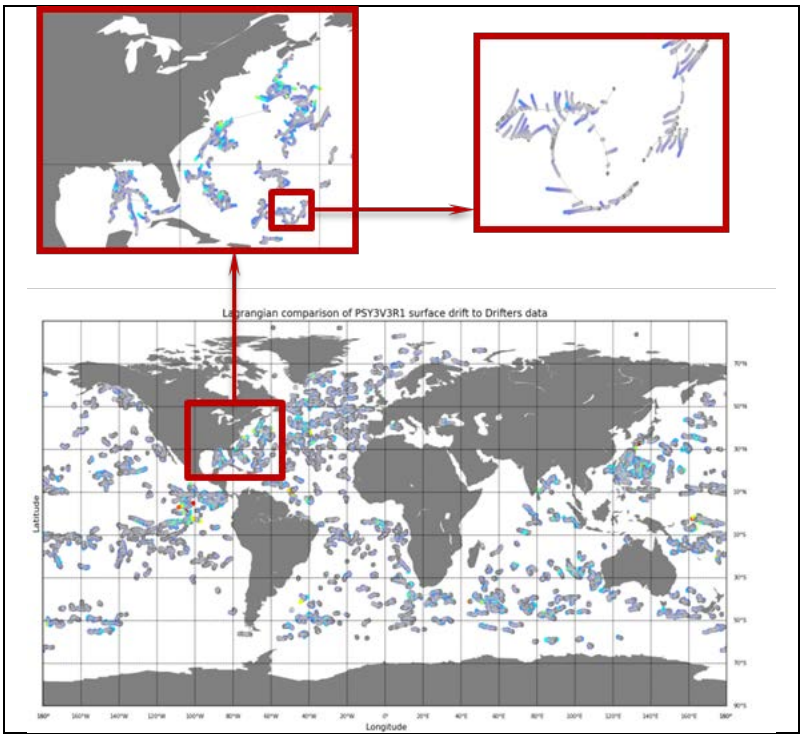

Figure 63: Example of the surface currents Lagrangian quality control algorithm on a global map (bottom panel) and zooms (upper panels).

Let us consider the example above (Figure 64). The thin grey line represents the trajectory of the drifter on a daily frequency. The thick ones represent the system drifting, starting from an observed point. Their colors show the distance to the corresponding point in the observed trajectory after D-days. Considering only this drifter, if we compute the D-days distance error starting from the t=0 observed point (01/02/2013 in the

example), we may compute it again only from the observed point t=D days. This way we may reasonably assume the two distance errors are uncorrelated and use most of the data (see ref 2 above).

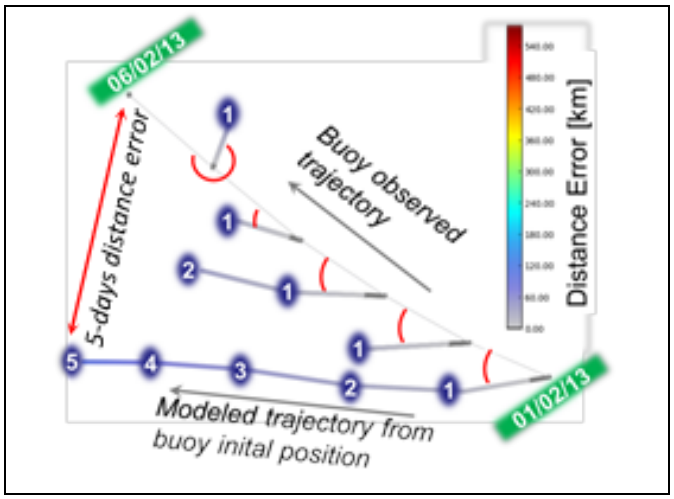

Figure 64: Illustration of the surface currents Lagrangian quality control algorithm.

References:

1- Ariane : utility developed at LPO (http://wwz.ifremer.fr/lpo_eng/Produits/Logiciels/ARIANE)
2- Scott, R. B., N. Ferry, M. Drevillon, C. N. Barron, N. C. Jourdain, J.-M. Lellouche, E. J. Metzger, M.-H. Rio, and O. M. Smedstad, Estimates of surface drifter trajectories in the equatorial Atlantic: A multi-model ensemble approach, Ocean Dynamics, 62, 1091-1109, 2012, doi:10.1007/s10236-012-0548-2.
3- M. Steele, J. Morison, W. Ermold, I. Rigor, and M. Ortmeyer(2004), Circulation of summer Pacific halocline water in the Arctic Ocean., J. Geophys. Res., 109,C02707,doi:10.1029/2003JC0022009109
4- Jackson, J. M., E. C. Carmack, F. A. McLaughlin, S. E. Allen, and R. G. Ingram (2010), Identification, characterization, and change of the near-surface temperature maximum in the Canada Basin, 1993–2008, J. Geophys. Res., 115, C05021, doi:10.1029/2009JC005265.

PSY4$_{PSY4V2R2}$ QUALITY SYNTHESIS, year *2014*

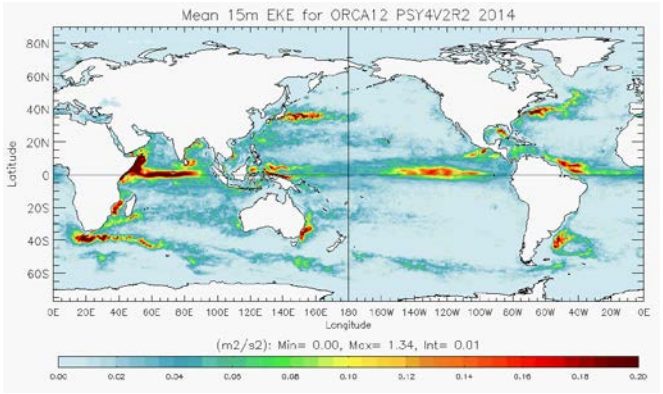

Figure 1: Eddy kinetic energy (EKE) averaged over the year 2014, calculated from the PSY4V2R2 daily 15m currents

The PSY4 global system with a 1/12 ° horizontal resolution provides a good representation of the global ocean circulation and the mesoscale features (Figure 1). This is the Mercator system that exhibits the best performance in terms of surface currents (Figure 2)

PSY4 also provides the best sea level anomalies forecast in all regions of the ocean, except in the Mediterranean where PSY2 is the most reliable of all Mercator Ocean systems.

Data assimilation in PSY4 is at the state-of-the-art like his contemporary systems PSY2 and PSY3.

PSY4 remains close to T and S in situ observations on average between 0 and 2000m. Differences with in situ observations reach amplitudes greater than 1 ° C and 0.2 psu only locally (in the thermocline, in regions of high variability).

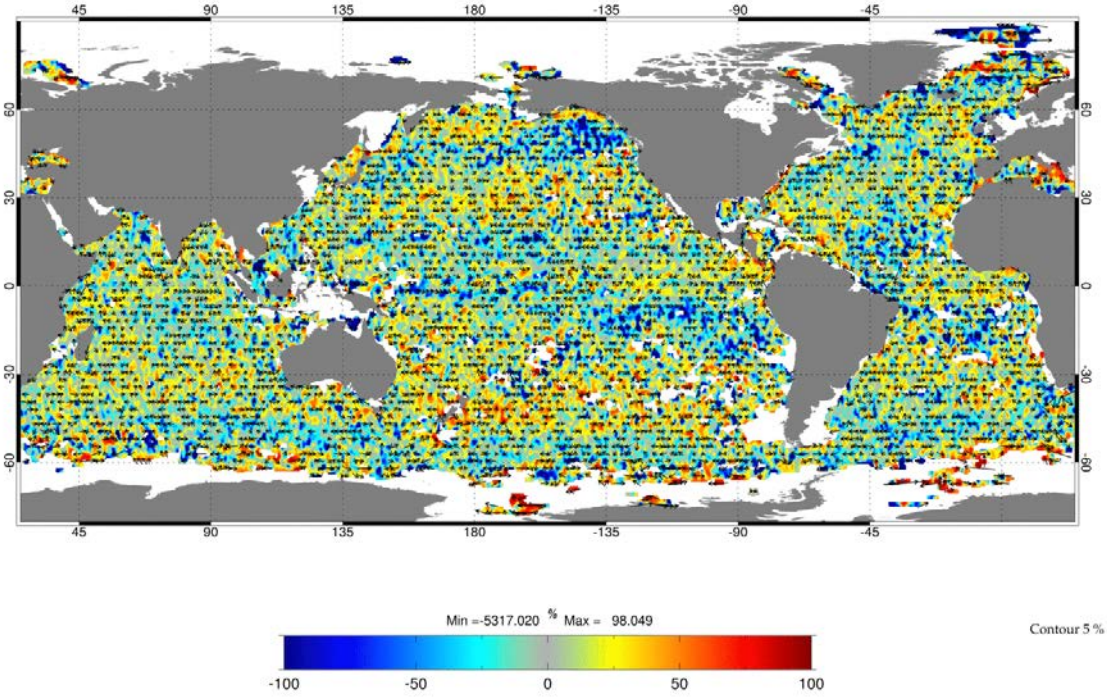

Figure 2: Relative error between the near surface(15 m) current velocities observed by drifting buoys and PSY4V2R2 velocities on average over the year 2014. The red (blue) indicates that PSY4V2R2 underestimates (overestimates) the current. The arrows indicate the direction of the difference between observations and PSY4V2R2, and are visible when zooming to 200%.

Globally, PSY4 underestimates the currents inside the gyres particularly the North and South Pacific and overestimates in the Gulf of Alaska and in the following Tropical currents:

- For the Pacific: the west side of the Equatorial Counter Current and the east part of the South Equatorial Current.
- For the Atlantic: the South Equatorial Current and the Brazil Current associated with the Equatorial Counter Current.

The Circumpolar current is also overestimated in the South Pacific Ocean and the south Indian Ocean

In global average the sea surface temperature is too warm (about 0.1°C), mainly in boreal fall and winter.

While the sea ice melts too much in the Arctic ice pack during summer, the sea ice extent is nevertheless overestimated in Arctic during boreal summer. For the Antarctic, the extension is underestimated during Austral summer and overestimated during Austral winter.

PSY2 *PSY2V4R4* QUALITY SYNTHESIS, *year 2014*

PSY2, the **Atlantic and Mediterranean system with 1/12 ° horizontal resolution** is operated since 2002 by Mercator. Designed as a test platform for PSY4, the global high resolution system at 1/12°, PSY2's performance has been gradually improving over the versions (Figure 1). The current PSY2V4R4, for which a 7-year time series is available, and the global 1/12 ° PSY4V2R2 display very similar results. Both PSY2 and PSY4 have more accurate surface fields (U, V, SSH, SST) than PSY3 which has a ¼° horizontal resolution. In 2014, PSY2 still provides the initial conditions and the boundary conditions for the IBI system. The global system PSY4 will progressively replace PSY2 for IBI and for all Mercator users in 2016.

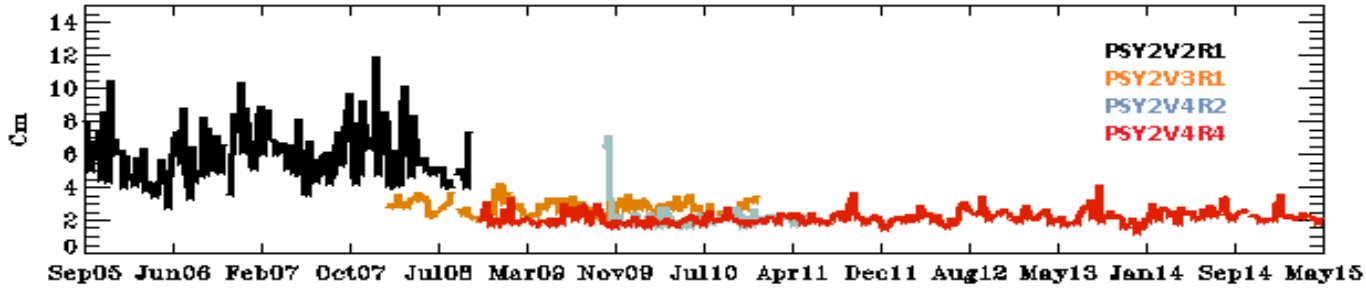

Figure 1: RMS difference between the SLA forecast of PSY2 systems since 2005 and SLA observations from Jason-1 and Jason-2, in an area near the southern boundary of the domain in the Tropical Atlantic west between 5 ° S and 10 ° S.

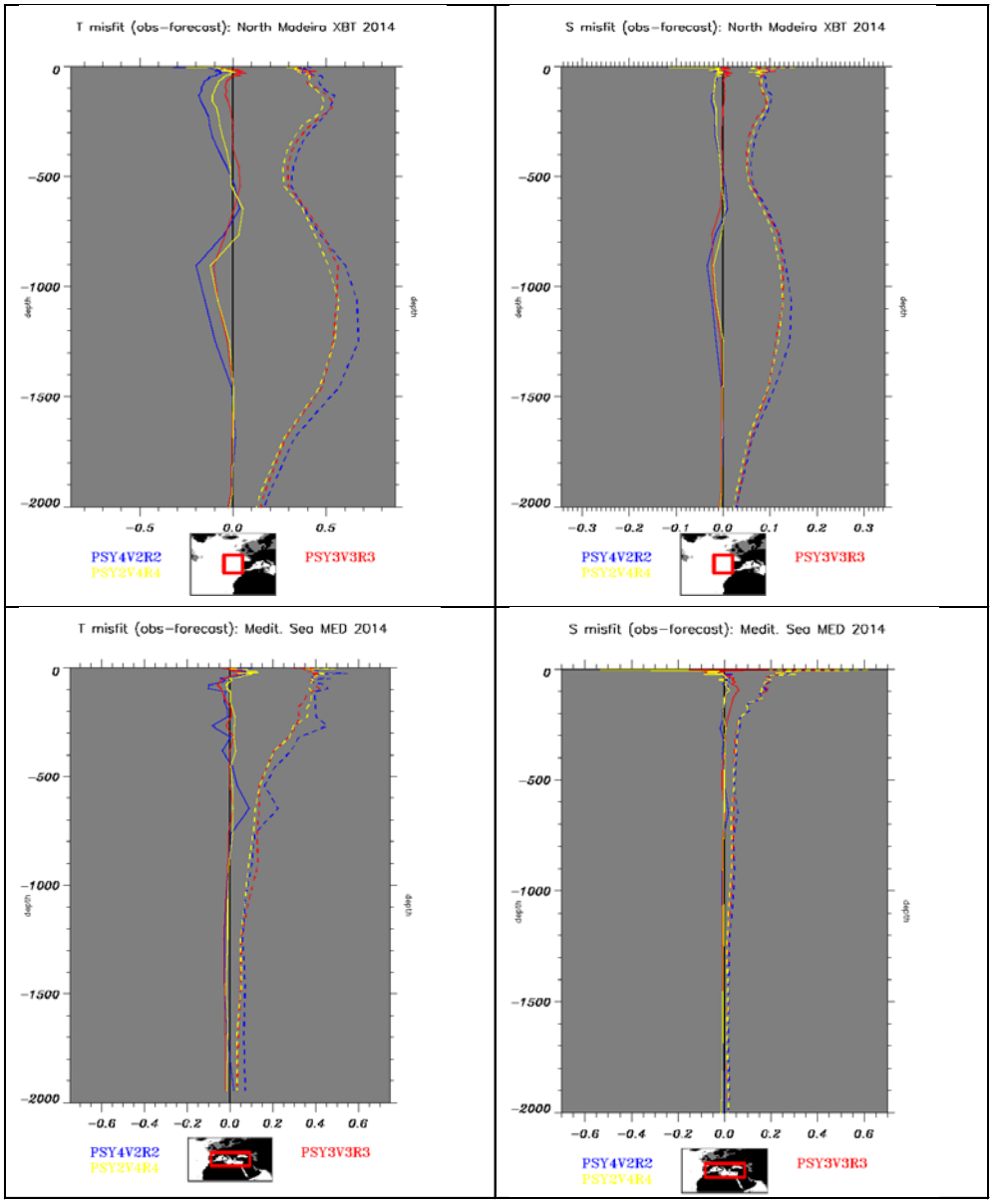

Figure 2 : Mean and RMS deviation of temperature (left) and salinity (right), for Mercator systems with respect to CORIOLIS in situ database in 2014, in the North East Atlantic (top) and the Mediterranean (bottom).

With almost identical model and data assimilation settings, the three Mercator systems PSY3, PSY2 and PSY4 show similar performance with respect to in situ profiles in 2014.
Globally, the high resolution systems PSY2 and PSY4 have slightly more accurate water masses especially in regions where finer structures need to be resolved, for instance in the Mediterranean Sea (Figure 2). PSY2 is preferred to PSY4 in 2014, as PSY4 is still close to his spin up phase.

.

Discrepancies with in situ observations reach amplitudes greater than 1 ° C and 0.2 psu only locally (in the thermocline, in regions of high variability). Some dense water masses are not represented by the system, for example some of the Levantine Intermediate Waters, the waters of the Labrador Current. The densest waters of the Bay of Biscay are well represented. Deficits of salt in the surface layers are generally related to errors in atmospheric forcing, while the denser bottom waters are under too much mixing.

IBI36 *IBI36V4 R1* QUALITY SYNTHESIS, *year 2014*

IBI36 (Iberia-Biscay-Ireland) is embedded into the PSY2 system (in 2014: PSY2V4R4) and has no data assimilation. IBI36 inherits from the water masses characteristics of PSY2. With higher spatial (1/36 °) and temporal resolution than PSY2 (hourly surface output), IBI36 is able to represent the tides with a mean square error between 11 and 12 cm for the semi-diurnal component M2 (Figure 1). Higher errors appear locally for instance on the Belgian coast and in the German Bight. The mean square error of residual height relative to observations is 11 cm on average (not shown).

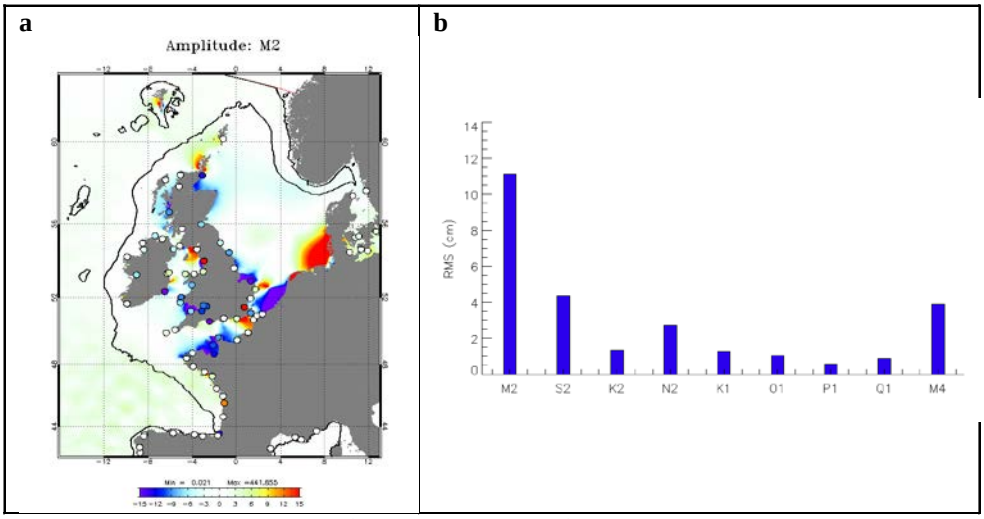

Figure 1: Error on the amplitude of the tidal components of IBI36 calculated with a harmonic analysis of the 2014 hourly surface elevation fields : (a). Difference in cm (zoom on the northern area) between the amplitude of the M2 tidal component of the FES2004 atlas and that of IBI36. The colored dots represent the difference between the amplitude of the M2 tidal component observed at tide gauges and that of IBI36 (b) RMS difference between the amplitudes of nine tidal components of tide gauges and those of IBI36.

The IBI36 model also benefits from more realistic physics than the other Mercator Ocean systems (vertical mixing, forcing bulk formulae and river inputs). Deviations from satellite observations of high-resolution SST are low on average over a large part of the domain (Figure 2). These discrepancies are greater on the shelf. Along the Moroccan and Iberian coasts where upwelling occurs (the model tends to be too warm). In the Irish Sea, English Channel and North Sea, the biases are linked to the mixing induced by the tides (the model tends to be too cold). Discrepancies are also noticeable in the Mediterranean Sea (in the Alboran Sea). The monthly evolution of errors shows a lower performance of the model from mid-spring to summer (maximum RMS) and in autumn (maximum bias in November).

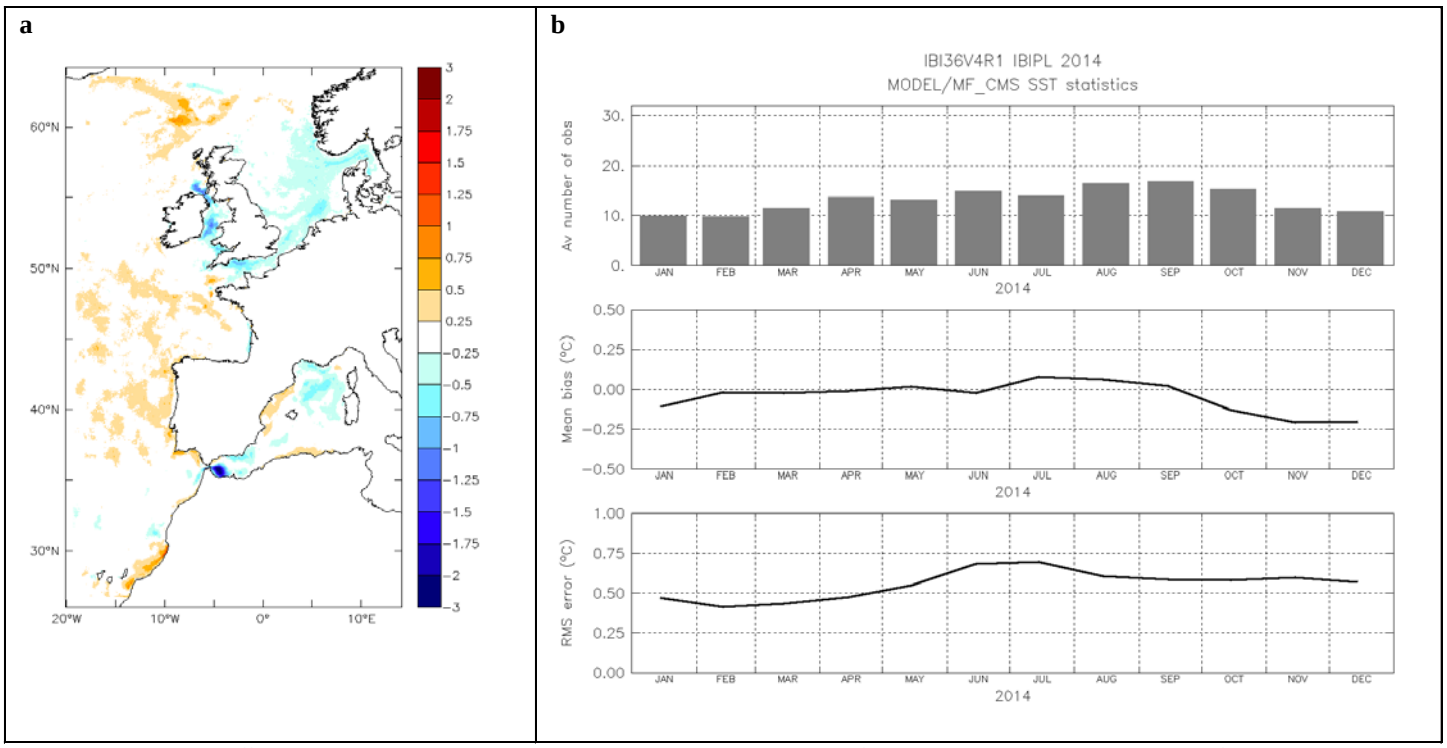

Figure 2 : (a) Average differences (°C) between IBI36 and SST satellite observations (SST L3S for the year 2014). (b) Average number of satellite observations by grid point and by month (top), monthly SST average (middle panel) and RMS (bottom panel) difference between IBI36 and satellite SST.

PSY3 *PSY3V3R3* QUALITY SYNTHESIS, *year 2014*

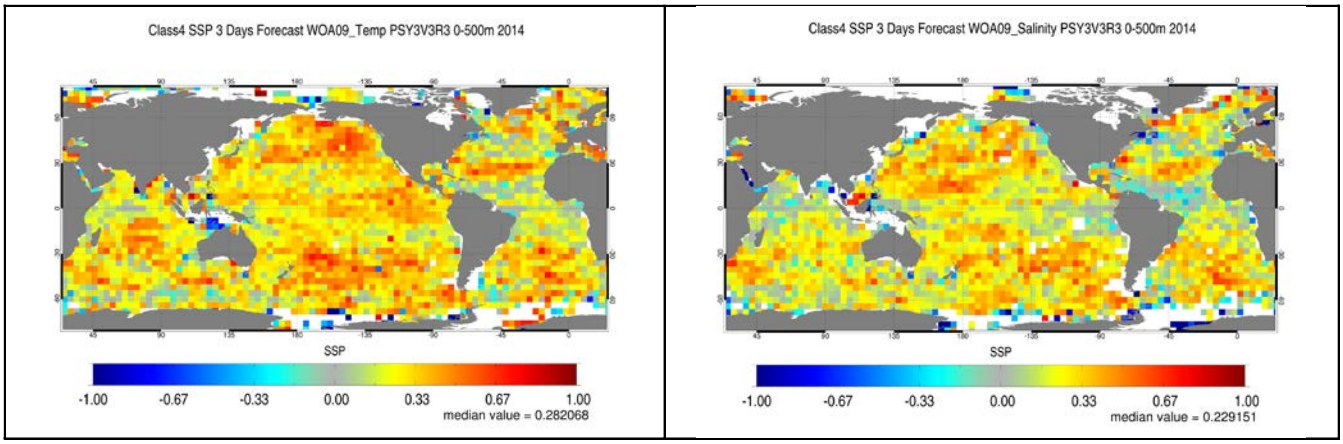

Figure 1: Murphy Skill Score for temperature (left) and salinity (right) on the layer 0-500m for the year 2014.The score is one minus the ratio between the 3-day forecast accuracy and the climatology accuracy. The accuracy is given by the mean square error between the in situ observation (ARGO) and the forecast or the World Ocean Atlas 2009 climatology. Therefore a positive score implies good predictive ability of the system.

The global ¼° PSY3 forecasts are clearly superior to climatology in the three oceans. The system's accuracy in terms of temperature (and to a lesser extent in terms of salinity, for which there are fewer observations) is particularly good in the mid-latitudes. Some regions are an exception, where the climatology is closer to the observations of salinity including: Arabian Sea, the Gulf of Guinea, the western Tropical Atlantic, the Japan Sea, the Weddell Sea, the Indonesian Throughflow, Southern Australia. The 3-day forecast is better than the persistence of the PSY3 analysis in certain areas only (not shown), particularly in the tropics.

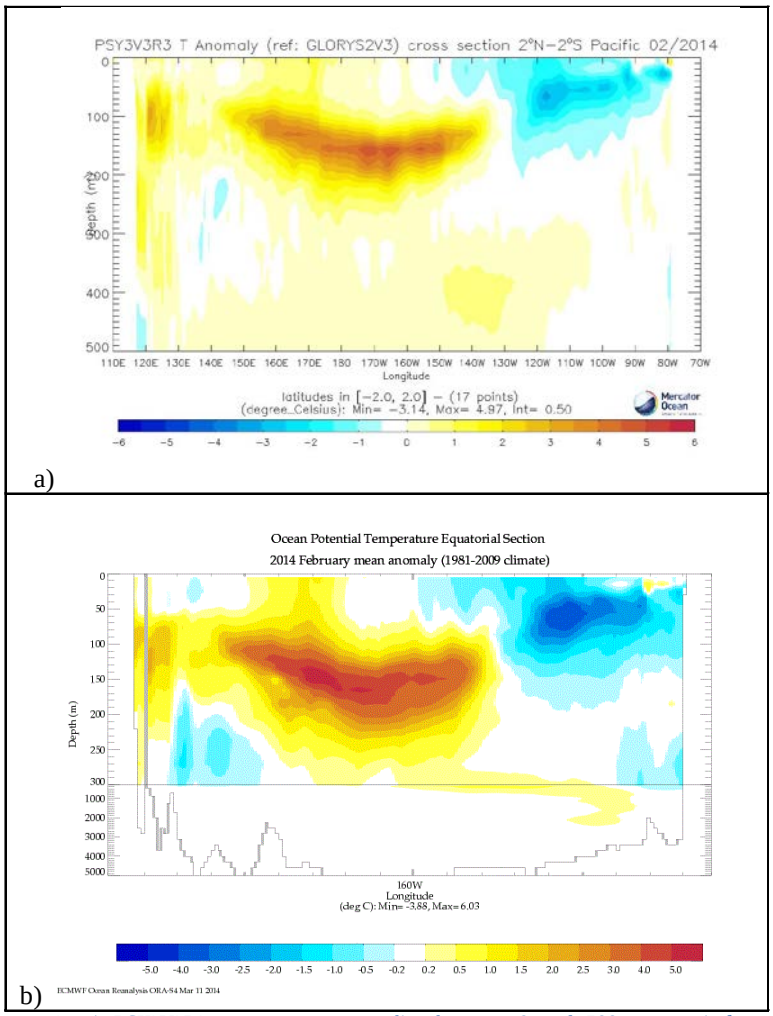

Figure 2: a) PSY3V3R3 temperature anomalies between 0 and 500 metres (reference: Glorys2v3 climatology), for February 2014, compared to b) that is the equivalent for ECMWF ocean reanalysis.

PSY3 analyses are used to create the initial conditions for the Météo-France ocean-atmosphere coupled system that provides seasonal forecasts. As illustrated on Figure 2, the "climatic" signal of PSY3 (temperature and heat content) is comparable to ECMWF reanalysis, particularly in zones of interest for seasonal forecast skill (convergence zones, tropics and equator).

PSY3 is very accurate in terms of concentration and extent of sea ice. Melting is nevertheless too strong in northern summer, because of a warm bias in the atmospheric forcings and relative high accumulation of sea ice in the Canadian basin due to a strong convergence which prevents the melting. In southern hemisphere, the sea ice extent is slightly overestimated during austral winter and underestimated during summer.

PSY3 provides a realistic estimate of the surface currents (especially in terms of direction), at the same order of PSY4, especially in the equatorial countercurrents. Subsurface equatorial currents are well represented, mostly west of equatorial basins.

BIOMER4V1R1 QUALITY SYNTHESIS, year *2014*

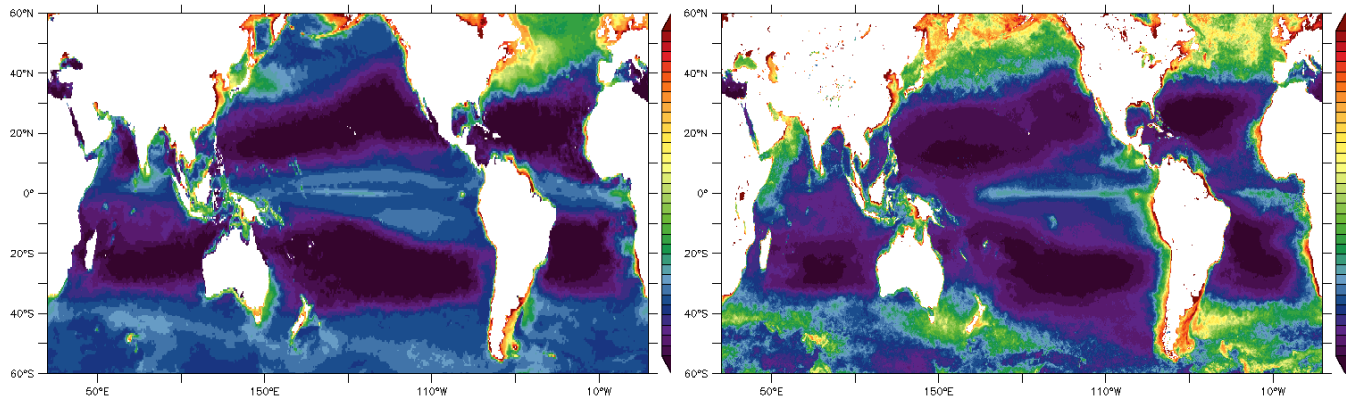

Figure 1: Concentration of chlorophyll a (mg Chl.m^{-3}) on average in 2014 (left) in the BIOMER system and (right) from the GlobColour observations (ocean colour data)

The global system BIOMER4V1R1 at 1/4° delivers weekly an estimate of the main biogeochemical variables in the ocean using the PISCES model and the physical fields of PSY3V3R3.
As can be seen on Figure 1, BIOMER reproduces the large scale structures of chlorophyll concentration corresponding to specific biogeographic zones (*eg.* double gyres, or the Antarctic Circumpolar Current). However, important biases remain in the tropics especially in the western tropical basins and in the southern ocean. Nitrate concentrations in the equatorial surface layer are too high (Figure2).

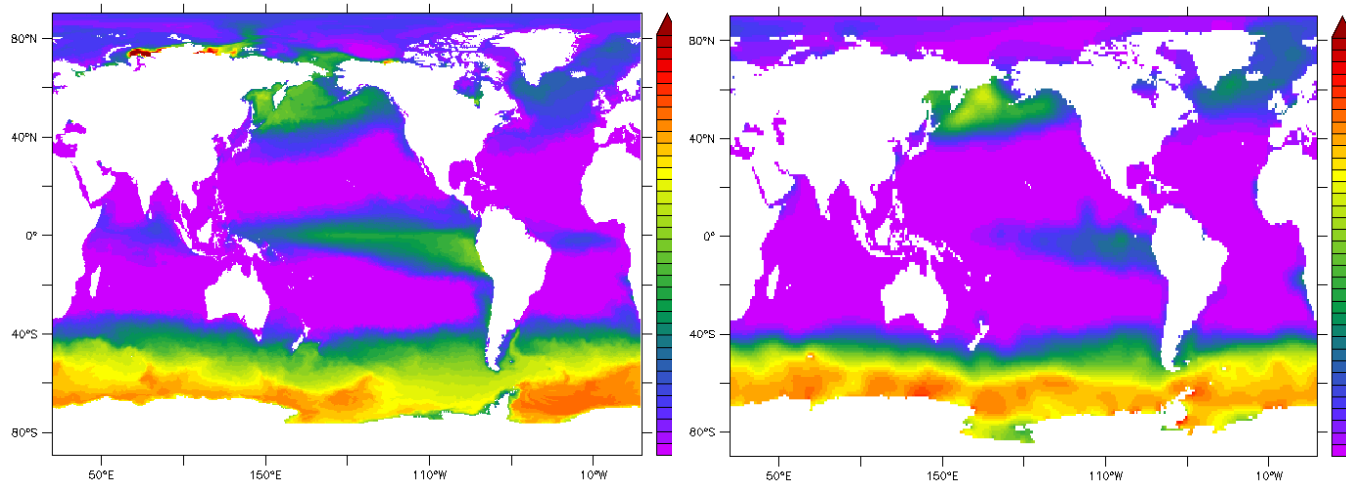

Figure 2: Nitrate concentrations in the layer 0-10m depth (µmol N L^{-1}) on average over the year 2014 (left) in the BIOMER system and (right) from the World Ocean Atlas 2009 climatology.

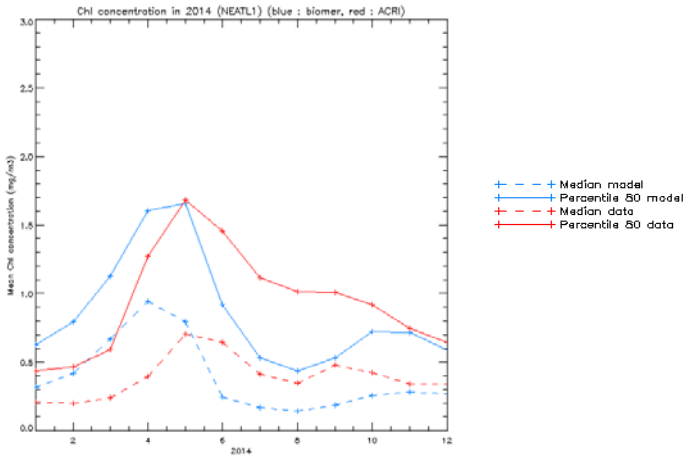

Figure 3: Median and 80th percentile time series for monthly chlorophyll concentrations (mg.m^{-3}) in 2014 in the North Atlantic Ocean. Blue: BIOMER4V1R1. Red : Globcolour

The seasonal cycle of surface chlorophyll is relatively well reproduced in the North Atlantic (Figure 3) with a spring and a fall bloom. However the onset of the spring bloom is not yet in line with the observations (one month delay) and chlorophyll concentrations are too low in summer.